EXPLORING MESENCHYMAL STEM CELL FUNCTION IN AN *IN-VITRO* EQUINE SYNOVITIS MODEL

A Dissertation

by

ANNE E. PETERS

Submitted to the Graduate and Professional School of
Texas A&M University
in partial fulfillment of the requirements for the degree of

DOCTOR OF PHILOSOPHY

Chair of Committee,	Michael Criscitiello
Committee Members,	Scott Dindot
	Jane Welsh
	Gus Wright
Head of Department,	Ramesh Vemulapalli

May 2022

Major Subject: Biomedical Sciences

ABSTRACT

After decades of research, the therapeutic mechanism of mesenchymal stem cells (MSC) remains unknown. While most agree that paracrine function is likely, little is known about the influence of cellular or tissue contact. Our objective was to develop a model of synovitis of the equine articular joint to further understand the role of cell-to-cell contact on MSC function. We tested four conditions (co-culture, transwell, conditioned media and co-culture with a cartilage explant) and found that contact with synovial cells (SCs) and chondrocytes in the presence of interleukin 1-beta (IL1-β) significantly altered cellular secretions. We then added synovial fluid to the cartilage co-culture model to examine the effects on MSCs and dermal fibroblasts (DFs). Compared to DFs, MSCs induced increased prostaglandin E_2 (PGE_2) in all conditions of contact, increased interleukin-6 (IL-6), decreased interleukin-10 (IL-10) and increased growth-related oncogene (GRO) in conditions of co-culture with and without a cartilage explant. The addition of synovial fluid to the cartilage co-culture had little effect on cytokine production, but resulted in SC death, mediated by an anti-bovine serum albumin (BSA) antibody. While soluble factors contribute to communication between SCs, MSCs, and chondrocytes, direct contact with MSCs altered the cellular function and secretome of SCs and MSCs. This work suggests that cross-talk in combination with cell-to-cell contact between MSCs, synovial cells and chondrocytes is important for MSC immunomodulation. While there is still much to discover about the MSC secretome and how paracrine signaling contributes to MSC function in tissue repair, this work sheds light on the complexity of cell-to-cell communication in the joint environment.

DEDICATION

I dedicate this dissertation to Dr. Ashlee Watts, who welcomed me into in the Comparative Orthopedic and Regenerative Medicine Laboratory when it was in its infancy. Together we tested and optimized cell culture techniques and built a successful program that impacted the lives of many horses and owners. After a year as the lab manager, I transitioned into graduate school and our program continued to grow and flourish. Ashlee has been a tremendous influence on my professional and personal life and an amazing mentor. She has a special talent for recognizing both our talents and deficits while encouraging independent growth. Each lab meeting was an opportunity to raise questions without judgement, deliberate on experimental design, or discover new concepts to learn and explore. She taught me how to get comfortable being uncomfortable. It wasn't just about earning a degree, but becoming an independent, confident scientist that understands that the more you learn, the more you learn you don't know- and that is how it should be.

ACKNOWLEDGEMENTS

There have been many influences in my academic career, but first I thank Ashlee Watts, who made all of this possible for me. I could not ask for a better mentor and I will forever appreciate her wisdom, honesty and sense of humor. I have the most incredible committee. Thank you to Mike Criscitiello for treating me like one of your own. I owe a special thank you to Gus Wright for joining my committee and taking extra time to help improve this dissertation and for his mentorship throughout my time here. I thank Jane Welsh for her kindness and mentorship over the past 8 years and Scott Dindot for sharing his lab (and his students) and also for challenging me to work harder.

I would also like to thank my family for their continued unwavering love and support, despite my setbacks. I thank my love, John Durst, for listening to me describe every detail of every experiment, for understanding me and for always being by my side. I thank our lab manager Hsing Fann, for her friendship, taking great care of our lab and for checking over my calculations anytime I asked. I thank my lab-mates for all of their support and teamwork. Particularly, I thank Cole Dahlstrom for bringing the final stages of my project to life. His ideas and enthusiasm helped push me to the end of this journey. There is amazing collaboration between colleagues here and I appreciate everyone's willingness to take the time to help one another and lend an ear whenever possible. Particularly, my friends on the 3rd floor of the research building who are always happy to exchange ideas and share supplies when someone is in need.

CONTRIBUTORS AND FUNDING SOURCES

Contributors

This work was supervised by a dissertation committee consisting of Ashlee Watts, Michael Criscitiello, Scott Dindot, Jane Welsh and Gus Wright.

Analysis of flow cytometry data for CD45 was performed by Gus Wright. Production of fluorescently labeled fetal bovine serum, fluorescent imaging, and flow cytometry of fluorescently labeled mesenchymal stem cells were performed by Cole Dahlstrom for undergraduate research credit. Chromatography of commercial equine serum for Chapter 4 was performed by Larry Dangott at the Texas A&M Protein Chemistry Laboratory.

All other work conducted for the dissertation was completed by the student independently.

Funding Sources

Graduate study was supported by a fellowship from Texas A&M University and a dissertation research fellowship from Link Foundation for Equine Research.

NOMENCLATURE

7AAD	7-Aminoactinomycin D
ADCC	Antibody-dependent cellular cytotoxicity
AD-MSC	Adipose derived mesenchymal stem cell
ATP	Adenosine triphosphate
bFGF	Basic fibroblastic growth factor
BM-MSC	Bone marrow derived mesenchymal stem cell
BSA	Bovine serum albumin
BHQ	Black Hole Quencher-2®
BME	2-Mercaptoethanol
BMP	Bone morphogenic protein
BMS	Bone marrow supernatant
CAC	Complement-assisted Antibody-mediated Cellular cytotoxicity
CD	Chemically defined
CM	Conditioned media
COX-2	Cyclooxygenase-2
DAMP	Danger associated molecular pattern
DF	Dermal fibroblast
DMMB	Dimethylmethylene blue
DMSO	Dimethyl sulfoxide
DPBS	Dulbecco's phosphate buffered saline
ELISA	Enzyme linked immunosorbent assay

EV	Extracellular vesicle
fFBS	FITC Labeled Fetal Bovine Serum
FGF	Fibroblastic growth factor
FITC	Fluorescein isothiocyanate
GAG	Glycosaminoglycan
GMP	Good manufacturing practices
GRO	Growth related oncogene
HRP	Horseradish peroxidase
IFN-γ	Interferon-gamma
IgE	Immunoglobulin E
IgG	Immunoglobulin G
IL-4	Interleukin-4
IL1-β	Interleukin 1-beta
IL-6	Interleukin-6
IL-8	Interleukin-8
IL-10	Interleukin-10
IL-13	Interleukin-13
IFN-γ	Interferon gamma
MEM	Minimum Essential Medium
MMP-13	Matrix metalloproteinase-13
MSC	Mesenchymal stem cell
PAMP	Pathogen associated molecular pattern

PBST	Phosphate buffered saline + Tween
PGE_2	Prostaglandin E2
PRR	Pattern recognition receptor
RT-qPCR	Real time quantitative reverse transcriptase PCR
SVF	Stromal vascular fraction
TBST	Tris buffered saline + Tween
TCEP	Tris (2-carboxyethyl) phosphine
TLR	Toll-like receptor
TNF-α	Tumor necrosis factor alpha

TABLE OF CONTENTS

Page

LIST OF FIGURES

LIST OF TABLES

CHAPTER I

INTRODUCTION

Stem Cell Therapy for Joint Disorders

Joint disease is extremely common and can result from autoimmunity, tissue injury and age. There are several types of joint diseases, including degenerative joint disease, inflammatory joint disease, and other less common joint diseases such as gout and joint infection. Degenerative joint disease is comprised of the diagnosis of osteoarthritis (OA). Inflammatory joint disease is comprised of the diagnosis of rheumatoid arthritis (RA), ankylosing spondylitis, and psoriatic arthritis (1). In OA, injury and aging process initiates the degeneration and inflammation of the joint, whereas, in RA the immune system mediates the destruction of the joint through autoantibodies directed against the joint tissues (2).

Despite different disease etiologies between OA and RA, in both cases, inflammation causes damage to articular cartilage within joints. The prevalence of RA in humans is near 1%, and it is characterized by synovitis, swollen joints and other systemic symptoms such as fatigue, anemia and weight loss (3). Compared to OA, the onset is faster, symptoms are systemic rather than local, and current treatments include disease modifying anti-rheumatic drugs (DMARDs) and biologic treatments instead of just pain management (2). In humans, OA is known to be a leading cause of disability which is particularly prominent in the knee and often leads to the need for joint replacement. It is the most prevalent disease of the adult articular joint (4), with extreme

financial burden (5) (6). In horses, it is also known to be a major cause of lameness and often occurs spontaneously (7). This has a major impact on the athletic careers and general wellbeing of the animals. Unfortunately, there is currently no treatment that can replace the damaged tissue and arthritis progresses further causing pain and debilitation. Modern therapies aim to stop the progression of inflammation in both RA and OA and possibly regenerate new cartilage.

Mesenchymal stem cell therapies are currently available in human and veterinary medicine, however, the mechanisms of how the stem cells therapeutically alleviate joint disease remain unknown. The long-term goal of this dissertation research is to understand the mechanism of action of the stem cells in the joint and establish the most efficacious treatments for tissue repair and regeneration. Both *in-vivo* and *in- vitro* studies aim to elucidate the mechanisms of action and gain better understanding of how to harness the regenerative power of stem cells. The overall objective of this research is to understand how MSCs function in the inflamed equine joint and contribute to the development of more functional therapeutic options.

Horses provide an appropriate model for translational studies of MSC therapy for joint injury and disease due to similarities in structure, strain and athleticism to humans. A recent study emphasized the use of equine models for microscopic examination of the effect of mechanical load at interface of bone and cartilage, which is not accurately mimicked in rodent models (8). Equine models of cartilage repair have shown that horses have similar thickness of articular cartilage and subchondral bone to humans, and that cartilage defect models in the horse can be used to successfully test the effect of

MSC treatment *in-vivo* (9). Naturally occurring arthritis is also common in horses, as in humans, providing another tool for translational study of MSC therapy (7). These applications are valuable in both human and veterinary medicine, emphasizing the utility of the horse as a translational model for studying joint damage and repair.

Joints are important structures that connect the bones of the skeletal system and provide support for the weight of an individual, allowing movement and preventing damage resulting from friction between bones. Damage to joints leads to pain, lack of mobility and inability to perform basic functions. One of the most studied and utilized MSC therapy includes the treatment of OA, which is common in many species (10) including humans (11) and horses (7).

Joint Structure, Function and Dysfunction

The articular joint is composed of a synovial capsule containing synovial tissue, cartilage, bone, ligaments and muscles. Joint function is based on the activity of cells in the joint, particularly synovial cells, chondrocytes, and underlying (subchondral) bone. Synovial cells produce synovial fluid to lubricate the joint, secrete cytokines and chemokines that participate in normal joint remodeling and participate in inflammation, resolution of inflammation and phagocytic activity to remove waste and debris (Figure 1). In the synovial lining, synovial macrophages have specialized roles in joint homeostasis and regulation of inflammation (12) (13) In the sub-lining layer, synovial fibroblasts secrete hyaluronic acid (HA) to provide viscosity and proteoglycan 4 (lubricin/PRG4) which regulates joint inflammation and synoviocyte proliferation (14).

Chondrocytes participate in homeostasis of extracellular matrix and cartilage turnover to ensure maximum functionality under optimal conditions. They synthesize and secrete proteins that make up the extracellular matrix (collagen, proteoglycans) and respond to stimuli such as damage and signals that regulate normal degradation and synthesis of cartilage (15).

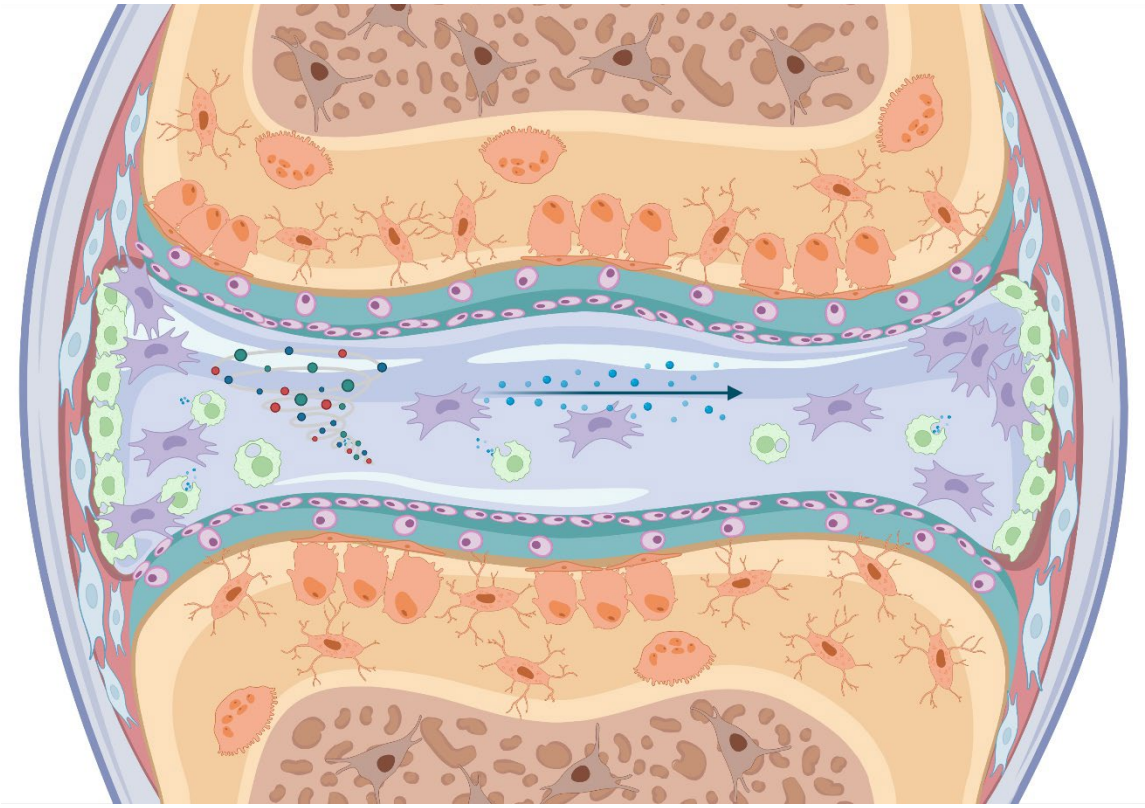

Figure 1. Cells within the synovial joint communicate through cellular signaling. In the lining and sub-lining layers, macrophage (green) and fibroblast like (blue) synoviocytes make up the tissue that surrounds the joint capsule. Chondrocytes (pink) within the articular cartilage communicate with other cells through the exchange of cytokines, chemokines and other chemical signals to maintain homeostasis and regulate inflammation. Mesenchymal stem cells (resident or therapeutic) participate in cellular communication with local cells to drive normal joint turnover and modulate inflammation. Mesenchymal stem cells are produced in the bone marrow. Created with BioRender.com

A problem arises when conditions within the synovial joint are not optimal due to injury, age or disease, leading to inflammation, followed by synovitis and eventual progression to arthritis. In recent years, OA has been implicated as an inflammatory condition, similar to rheumatoid arthritis (RA), but originating from age or injury rather than autoimmunity. While originally thought to be driven by chondrocytes within the articular cartilage, it is now understood that cells within the synovial tissue and subchondral bone communicate, and all have a role in initiating and mediating inflammatory processes (15).

In OA, initial inflammation causes synovitis, which is mediated by synovial macrophages, fibroblasts and chondrocytes. There is intricate signaling between resident and infiltrating cells that orchestrate a coordinated and continuous inflammatory response (16). Synovial macrophages secrete pro-inflammatory cytokines IL1-β, TNF-α, and IL-6 which activate synovial fibroblasts to secrete proteases that degrade the articular cartilage. Synovial cells also recruit infiltrating synovial fibroblasts and other immune cells which, along with chondrocytes, enhance secretion of the same pro-inflammatory cytokine milieu of interleukin 1-beta (IL1-β), interleukin-6 (IL-6) and tumor necrosis factor-alpha (TNF-α) that increase expression and secretion of matrix metalloproteases (MMPs) which degrade the extracellular matrix leading to continued inflammation, secretion of more pro-inflammatory cytokines and further damage (15). A recent study using single cell RNA-sequencing in joint tissue from patients undergoing joint replacement showed that some cytokines (TNF, IL1-β and IL-6) are secreted

exclusively by synoviocytes, illustrating the importance of communication between synoviocytes and chondrocytes in the development of OA (17).

Subchondral bone also communicates with the joint environment, playing a role in the pathogenesis of OA. Importantly, cross-talk between bone and cartilage contributes to the pathogenesis of OA and pain associated with damage to cartilage (18). Synovial cells also contribute to bone changes in OA through secretion of bone morphogenic proteins (BMPs) that contribute to bone remodeling and osteophyte formation (19). Subchondral bone sclerosis and osteophytes are hallmark features of OA, resulting from communication at the osteochondral junction where synovial fluid can contact bone and cartilage cells in areas of damage, recruiting cells to secrete cytokines that direct bone remodeling (20).

The Role of Innate Inflammation in Osteoarthritis

When disrupted by acute injury, overloading or age, complex interplay between synovial macrophages and fibroblasts creates a cascade of inflammation and degradation of the articular cartilage that protects subchondral bone and facilitates movement. Initial damage is recognized by pattern recognition receptors such as toll like receptors (TLRs) on macrophages as damage associated or pathogen associated molecular patterns (DAMPs or PAMPs), activating downstream pathways (NFκB) to secrete pro-inflammatory cytokines and chemokines (21). Toll-like receptors and complement activation, part of the innate immune system, play a role in cartilage degradation resulting in release of inflammatory mediators that contribute to catabolism of cartilage

(22). The complement cascade, which is influenced by pro-inflammatory cytokines, has been shown to participate in the pathogenesis of OA (23).

Many studies aim to discover and target anti-inflammatory pathways to resolve inflammation and reduce cartilage destruction. Recently, resident macrophages were shown to suppress secretion of IL1-β through a pathway involving IL-10 inhibition of IL1-β processing. (24). Anti-inflammatory actions of IL-10 involve chondroprotective effects such as reduced apoptosis and expression of cartilage degrading enzymes (25). In a recent study in horses, overexpression of *IL-10* led to decreased expression and secretion of pro-inflammatory cytokines and cartilage degrading enzymes by MSCs and chondrocytes stimulated with TNF-α or IL1-β (26).

Macrophage Subtypes

Macrophages are important in innate immunity for both homeostasis and regulation of inflammation, and their phenotype determines their secretion of cytokines that result in exacerbation or resolution of inflammation. Synovial macrophages act as immune cells in the synovial joint and their activation or polarization to a particular phenotype (M1 or M2) is driven by the surrounding environment. The M1 phenotype occurs in a pro-inflammatory environment (IL1-β, TNF-α) after activation by TLRs while polarization to M2 (anti-inflammatory) is based on the present balance of cytokines (IL-4, IL-6, IL-10, IL-13, IFN-γ) (27). However, rather than a clear definition how cytokines activate polarization to a particular phenotype, recent research has shown that macrophages display great plasticity, and there are many more factors that

contribute to polarization than previously thought (27). A recent systematic review of macrophage phenotype in OA emphasized that they should be further categorized with emerging technologies to accurately identify specific roles of each subtype (28). There is much current research involving macrophage polarization phenotypes and these studies have uncovered new complexities in how synovial macrophage phenotypes affect function and regulation of homeostasis and inflammation (12). Exciting progress has been made in recent years involving our understanding of macrophage polarization. One important study uncovered the existence of a population of epithelial-like resident macrophages that form an immunological barrier in the synovial lining through tight junctions that are not derived from monocytes and express CX3CR1, a receptor for the chemokine fractalkine, which is involved in cellular recruitment and activation (13). In another recent publication with chimeric mice, gain and loss of function studies uncovered important cellular pathways and revealed that tissue resident macrophages engage in efferocytosis of apoptotic cells and recruit granulocytes that produce reactive oxygen species, which contributes to tissue regeneration. These discoveries are a tremendous contribution to the understanding of OA pathology and tissue regeneration.

Cellular Metabolism

Mammalian cells need nutrients and amino acids for growth and proliferation, as they are unable to biosynthesize all of the nutrients required for proliferation and cellular function (metabolic and communicative). Therefore, these are acquired by use of transporters, which bring in glucose, amino acids and other small molecules, along with

endocytosis and micropinocytosis. These processes are regulated by growth factors and sensors that may be intrinsic or extrinsic to the cell (29). Endocytosis can be described broadly as the formation of internal membranes from the outer plasma membrane of a cell. It includes phagocytosis, autophagy and micropinocytosis and is controlled by a number of pathways that lead to nutrient acquisition, cell signaling, antigen presentation, adhesion, migration, growth, differentiation, and receptor expression (30). Endocytosis is also important in the internalization and formation of vesicles that may be recycled in lysosomes or secreted as extracellular vesicles (EVs) (31). Macropinocytosis is now recognized as an important means for antigen processing and presentation. Innate immune cells have recently been attributed to utilizing micropinocytosis as part of their surveillance machinery (32). Innate immune cells, such as synovial macrophages, likely use micropinocytosis to engulf antigens and other molecules to drive the pathogenesis of arthritis.

Fetal Bovine Serum in Cell Culture

Cell culture and expansion is necessary for laboratory research and therapeutic use of mammalian cells. The gold standard for mammalian cell expansion is media supplementation with fetal bovine serum (FBS), which contains growth factors and proteins that support cell proliferation. However, FBS contains xenogeneic proteins which creates an opportunity for immune recognition by processing and recognition by the immune system. It has been shown that intra-articular injection of FBS supplemented MSCs results in adverse clinical responses (effusion, edema, lameness) in horses (33)

(34). Due to ethical, safety and production concerns, the use of serum replacements or serum free media is being explored (35). For therapeutic MSCs, our group developed a system in which cells are starved of FBS and supplemented with media containing 10% autologous serum 48 hours prior to cryopreservation. Although the majority of bovine proteins are expelled within that time frame, we found that bovine proteins were still present in the cells after FBS starvation at 48 hours (34). Additionally, due to vaccination, horses possess anti-bovine antibodies that may induce cellular cytotoxicity and MSC death in cells grown in FBS supplemented media (33). Reduced cell viability is likely to alter the efficacy of therapeutic MSCs and any *in-vitro* studies of OA in which MSCs are exposed to synovial fluid or serum containing antibodies are likely to be affected by reduced viability due to cell or antibody mediated cytotoxicity. To resolve this problem, our group has developed and tested a xenogen-free culture supplement from bone marrow supernatant (BMS) with improved clinical outcomes *in-vivo* and no cell death *in vitro* compared to FBS supplemented cells after exposure to anti-bovine antibodies (33).

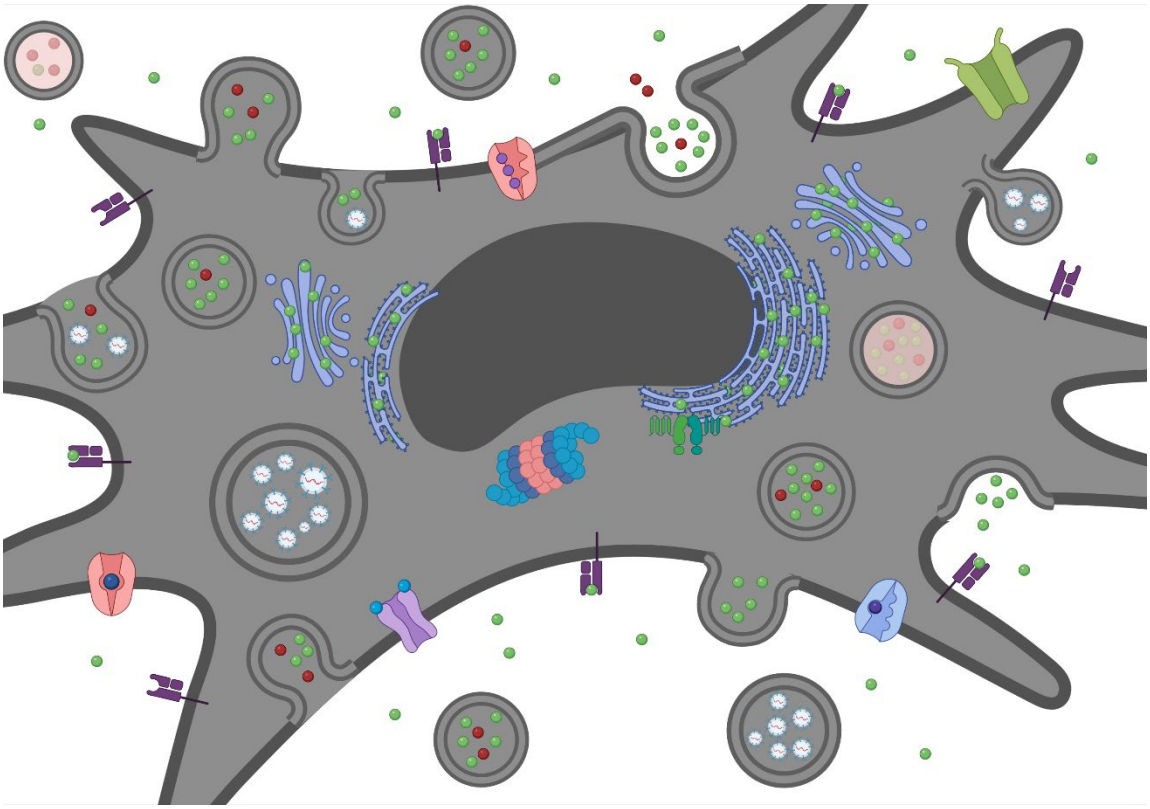

Figure 2. Cellular metabolism and antigen presentation. Mammalian cells maintain homeostasis and participate in immune responses through the uptake of nutrients and other small molecules by use of various channels and transporters, micropinocytosis, packaging and exocytosis of extracellular vesicles. Proteasomes process peptides for antigen presentation or lysosomal recycling. Bovine antigens (green) are taken up, processed and potentially presented on the cell surface by MHCI or adhered to the cell surface for recognition by the immune system. Cytokines (red) may also be secreted or degraded by lysosomes. Created with BioRender.com

Intercellular Communication in the Synovial Joint

Within the joint, juxtacrine (contact-dependent) signaling is important for homeostasis and regulation of inflammation. In the Notch signaling pathway, the Notch protein extends from the membrane to bind with proteins that extend from an adjacent cell, initiating cleavage by a protease and transport of the intracellular domain to the

nucleus for activation of transcription (36) (37). Communication between resident synovial macrophages and fibroblasts through Notch signaling has been shown to participate in the pathogenesis of inflammatory arthritis (38). Additionally, MSCs express, secrete and communicate through Notch signaling (39). In another form of juxtacrine signaling, gap junctions allow small molecules such as calcium, adenosine triphosphate (ATP) and prostaglandin E_2 (PGE_2) to pass to adjacent cells in gap-junctional intercellular communication (GJIC) (39). Chondrocytes have been shown to communicate and exchange nutrients through gap junctions to maintain homeostasis (40). Additionally, chondrocytes, bone cells and synovial cells exchange signaling molecules through channels formed by connexin 43 (Cx43), resulting in crosstalk between cells in the synovial joint (41). Cross-talk involving IL-6 between chondrocytes and synovial fibroblasts has been reported in patients with OA (42). Expression of Cx43 has been shown to be regulated by the exchange of calcium, which is influenced by IL1-β present during inflammation (43). Calcium is a crucial second messenger that participates in an extensive amount of signaling processes, operating in a wide range of time frames and aiding to controlled expression of proteins that participate in these signaling pathways (44).

Paracrine signaling, which involves the exchange of materials between cells or cells and their environment without direct contact, is crucial for normal joint function and immunomodulation. Cells deliver chemical signals such as cytokines and chemokines through the use of vesicles that are released into the extracellular

environment. The coupling of endocytosis and exocytosis is critical for vesicle formation and release (45).

In-vitro models have been used to study paracrine signaling by MSCs and recent work has demonstrated that pre-conditioning equine MSCs with tumor necrosis factor alpha (TNF-α) and/or interferon gamma (IFN-γ) increased their capacity to inhibit T-cell proliferation *in-vitro*, which supports the notion that paracrine activity is important for MSC immunomodulation (46). Transwell membranes have been utilized *in-vitro* to explore how cells behave when they are not in direct contact, and studies illustrate that both paracrine signaling and direct cell-to-cell contact are important (47).

The Future of Regenerative Medicine

Although MSC therapy for regenerative medicine is heavily studied and is already clinically applied for the treatment of OA, there is no federal regulatory marketing approval in the United States. This is likely due to discrepancies in preparation technique and efficacy of allogeneic versus autologous MSC therapy. There are numerous studies testing the efficacy of each in humans (48) and horses (49), both with promising outcomes. However, allogeneic therapies may not be as efficacious as previously thought, due to recognition by the host immune system (50) (51) (52). Based on our group's clinical experience, autologous therapies come with a time delay and high expense due to isolation and expansion, plus the effect of patient health and age must be considered. Given the challenges in both, alternative methods of delivering MSC therapy are being examined.

Cell-free therapy avoids immune recognition of allogeneic cells and bypasses the need for autologous MSC therapy. Development of cell-free therapy, which has become a focal point, involves harnessing the MSC secretome, including EVs and exosomes containing soluble factors that participate in tissue repair, cellular proliferation and immune modulation (53) . Although other cell free therapies, such as platelet rich plasma (PRP) and stromal vascular fraction (SVF) have been explored, recent focus is directed at MSC secretions that can deliver signaling molecules and influence gene expression of local cells (4). Exosomes are membrane bilayer enclosed vesicles packaged with lipids, proteins and nucleic acids that can be exchanged through paracrine signaling for homeostasis, but they become altered during OA and have thus become a target for therapeutic strategies (54). Clinical use of MSC secretions have yielded encouraging results, but there is much more to be understood before therapeutic treatments can be developed due to differences in MSC secretions between individuals and adherence to federal regulations (55). A recent study treated equine chondrocytes with MSC derived EVs during exposure to IL1-β and TNF-α and found a reduction in matrix metallopeptidase-13 (MMP-13) (56), one of the key enzymes of joint degradation in OA. Another publication showed that exosomes derived from MSCs treated with TNF-α and IFN-γ promoted regulatory T-cell (Treg) differentiation from peripheral blood mononuclear cells (PBMCs) (57). While this evidence is promising for the utilization of cell-free therapy, these treatments likely have reduced efficacy due to lack of juxtacrine communication between implanted MSCs and the local cells. It is possible that without

cellular contact, cross-talk between signaling pathways is reduced so that cell-free therapies will not achieve the same effect as viable cells.

A critical gap in our knowledge is how the MSCs or secretomes exert their effect in the articular joint. *In-vitro* evidence demonstrates that paracrine signaling occurs through secretion of mediators and EVs containing soluble mediators working through trophic mechanisms of immunomodulation or stimulation of endogenous progenitors (58). It has been shown that MSCs recruit endogenous progenitors, rather than persisting in the joint 30 days after MSC injection (50). In one study from our group, colony forming units (CFU) from the synovial fluid of allogeneic MHC matched MSC injected equine metacarpophalangeal joints proved to be of recipient origin rather than donor (50). It is not clear however whether the presence of viable cells with continued secretion of chemokines was necessary because synovial fluid was collected 30 days after injection.

In-vitro models of MSC interaction within the articular joint are useful for studying cellular communication in inflammation. Co-culture systems, including direct (cellular contact) and indirect (separation with a transwell membrane) have contributed greatly to the problem of cartilage injury and repair with respect to the regeneration of cartilage and understanding the pathogenesis of arthritis. Some have explored MSCs in co-culture with articular chondrocytes to aid in the regeneration of cartilage (59) (60) (60), while others have shown that cartilage formation in co-cultures results from paracrine signaling rather than differentiation (61). This has led to some discrepancies

about the paracrine function of MSCs in tissue repair. We aim to explore how different contact mechanisms affect MSC function in early synovitis.

If we understand the underlying mechanisms of MSC action in the inflamed synovial joint, we can develop better treatments, making it possible to identify which molecules that MSCs exert their effect. Because one universal therapy cannot be applied to each possible application of MSC therapy, we need to optimize a variety of therapies, including MSC secretions, small molecule pharmaceuticals, cytokine primed and genetically modified MSCs. Gene therapy and cell-free therapies can be optimized to create specific treatments for many diseases. Because the function of cellular contact with local cells after MSC administration in horses or humans is not clearly defined, our aim was to develop and test a model of equine synovitis to help elucidate MSC function in the inflamed joint. We hypothesized that juxtacrine and paracrine signaling play a role in MSC therapeutic effects through immune modulation.

In the following chapters, the effect of contact between cells will be explored, along with the of effect of healthy and inflamed synovial fluid on SCs co-cultured with cartilage explants and MSCs or DFs. Because the addition of synovial fluid affected cell viability, we purified an anti-bovine antibody and identified xenogeneic contamination in cells supplemented with fetal bovine serum during expansion. We discovered that contact with synovial cells and chondrocytes alters the joint secretome and confirmed that equine cells cultured with fetal bovine serum contain anti-bovine antibodies that lead to cellular cytotoxicity which may affect the efficacy of MSC treatment. We propose the use of an autologous culture supplement for expansion of MSCs and deeper

exploration of the synovitis model with the addition of synovial fluid and IL1-β to further investigate the role of MSCs after intra-articular injection.

CHAPTER II

EQUINE SYNOVIAL CELLS AND MESENCHYMAL STEM CELLS IN CLOSE CONTACT SECRETE PRO-INFLAMMATORY CYTOKINES IN RESPONSE TO INTERLEUKIN 1-BETA

Introduction

Mesenchymal stem cell (MSC) based therapies are being used for the treatment of joint injury and disease, but many challenges remain before the full potential of therapeutic use of MSCs can be realized. Intra-articular injection of MSCs in horses has resulted in improved tissue integrity (62), reduced lameness and slowed progression of joint disease (63). Unfortunately, a major obstacle is that we do not fully understand the mechanisms of improved tissue repair and regeneration.

Paracrine activity leading to immunomodulation rather than cell replacement is the current leading theory to explain how MSCs contribute to repair. However, it is important to best utilize MSCs to achieve the most efficacious therapeutic. Although cytokine, chemokine and growth factor secretion by MSCs are known to contribute to immunomodulation, the mechanism by which MSC function is affected by cellular contact within the synovial joint is unknown. Without the ability of cells to communicate through direct contact, many signaling cascades may be interrupted.

Cellular therapy involves the use of autologous or allogeneic cell preparations to treat injury or disease. To date, many publications use allogeneic cell preparations to test MSC efficacy *in-vivo* (64). Allogeneic cells must be cross-matched to evade immune

recognition (65) and autologous preparations are burdened by inconsistencies in preparation (33). Therefore, a growing interest in cell-free therapy has emerged which potentially circumvents any adverse effects associated with cellular therapy.

Cell-free therapy utilizes the MSC secretome as a therapeutic. Treatment with MSC derived exosomes (66), often pre-conditioned with cytokines, growth factors or other enrichments (67) has been evaluated in the synovial joint with positive outcomes but there are many hurdles. Current research is also focused on using MSC conditioned medium (CM) concentrates (68) or extracellular vesicles (EVs) (69) to treat diseases in which cellular therapy has been employed, but the efficacy of these treatments remains unclear.

Our objective was to evaluate MSC function with and without cellular contact in an *in-vitro* model of the inflamed synovial joint during articular inflammation. We used a benchtop model of synovitis to investigate the function of MSCs versus that of skin fibroblasts in four different contact conditions in the early phases of inflammation. We hypothesized there would be differences in mitigation of inflammation by different model conditions and our results suggest that contact between MSCs and synovial cells (SCs) significantly changed their cellular function and secretome. Our concurrent use of conditioned medium suggests that harnessing the MSC paracrine function from a short time period is less effective than allowing MSC contact during inflammation. Juxtacrine signaling mediates many processes and without it, we expect that cellular communication is interrupted. Perhaps a combination of contact between cells with optimized cell-free therapy would result in better clinical outcomes.

Methods

In preliminary tests, synovial cells were exposed to interleukin 1-beta (IL1-β) to mimic an inflammatory environment and co-cultured with MSCs or dermal fibroblasts (DFs) in direct contact as a control. We examined differences between cells treated with IL1-β compared to controls and determined that 10 ng/ml IL1-β was sufficient to elicit cytokine secretion from one or both cell types. The experimental model consisted of four conditions of contact: (1) direct contact in which MSCs or DFs were seeded on top of synovial cells, (2) indirect contact in which cell types were separated by a transwell membrane, (3) CM in which synovial cells were treated with IL-β and the CM was added to MSC/DF monocultures and (4) direct contact with the addition of a donor cartilage explant. Culture supernatant and cartilage explants were collected and stored for subsequent assays. Cells were lysed and stored for RNA isolation and gene expression analysis.

Tissue Collection, Cell Isolation and Culture

Synovial Cells

Synovial tissue was aseptically dissected from the front and back metacarpophalangeal joints immediately post-mortem. Between 3 and 12 g of tissue was collected into a glass media bottle containing 250 ml Dulbecco's phosphate buffered saline (DPBS)[i] supplemented with 10,000 U/ml Penicillin, 10 mg streptomycin sulfate, 25 μg/ml amphotericin B[ii]. Synovium digestion was performed by incubating synovial tissue in 10 ml sterile filtered digest media per gram of tissue for 4 hours at 37°C with

gentle agitation. Digest media consisted of synoviocyte growth medium [Dulbecco's modified Eagle's medium[iii] (DMEM) 4.5 g/l glucose supplemented with 10,000 U/ml Penicillin, 10 mg streptomycin sulfate, 25 µg/ml amphotericin B, HEPES buffer[iv], and 10% fetal bovine serum (FBS)[v]] and 1.5 mg type II collagenase[vi] per ml digest media prepared. The digested tissue and media were centrifuged at 600 x G for 5 minutes at 4°C to pellet the cells. After aspirating the supernatant, the pellet was re-suspended in synoviocyte isolation medium and a 100 µl sample was used to manually count nucleated cells with fluorescein diacetate[vii] and propidium iodide[viii]. The remaining volume was seeded at 10,000 cells/cm^2 into tissue culture flasks[ix] and maintained at 37°C in 5% CO2 humidified air for 2-4 days. Cells were detached for cryopreservation at passage 0 with 0.25% Trypsin EDTA[x], washed, counted and cryopreserved in 80% synoviocyte isolation media, 10% dimethyl sulfoxide (DMSO)[xi], and 10% FBS.

MSCs

Sternal bone marrow was collected from each horse immediately post-mortem, followed by red blood cell lysis as previously described (70) and isolation and expansion to passage 4 as previously described (71).

Dermal Fibroblasts

Prior to dissection, a skin flap was aseptically reflected to expose the metacarpophalangeal joint. For each horse, six approximately 5 mm dermal punches, dissected by hand, were immediately placed in a 50 ml conical tube containing 35 ml

fibroblast isolation medium [DMEM/Ham's F-12 50/50 supplemented with 10,000 U/ml Penicillin, 10 mg streptomycin sulfate, 25 µg/ml amphotericin B, HEPES buffer, 10 µg/ml human recombinant basic fibroblastic growth factor and 10% FBS]. Punches were placed epidermal side down in 6 well culture dishes[xii] for explant culture with 3 ml fibroblast isolation media. After 4 days, tissues were removed, and media exchanged. Migrated DFs were maintained with fibroblast growth medium, which was exchanged three times per week. Cells were detached from tissue culture dishes with 0.25% Trypsin EDTA and transferred to 175 cm^2 tissue culture flasks for expansion at the first passage. Cultures were maintained until reaching 70-80% confluence and then lifted with 0.25% Trypsin EDTA at each passage until reaching passage 4. Upon reaching 80% confluence, cells were cryopreserved in 80% fibroblast isolation media, 10% DMSO, and 10% FBS.

Cartilage Explants

Cartilage explants were collected from 5 horses that were euthanized for reasons unrelated to this study. Collection was performed immediately post-mortem. Stifle joints were aseptically dissected to expose the lateral and medial trochlear ridges on the femur. An 8 mm biopsy punch[xiii] was pressed into the articular cartilage to create a uniformly sized explant. To remove explants, a scalpel blade was passed beneath the explant to release it from the underlying cartilage/subchondral bone. Explants were placed into a glass media bottle containing 250 ml DPBS supplemented with 10,000 U/ml Penicillin,

10 mg streptomycin sulfate, 25 µg/ml amphotericin B and stored on ice for transport to the lab. Each donor horse provided explants for two co-culture experiments.

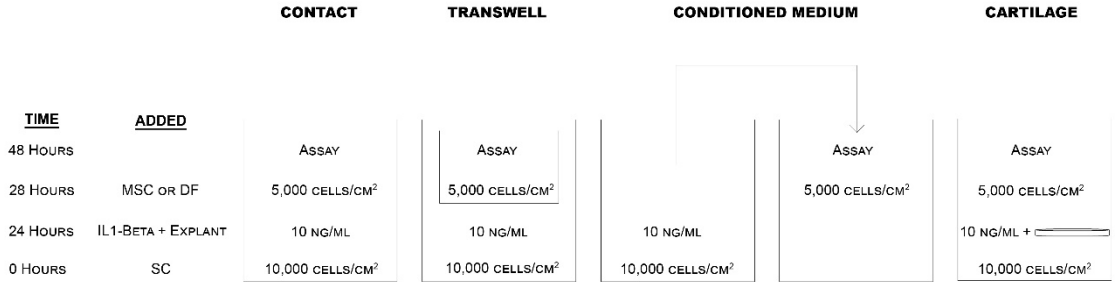

Figure 3. Experimental model of co-culture under different conditions of contact. Cells were harvested from the metacarpophalangeal joints and clean incision areas. Bone marrow was harvested from the sternum. Synovial cells (SCs), dermal fibroblasts (DFs) and mesenchymal stem cells (MSCs) were cryopreserved and later seeded onto 6 well plates. After overnight recovery, the cells were exposed to 10 ng/ml interleukin 1-beta (IL1-β) for 4 hours before treatment with MSCs or DFs. In the co-culture condition, cells were in direct contact while in the transwell condition, cells were separated by a transwell membrane that allowed media to pass between both cell types. In the conditioned medium condition, media was moved from the synovial cells after IL1-β exposure then used to seed MSCs or DFs for overnight culture. In the cartilage condition, cells were in direct contact with the addition of a donor cartilage explant. Following treatment and overnight culture, media and cell lysates were collected and stored for future assays.

Contact Co-culture

Cryopreserved SCs were thawed and seeded onto 6 well culture dishes at a density of 10,000 cells/cm^2 on synoviocyte isolation media [Dulbecco's modified Eagle's medium (DMEM) 4.5 g/l glucose supplemented with 10,000 U/ml Penicillin, 10 mg streptomycin sulfate, 25 µg/ml amphotericin B, HEPES buffer, and 10% fetal bovine serum (FBS)]. Following overnight recovery, all wells were washed, and media replaced with 2 ml control or inflamed media. Media preparations consisted of serum

free MSC isolation medium [DMEM 1g/l glucose supplemented with 10,000 U/ml Penicillin, 10 mg streptomycin sulfate, 25 µg/ml amphotericin B, HEPES buffer, 10 µg/ml human recombinant bFGF and 1% ITS+ Premix[xiv]] plus sterile 0.1% bovine serum albumin[xv] (BSA) (control media) or 10 ng/µl IL1-β[xvi] (inflamed media) reconstituted in sterile 0.1% BSA for a final concentration of 10 ng/ml inflamed media. The volume of BSA added to the control media was equal to the volume of IL1-β added to the inflamed media. After 4 hours, MSCs or dermal fibroblasts were thawed, resuspended in control or inflamed media and then added to each well at a density of 5,000 cells/cm^2 with a final volume of 3 ml. After 24 hours, the cell culture supernatant was collected and stored at -80°C for enzyme-linked immunosorbent assay (ELISA). Each well was then washed with DPBS before cell lysing solution, premixed with tris (2-carboxyethyl) phosphine (TCEP[xvii]) at a concentration of 1%, was added according to the manufacturer instructions directly to each well. Culture dishes were stored at -80°C for later RNA isolation.

Transwell Co-culture

Synovial cells were thawed on day 1 and seeded onto the bottom wells of 6 well culture dishes containing transwell inserts[xviii] at a density of 10,000 cells/cm^2. Following overnight recovery, all wells were washed, and media replaced with 2 ml control or inflamed media. After 4 hours, MSCs or dermal fibroblasts were thawed, resuspended in control or inflamed media and then added to each of the transwell inserts each at a density of 5,000 cells/cm^2 with a final volume of 3 ml. After 24 hours, the cell culture

supernatant was collected and stored at -80°C for ELISA. Each well was then washed with DPBS before cell lysing solution, premixed with TCEP at a concentration of 1%, was added according to the manufacturer instructions directly to each well. Culture dishes containing two cell types were separated for cell lysis. After rinsing, transwell inserts were removed and placed into a fresh 6 well culture dish before lysing solution was added to the wells. Cell lysate was removed from transwell inserts and pipetted into clean wells. Culture dishes were stored at -80°C for later RNA isolation.

Conditioned Media Experiment

Conditioned media production was initiated by thawing synovial cells and seeding onto 6 well culture dishes at a density of 10,000 cells/cm^2. Following overnight recovery, all wells were washed, and media replaced with 2 ml control or inflamed media. After 4 hours, CM was collected, and 2 ml added to clean 6 well culture dishes. At the same time, MSCs or DFs were thawed, resuspended in control or inflamed media and then added to each well containing control or inflamed CM media at a density of 5,000 cells/cm^2 with a final volume of 3 ml. After 24 hours, the cell culture supernatant was collected and stored at -80°C for ELISA. Each well was then washed with DPBS before cell lysing solution, premixed with TCEP at a concentration of 1%, was added according to the manufacturer instructions directly to each well. Culture dishes were stored at -80°C for later RNA isolation.

Cartilage Explant Contact Co-culture

Synovial cells were thawed on day 1 and seeded onto 6 well culture dishes at a density of 10,000 cells/cm^2. Following overnight recovery, all wells were washed, fresh cartilage explants were added to each well and the media was replaced with 2 ml of inflamed media. After 4 hours, MSCs or dermal fibroblasts were thawed, resuspended in inflamed media and then added to each well at a density of 5,000 cells/cm^2 with a final volume of 3 ml. After 24 hours, the cell culture supernatant was collected and stored at -80°C for ELISA. Cartilage explants were then removed from the wells and stored at -80°C. Each well was then washed with DPBS before cell lysing solution, premixed with TCEP at a concentration of 1%, was added according to the manufacturer instructions directly to each well. Cell lysate was stored at -80°C.

Enzyme Linked Immunosorbent Assay

Cell culture supernatants were used at a 3 to 10-fold dilution at the first freeze thaw with the Prostaglandin E2 Parameter Assay Kit[xix], Equine IL-6[xx] and IL-10[xxi] DuoSet ELISA kits according to the manufacturer's instructions.

Magnetic Bead Assay

Undiluted cell culture supernatants were used to perform a 23-analyte magnetic bead assay[xxii] to assess cytokine/chemokine production by synovial cells co-cultured

with MSCs or DFs. Supernatants and standards were incubated with magnetic beads according to the manufacturer's instructions to produce analyte concentrations[xxiii].

Reverse Transcriptase Quantitative Polymerase Chain Reaction

Cells from 6 well dishes in the cartilage co-culture were treated with lysing solution and TCEP before RNA isolation[xxiv]. Quality and quantity of total RNA were evaluated[xxv] before gene expression was measured. One-step reverse transcriptase quantitative polymerase chain reaction (RT-qPCR) was performed with a dual labeled probe and primers designed by Sigma OligoArchitect[xxvi] with KiCqStart One-Step Probe based PCR Mastermix[xxvii]. Expression of interleukin-6 (IL-6), cyclooxygenase-2 (COX-2), and IL1-β were measured by relative quantification (ΔΔ Cq) and glyceraldehyde 3-phosphate dehydrogenase (GAPDH) was used as a reference gene. Probe oligonucleotides were dual labeled with reporter Texas Red (TxRed) at the 5' end and Black Hole Quencher®-2 (BHQ2) at the 3' end.

Table 1. Primer and probe sequences for RT-qPCR. Primer and probe sequences (5' to 3') for measuring expression of interleukin-6 (IL-6), cyclooxygenase-2 (COX-2), interleukin 1-beta (IL1-β) and glyceraldehyde 3-phosphate dehydrogenase (GAPDH) by reverse transcriptase polymerase chain reaction (RT-PCR)

Primer and probe sequences for RT-qPCR			
Gene	Forward Primer (5'-3')	Reverse Primer (5'-3')	Dual Labeled Probe (5'-3')
IL-6	CACTCCAGTTGCCTTCTC	CCGAGGATGTACTTAATGTG	CTGCTCCTGGTGATGGCTACT
COX-2	CCAACCTCTCGTATTACA	GGGATGAACTTTCTTCTTAG	TCTTCCTCCTGTGGCTGACG
IL1-β	CACTCCAGGATTCTGTTC	TGCCCTTCATCTGTTTTG	AACAGGTCATTCTCATTGCCGC
GAPDH	CTCACTTGAAGGGTGGAG	GAGGCATTGCTGACAATC	TCATCATCTCTGCTCCTTCTGCTG

Dimethylmethylene Blue Assay

Glycosaminoglycan (GAG) content was measured by spectrophotometry. Sample preparation and assay were adapted from previous literature (72). Media and cartilage explants were digested with 5 mg/ml papain[xxviii] (media dilution 1:3, cartilage explant dilution 1:20) for 4 hours at 65°C. In a 96 well plate, 25 µl of diluted cell culture supernatant or digested tissue was added to the plate before adding 200 µl of dimethylmethylene blue (DMMB) dye and reading at 525 nm[xxix] immediately. Concentrations of GAG in each sample were interpolated using a chondroitin sulfate[xxx] standard curve. The percentage loss of GAGs from cartilage explants was calculated by dividing the difference in the total GAGs and the weight adjusted (g) GAG concentrations in the tissue by the total GAGs (media + weight adjusted (g) tissue).

Histology

Cartilage explants were processed, embedded and sectioned at 4 µm prior to staining with Safranin O[xxxi] and Fast Green[xxxii]. Slides were observed with an Olympus CKX41 light microscope and pictures taken with an Olympus DP73 camera mounted to

the microscope and captured with cellSens[xxxiii] software before pictures were evaluated using and adaptation of the Modified Mankin Scoring System (Table 2) (73) (74) (75) (76) . Additionally, images were randomized using an online program (http://random.org/) and scored for loss of Safranin-O stain by drawing a line at the interface of stain loss and measuring the distance in pixels from the surface using Image J[xxxiv] software. Values obtained by two individuals were averaged.

Cell Surface Marker Expression

Two horses were chosen for CD45RB expression based on their secretion of IL-6. Synovial cells, MSCs and DFs were thawed and prepared for flow re-suspended at a concentration of 10 million cells/ml in DPBS. One million cells of each type were aliquoted into microcentrifuge tubes for the following conditions: unstained control, secondary antibody control, and CD45RB[xxxv] + secondary antibody. Cells were labeled with CD45RB by adding 100 µl staining buffer to the tube containing cells in the CD45RB + secondary antibody condition followed by the addition of 3 µl CD45RB and incubation in the dark for 15 minutes. Following incubation, 2 washes in 100 µl DPBS were performed by centrifugation at 400 X G for 3 minutes. Secondary antibody controls and CD45RB + secondary antibody tubes were labeled with F(ab')2-goat anti-mouse IgG conjugated to fluorescein and incubated in the dark for 15 minutes. All tubes were washed by centrifugation at 400 X G for 5 minutes, followed by resuspension in 150 µl DPBS and the addition of 7-Aminoactinomycin D[xxxvi] (7AAD) prior to flow cytometry using an Amnis CellSteam[xxxvii] flow cytometer with a 488 nm laser.

Statistical Analysis

All statistical analyses and graphs were created using GraphPad Prism[xxxviii] software. Data from co-cultures in all assays except the RT-PCR were compared using paired Wilcoxon Signed Rank. Relative quantification (ΔΔ Ct) was used to observe fold-change expression of *IL-6*, *COX-2* and *IL1-β* in MSC co-cultures relative to dermal fibroblast co-cultures (control) using GAPDH as a reference gene. Modified Mankin scores and percent GAG loss from MSC and DF co-culture cartilage explants were compared using paired Wilcoxon Signed Rank.

Results

Table 2. Summary of median cytokine concentrations in the contact co-culture condition measured by enzyme-linked immunosorbent assay (ELISA). (SC = synovial cell monoculture, MSC = mesenchymal stem cell monoculture, DF = dermal fibroblast monoculture, SC/DF= SC/DF co-culture, SC/MSC = SC/MSC co-culture).

Contact Co-Culture Cytokine Concentrations						
Condition	**Control [pg/ml]**			**IL1-β [pg/ml]**		
	PGE_2	**IL-6**	**IL-10**	**PGE_2**	**IL-6**	**IL-10**
SC	102	1	1	643	156	1
MSC	66.1	1	1	883	81	1
DF	160	1	1	543	1	1
SC/MSC	231	1	1	3,645	372	1
SC/DF	260	1	1	1,420	108	1

Table 3. Summary of median cytokine concentrations in the transwell co-culture condition measured by enzyme-linked immunosorbent assay (ELISA). (SC = synovial cell monoculture, MSC = mesenchymal stem cell monoculture, DF = dermal fibroblast monoculture, SC/DF = SC/DF co-culture, SC/MSC = SC/MSC co-culture).

Transwell Co-Culture Cytokine Concentrations						
Condition	**Control [pg/ml]**			**IL1-β [pg/ml]**		
	PGE_2	**IL-6**	**IL-10**	**PGE_2**	**IL-6**	**IL-10**
SC	92	1	2	297	2	1
MSC	82	1	2	364	1	2
DF	122	1	9	286	1	4
SC/MSC	185	1	6	1,029	4	17
SC/DF	188	1	7	565	1	17

Table 4. Summary of median cytokine concentrations in the conditioned media (CM) condition measured by enzyme-linked immunosorbent assay (ELISA). (MSC = mesenchymal stem cell monoculture, DF= dermal fibroblast monoculture).

Conditioned Media Cytokine Concentratiosn						
Condition	**Control [pg/ml]**			**IL1-β [pg/ml]**		
	PGE_2	**IL-6**	**IL-10**	**PGE_2**	**IL-6**	**IL-10**
MSC	206	1	7	486	92.1	1
DF	42.98	1	1	1,196	1	4

Table 5. Summary of median cytokine concentrations in the cartilage co-culture condition measured by enzyme-linked immunosorbent assay (ELISA). (SC = synovial cell monoculture, MSC = mesenchymal stem cell monoculture, DF= dermal fibroblast monoculture, SC/DF= SC/DF co-culture, SC/MSC = SC/MSC co-culture).

Cartilage Co-Culture Cytokine Concentrations						
Condition	**Control [pg/ml]**			**IL1-β [pg/ml]**		
	PGE_2	**IL-6**	**IL-10**	**PGE_2**	**IL-6**	**IL-10**
SC	468	0	1	3,012	4,680	1
SC/MSC	551	43	20	96,337	9,334	64
SC/DF	681	0	47	7,551	3,924	185

PGE_2 secretion is increased the presence of IL1-β and MSCs regardless of contact

Co-cultures not exposed to IL1-β secreted little to no cytokines, indicating that co-culture with a pro-inflammatory cytokine stimulates cellular secretions and communication. Co-culture alone stimulated some production of PGE_2, indicating juxtacrine signaling between cells without pro-inflammatory stimulation (Figure 4). After exposure to IL1-β, as detected by ELISA, synovial cells and MSCs in all conditions of contact significantly increased production PGE_2 (Figure 5) compared to SC/DF co-cultures (co-culture $p= 0.0009$, transwell $p= 0.03$, CM $p= 0.02$, cartilage co-culture $p = 0.02$). These findings were confirmed by the up-regulation of COX-2 ($p= 0.002$) in the cartilage co-culture (Figure 7).

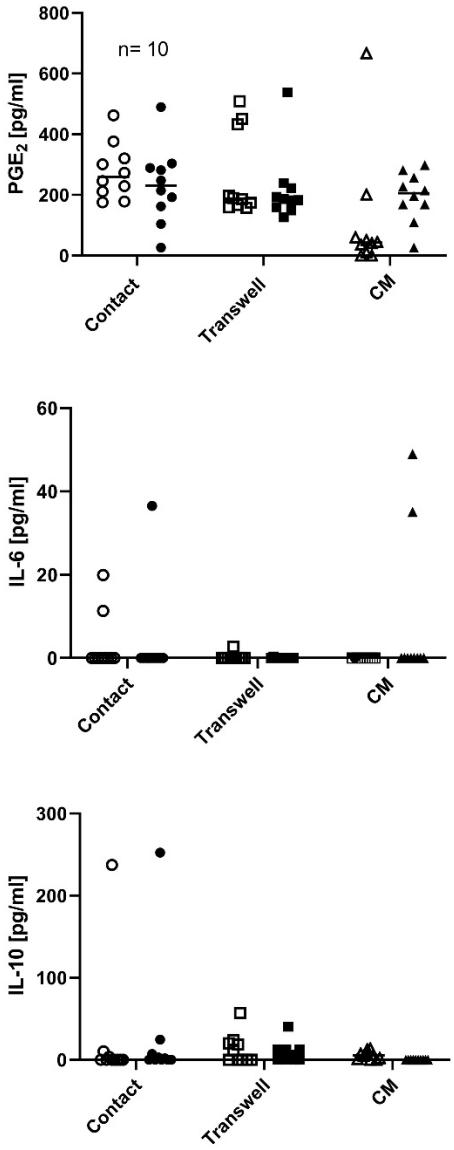

Figure 4. Cytokine concentrations of co-cultures without IL1-β exposure. Open shapes represent synovial cell (SC)/mesenchymal stem cell (MSC) co-cultures and closed shapes represent SC/dermal fibroblast (DF) co-cultures. Cytokine production was measured by enzyme linked immunosorbent assay (ELISA) using cell culture supernatants of co-cultures not treated with interleukin 1-beta (IL1-β). The cartilage co-culture is not shown.

Cytokine secretion/stimulation between MSCs and DFs is not identical

In the contact (SC/MSC p= 0.002, SC/DF p= 0.002), transwell (SC/MSC p= 0.002, SC/DF p= 0.002) and CM (SC/MSC p= 0.003, SC/DF p= 0.002) formats, cells secreted significantly more PGE_2 (Figure 5) than unstimulated controls (Figure 4). IL-6 secretion, possibly by MSCs and/or SCs is increased by the presence of IL1-β conditioned medium, as cells in the MSC condition secreted significantly more IL-6 compared to unstimulated controls (p= 0.007) while cells in the DF condition did not. There is an inhibitory effect of contact between MSCs/DFs and SCs on IL-10 secretion in the absence of cartilage. Secretion of IL-10 was only elevated compared to unstimulated controls in the MSC transwell (p= 0.03) and CM (p= 0.02) co-cultures. DFs do not secrete or stimulate secretion of IL-10 in the absence of chondrocytes.

Synovial cells and MSCs in close contact increase expression and secretion of IL-6

In conditions of co-culture (p= 0.01) and cartilage co-culture (p= 0.03) IL-6 was increased in MSC compared to DF co-cultures as detected by ELISA. To corroborate this finding, expression of *IL-6* was upregulated in the SC/MSC co-culture compared to the SC/DF co-culture (Figure 5). Steady state RNA levels of *IL-6* were higher in the SC/MSC co-culture compared to the SC/DF co-culture (p= 0.002, Figure 7). Production of IL-6 was elevated in the SC/MSC co-culture, cartilage co-culture and conditioned media formats, but not the transwell co-culture as detected by the magnetic bead assay. A significant difference in IL-6 concentrations was observed between MSC and DF co-

cultures in the co-culture and conditioned media formats (Figure 6). Although not significantly different between SC/MSC co-cultures and SC/DF co-cultures, IL-6 concentrations produced by several horses (Figure 6) detected by this assay were markedly higher in the cartilage co-culture, indicating that the presence of chondrocytes impacted secretion of IL-6.

The addition of chondrocytes led to altered secretory activity and gene expression

Decreased IL-10 in MSC compared to DF co-cultures was detected in the presence of a cartilage explant ($p= 0.01$) while separation of the cell types did not result in increased cytokine production (Figure 5). To corroborate this finding, expression of *IL-6* and *COX-2* were upregulated in the MSC co-culture compared to the dermal fibroblast control (Figure 7). In the magnetic bead assay, 23 analytes were provided by the manufacturer and four were detectable in the culture supernatants: IL-6, growth related oncogene (GRO), interleukin-8 (IL-8) and fibroblastic growth factor (FGF). In the conditions of contact and CM, significant increases in GRO (co-culture $p= 0.002$, CM $p= 0.007$) and IL-6 (co-culture $p = 0.002$, CM $p= 0.003$) concentrations were observed in SC/MSC co-cultures compared to SC/DF co-cultures. There was no difference in IL-8 or FGF concentrations between MSC and DF co-cultures (Figure 6).

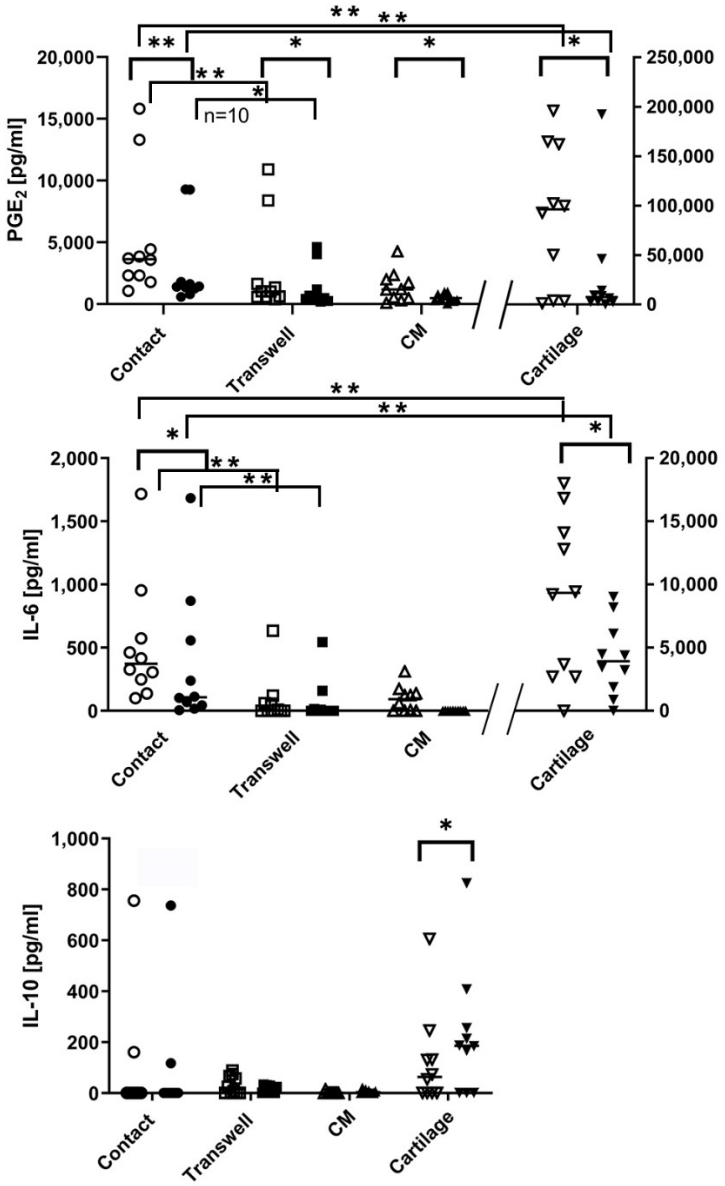

Figure 5. Cytokine concentrations measured by ELISA. Open shapes represent synovial cell (SC)/ mesenchymal stem cell (MSC co-cultures) and closed shapes represent synovial cell (SC)/dermal fibroblast (DF) co-cultures. Cytokine production was measured by enzyme linked immunosorbent assay (ELISA) using the cell culture supernatants. SCs and mesenchymal stem cells MSCs secreted significantly more prostaglandin E_2 (PGE_2) than SCs and dermal fibroblasts (DFs) in co-culture in all conditions of contact after 4 hours of exposure to 10 ng/ml interleukin 1-beta (IL1-β) and overnight co-culture (Wilcoxon signed rank, contact p = 0.009, transwell p= 0.03, CM p= 0.02, cartilage p= 0.02). Interleukin-6 (IL-6) concentrations were significantly higher in MSC compared to DF co-cultures in the contact (p= 0.01) and cartilage (p=

0.03) conditions. IL-10 concentrations were higher in the DF compared to MSC co-cultures only with the addition of a cartilage explant (p= 0.01). SC/MSC and SC/DF co-cultures secreted significantly higher amounts of PGE_2 (SC/MSC p= 0.004, SC/DF p= 0.02) and IL-6 (SC/MSC p= 0.004, SC/DF p= 0.004) in the cartilage co-cultures compared to co-culture without cartilage. Concentrations of PGE_2 in SC/MSC co-cultures (p= 0.002) and SC/DF co-cultures (p= 0.002) were significantly higher compared to transwell co-cultures. Concentrations of IL-6 in SC/MSC co-cultures (p= 0.002) and SC/DF co-cultures (p= 0.01) were significantly higher compared to transwell co-cultures.

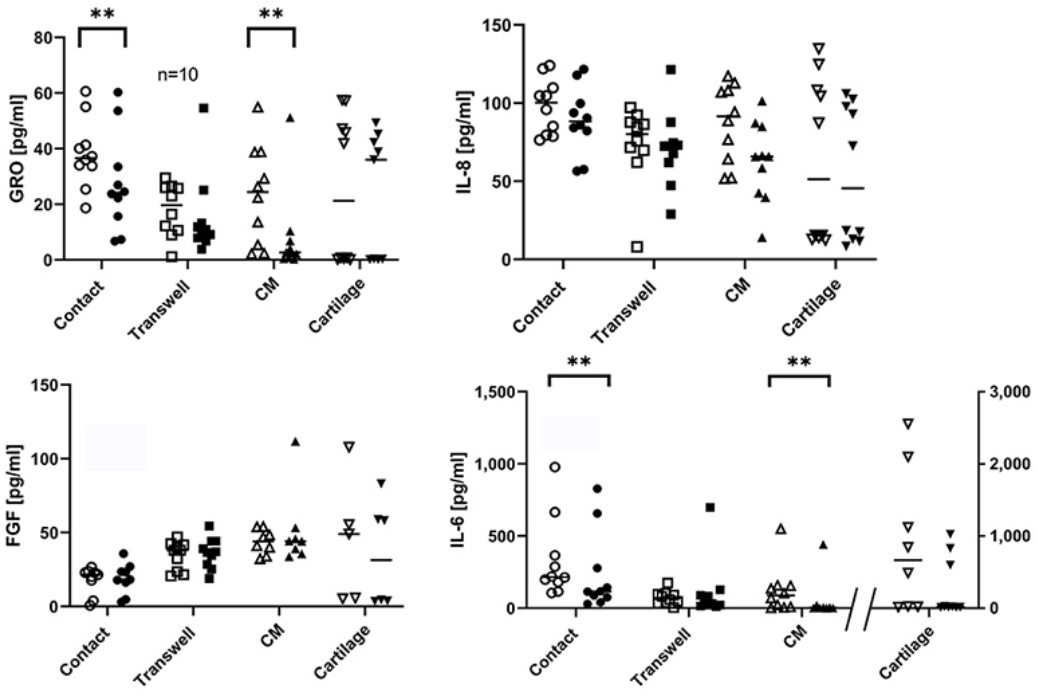

Figure 6. Cytokine concentrations measured by magnetic bead assay. Open shapes represent synovial cell (SC)/ mesenchymal stem cell (MSC co-cultures) and closed shapes represent synovial cell (SC)/dermal fibroblast (DF) co-cultures. When SC/MSC co-cultures and SC/DF co-cultures were compared, significantly increased growth-related oncogene (GRO) concentrations were observed in the conditions of contact (p= 0.002) and conditioned media (p= 0.007). Increased interleukin (IL-6) concentrations were observed in MSC co-cultures by Wilcoxon signed rank in the contact (p= 0.002) and conditioned media (p= 0.003) conditions. No significant differences were in interleukin-8 (IL-8) or fibroblastic growth factor (FGF) concentrations were observed between MSC and DF co-cultures.

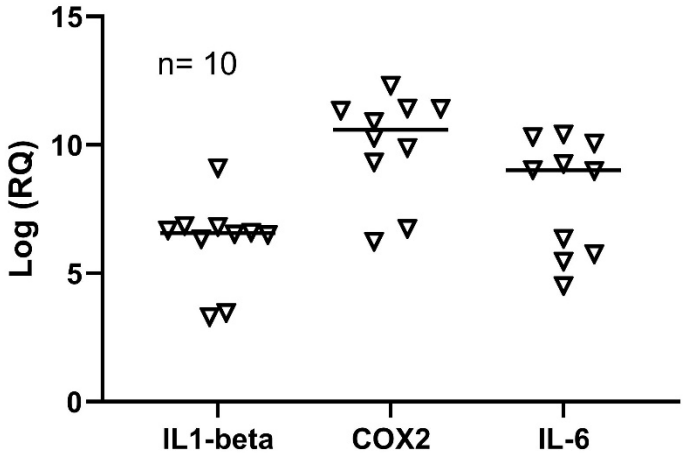

Figure 7. Relative quantification of gene expression. Steady state RNA levels (ΔΔ Ct, log transformed) of interleukin-6 (*IL-6*), cyclooxygenase-2 (*COX-2*) and interleukin 1-beta (*IL1-β*) in synovial cell (SC)/mesenchymal stem cell (MSC) cartilage co-cultures compared to SC/dermal fibroblast (DF) co-cultures as a control using glyceraldehyde 3-phosphate dehydrogenase (*GAPDH*) as a reference gene. In the SC/MSC co-culture, ΔCt values were higher than in the SC/DF co-culture (p= 0.002, Wilcoxon signed rank).

Cartilage integrity was not affected by IL-β exposure or proximity to MSCs or DFs

There was no significant difference in GAG loss (Figure 8), proteoglycan staining (Figure 9), or morphology (Figures 10, 11) in cartilage explants in co-culture with SCs and MSCs or DFs. This finding shows that a short incubation period with IL1-β did not result in substantial changes articular cartilage structure.

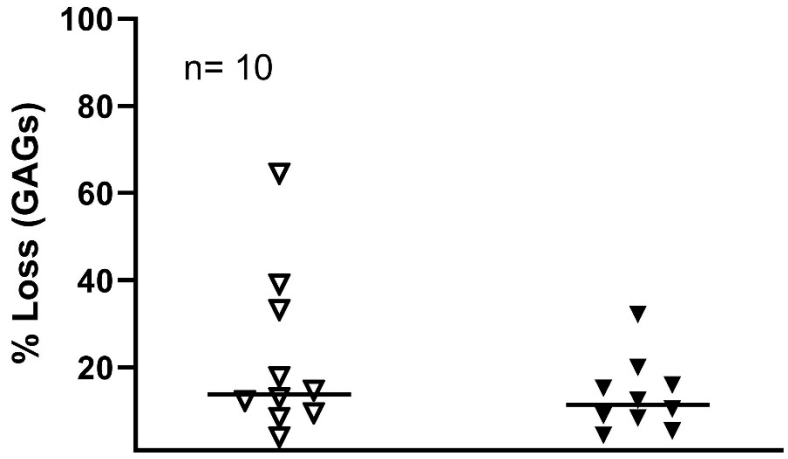

Figure 8. Percent loss of GAGs by cartilage explants. Dimethylmethylene blue (DMMB) assay was performed with cell culture supernatants and cartilage explants to evaluate proteoglycan loss by explants in culture after exposure to 10 ng/ml interleukin 1-beta (IL1-β). No significant difference (Wilcoxon signed rank) in sulfated glycosaminoglycan (GAG) loss was observed between synovial cell (SC)/mesenchymal stem cell (MSC) co-cultures (open triangles) compared to SC/dermal fibroblast (DF) co-cultures (closed triangles).

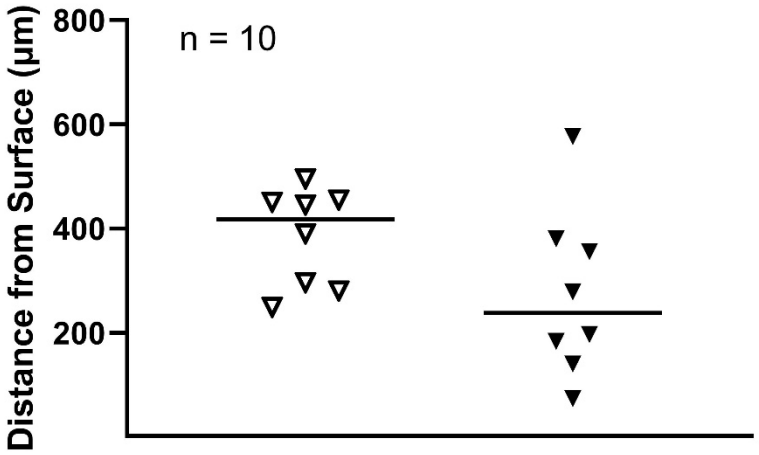

Figure 9. Cartilage histology: loss of Safranin O stain by cartilage explants. The distance from the articular cartilage surface to the margin of stain loss was visually determined by drawing a line at the interface of stain loss. The distance was measured in pixels from the center of the image at the surface of the cartilage to the line. There was no difference

(Wicoxon signed rank) in distances between synovial cell (SC)/mesenchymal stem cell (MSC) co-cultures (open triangles) compared to synovial cell SC/dermal fibroblast (DF) co-cultures (closed triangles).

Table 6. Modified Mankin Scoring System. Cartilage integrity was graded based on a modified scoring system based on proteoglycan staining with Safranin-O, chondrocyte morphology, and structure of the articular cartilage surface.

Table 2.3 Modified Mankin Scoring System					
Staining	**Score**	**Cells**	**Score**	**Structure**	**Score**
Uniform	0	Normal	0	Normal	0
Loss of staining into superficial zone	1	Small superficial clusters	1	Irregular surface/fissures	1
Loss of staining extending to middle zone	2	Clusters/cloning	2	Surface fissures into mid zone	2
Loss of staining extending > ½ middle zone	3	Hypocellularity	3	Surface fissures into deep zone	3
Loss of staining extending into deep zone	4			Complete disorganization	4

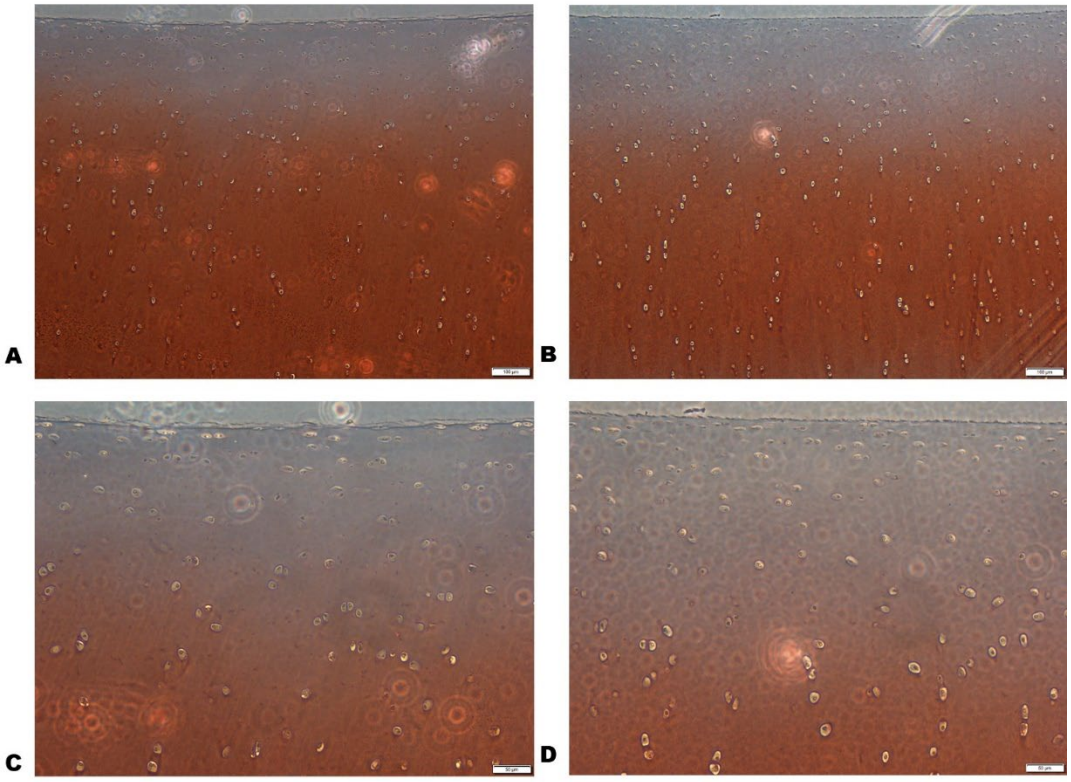

Figure 10. Cartilage Histology: Representative images of cartilage explants. Representative example of cartilage explants from mesenchymal stem cell (MSC) and dermal fibroblast (DF) co-cultures after tissue processing, sectioning, and staining with Safranin O and Fast green to visualize proteoglycan loss at the surface of the articular cartilage, chondrocyte morphology, and articular cartilage structure. (A) MSC co-culture at 100x magnification (B) DF co-culture at 100x magnification (C) MSC co-culture at 200x magnification (D) DF at 200x magnification.

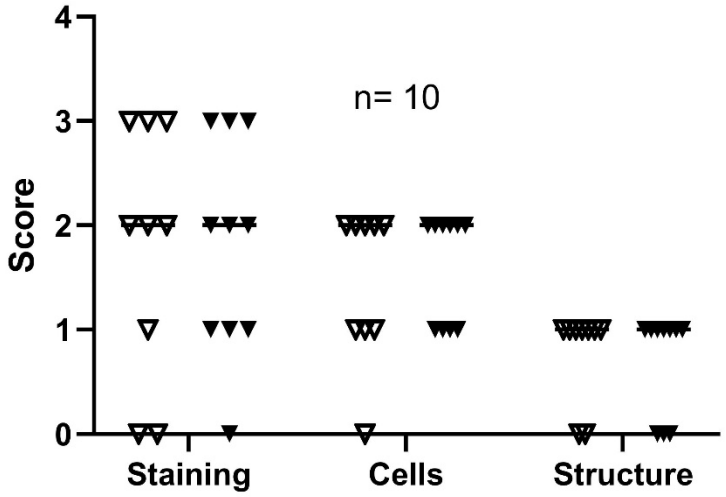

Figure 11. Cartilage Histology: Modified Mankin scores of cartilage explants. There were no differences (Wilcoxon signed rank) in loss of staining by visual observation into the superficial, middle or deep zones, chondrocyte clustering, cloning or hypocellularity and structure at the articular surface between synovial cell (SC)/mesenchymal stem cell (MSC) co-cultures (open triangles) compared to synovial cell SC/dermal fibroblast (DF) co-cultures (closed triangles).

Table 7. Cartilage histology scores. Modified Mankin scores of articular cartilage explants in mesenchymal stem cell (MSC) co-cultures (M) and dermal fibroblast (DF) co-cultures (F). Loss of stain at the surface, chondrocyte morphology and articular cartilage surface were evaluated to determine the effects of overnight incubation with synovial cells (10,000 cells/cm2), 10 ng/ml interleukin 1- beta (IL1-β) and either MSCs or DFs (5,000 cells/cm2) overnight.

Cartilage Histology Scores						
Horse	**Staining**		**Cells**		**Structure**	
	M	F	M	F	M	F
1	3	3	1	2	0	0
2	3	3	2	2	1	1
3	2	1	2	2	1	1
4	2	2	2	2	1	1
5	0	0	0	1	1	0
6	1	1	2	1	1	1
7	2	2	2	2	1	1
8	0	1	2	1	0	1
9	3	2	1	1	1	1
10	2	3	1	2	1	0

Table 8. Signalment of Horses from which Experimental cell lines were isolated.

Signalment: Experimental Cell Line Donors			
Horse ID	**Age**	**Breed**	**Sex**
1	2	QH	Mare
2	3	QH	Mare
3	3	QH	Mare
4	6	QH	Gelding
5	2	QH	Gelding
6	4	QH	Gelding
7	2	QH	Mare
8	4	QH	Mare
9	3	QH	Mare
10	4	QH	Gelding

Table 9. Signalment of cartilage donors. Each donor provided cartilage explants for two experiments.

Signalment: Cartilage Explant Donors			
Horse ID	**Age**	**Breed**	**Sex**
11	13	Hanoverian	Gelding
12	4.5	QH	Gelding
13	5	QH	Mare
14	4.5	QH	Mare
15	3	QH	Mare

Synovial cells, MSCs, and DFs communicate through juxtacrine signaling

Concentrations of PGE_2 were significantly higher in SC/MSC co-cultures compared to SC/MSC transwell co-cultures ($p= 0.002$). Concentrations of PGE_2 were also significantly higher in SC/DF co-cultures compared to SC/DF transwell co-cultures ($p= 0.002$) (Figure 5). Additionally, concentrations of IL-6 were significantly higher in

SC/MSC co-cultures compared to SC/MSC transwell co-cultures (p= 0.002, Figure 5) as well as in SC/DF co-cultures compared to SC/DF transwell co-cultures (p= 0.01, Figure 4).

Stimulation with IL1-β was required for SCs and MSCs to secrete IL-6 and PGE_2

Synovial and MSC monocultures in the presence of IL1-β (Figure 12) secreted significantly more PGE_2 (p= 0.004) and IL-6 (0.004) compared to unstimulated controls while DFs did not produce a significant amount of PGE_2, IL-6 or IL-10 in monoculture with or without IL1-β stimulation (control comparison to IL1-β not shown).

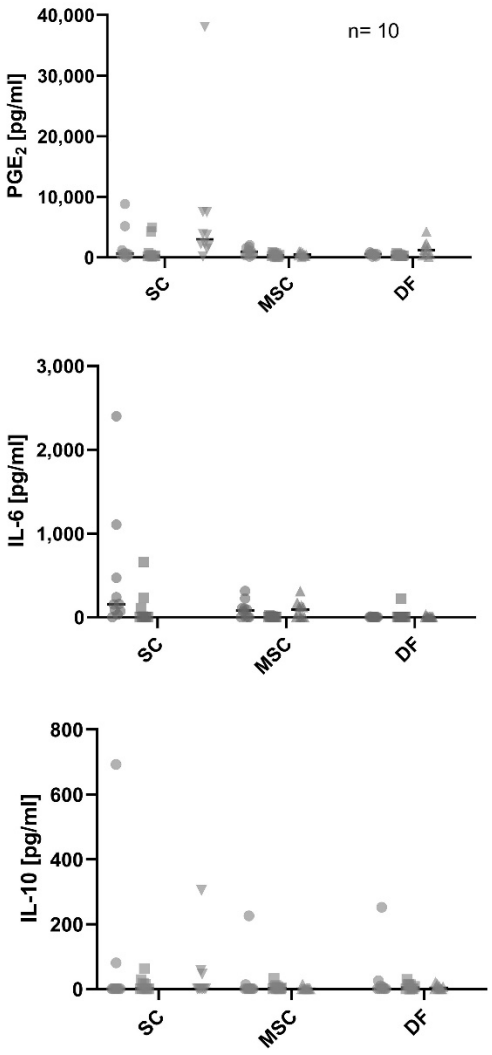

Figure 12. Monoculture cytokine concentrations measured by ELISA. Circles represent cells (SC = synovial cell, MSC = mesenchymal stem cells, DF = dermal fibroblasts) in the contact co-culture, squares represent cells from the transwell co-culture, triangles represent cells from the conditioned media (CM) condition and upside-down triangles represent cells from the cartilage co-culture. Cytokine production was measured by enzyme linked immunosorbent assay (ELISA) using the cell culture supernatants. SCs and mesenchymal stem cells MSCs secreted significantly more prostaglandin E2 (PGE_2) and interleukin-6 (IL-6) after exposure to 10 ng/ml interleukin 1-beta (IL1-β) and overnight co-culture compared to stimulated controls (Wilcoxon signed rank, SCs p= 0.004, MSCs p= 0.004)

Co-culture in contact and with cartilage amplified cytokine secretion by SCs, MSCs and DFs

Co-culture in the presence of cell-to-cell contact without cartilage resulted in significantly higher secretion of PGE_2 in SC/MSC co-cultures ($p= 0.002$) compared to the addition of SC and MSC monocultures while there was no significant difference in IL-6. No differences were detected in PGE_2 or IL-6 between the addition of SC and DF monocultures compared to SC/DF co-cultures, indicating that the effect was additive (data not shown). In the presence of cartilage explants however, PGE_2 was significantly increased compared to addition of monocultures in both SC/MSC ($p= 0.002$) and MSC/DF ($p= 0.02$) co-cultures (data not shown). To corroborate this finding, PGE_2 was significantly higher in SC/MSC cartilage co-cultures ($p= 0.004$) and SC/DF co-cultures ($p= 0.02$) compared to co-culture in contact but without cartilage (Figure 5).

Cell populations contain immune cells that may be responsible for secreting IL-6

Horse 3 had very low levels of CD45 expression on the surface of SCs, MSCs and DFs while horse 4 (high responder) had low levels of CD45 expression in SCs and DFs, but 24.2.5 CD45+ MSCs, indicating the presence of immune cells.

Table 10. Cell surface marker expression of CD45 in low responder and high responder

% Positive Cell Surface Expression of CD45			
Horse ID	SCs	MSCs	DFs
3 (high)	3.50	2.31	2.49
4 (low)	1.74	24.2	0.45

Discussion

Our overall goal is to better understand how MSCs function after they have been injected into a patient. We created an *in-vitro* model of the inflamed equine synovial joint and designed a series of experiments to investigate the secretory actions of both MSCs and synovial cells in direct and indirect co-culture. Early passage synovial cells (P1) were used in an effort to isolate synovial macrophages and fibroblasts due to the known importance of communication between cell types and macrophage activation in synovitis. Notably, the SC cell populations of both the low and high responding horses had very low CD45 expression, while the high responding horse had 24% CD45+ MSCs, which was unexpected. Immune cells within the MSC population likely influenced PGE_2 and IL-6 secretion, as macrophages are known to activate synovial fibroblasts to secrete pro-inflammatory cytokines. We found that MSC/DF contact with both synovial cells and chondrocytes affects the secretome of one or more cell types (synovial cells, chondrocytes, MSCs) in our model of synovitis, indicating the importance of juxtacrine signaling in cellular communication during inflammation.

To confirm that our synovitis model mimics inflammation, IL1-β expression was upregulated in the cartilage co-culture (Figure 7). Continued presence of IL1-β in the inflamed synovial joint is known to contribute to the infiltration of synoviocytes that produce pro-inflammatory cytokines resulting in joint destruction (77). These results support the use of IL1-β in an *in-vitro* model of synovitis.

After exposure to inflammatory cytokine IL-1β in combination with MSCs in co-culture, all conditions of contact induced increased PGE_2 production, indicating a robust

response to inflammatory stimulation. In both SC/MSC and SC/DF co-cultures, IL-β treated cells secreted significantly more PGE_2 than unstimulated controls, indicating that DFs have secretory/stimulatory activity and may not serve as an appropriate control for this model. In accordance with the present results, previous studies have demonstrated that DFs have immunomodulatory capability (78) (79). However, this study did provide evidence that secretion between MSCs and DFs is not identical, proving that further research is needed to determine the immunomodulatory behavior of both cell types. Because our data shows significantly increased gene expression and cytokine (PGE_2, IL-6) secretion in MSC co-cultures compared to DF, it is likely that MSCs have increased immunomodulatory capability. In OA synoviocytes, PGE_2 production is increased by stimulation with IL1-β (80), which was confirmed by secretion of PGE_2 regardless of contact. Gene expression of pro-inflammatory cytokines corroborated with protein production as evidenced by cell culture supernatant data. Significantly higher *COX2* ΔCt values in the SC/MSC cartilage co-culture should be expected with high PGE_2 production. In horses, synovitis has been induced with IL1-β, leading to secretion of PGE_2, which is consistent with our findings (81).

We discovered that IL-6 secretion increased when synovial cells and MSCs were in close contact and that the addition of chondrocytes significantly amplified PGE_2 and IL-6 production by synovial cells and/or MSCs. This finding was reflected by upregulation of *IL-6* and *COX2* in the SC/MSC co-culture. It is known that IL-6 is present in arthritic joints and has a role in the changes between acute and chronic inflammation (82) and has been shown to inhibit proteoglycan synthesis (83). Other

studies have shown that it is present in the synovial fluid of patients with osteoarthritis (84) and rheumatoid arthritis (85). Our data provides further evidence that IL-6 secretion is triggered in the presence of pro-inflammatory cytokines and provides evidence for juxtacrine signaling through contact based on significant differences between co-cultures in contact and transwell co-cultures. While regenerative/reparative properties of MSCs are thought to result from immune modulation, we observed a pro-inflammatory environment with the addition of MSCs and DFs. This finding reflects early inflammation, and it is possible that an increase in pro-inflammatory cytokines may lead to a switch of macrophage polarization to an anti-inflammatory phenotype which was not observed during the short incubation period. A previous study in horses did not detect IL-6 in equine SCs co-cultured with injured cartilage (not in direct contact) (86). While the authors suggest that the fibroblastic, rather than macrophage phenotype may have contributed to their findings, a transwell membrane was used to separate the cells from the cartilage explant, indicating that contact plays a vital role in cellular communication. Additionally, cells were not stimulated with IL1-β, but rather the cartilage explant was mechanically injured prior to co-culture. Both aspects likely contributed to the lack of IL-6 secretion by SCs. In our model, it is possible that the cartilage explants mimicked injured cartilage rather than healthy cartilage, triggering a pro-inflammatory environment.

Interestingly, IL-6 production was not significantly different from the unstimulated control in the transwell MSC or DF co-culture, but significant differences were noted the CM co-culture ($p= 0.007$). This leads to the conclusion that some IL-6

may be packaged in vesicles that are larger than the pore size of the transwell membrane. Some EVs are known to be up to 1,000 nm in diameter (87) and the transwell pore size (400 nm) would prevent some of the larger vesicles from reaching the cells beneath the membrane, thus preventing the exchange of soluble factors. It is likely that IL-6 is packaged in both larger and smaller vesicles. This may explain the differences in responses to CM, which contain everything released by synovial cells and suggests paracrine signaling through vesicles. However, further support for the role of contact in IL-6 production is provided by a study that found positive regulation of *IL-6* expression by Notch, a juxtacrine signaling protein, in macrophages through NFκB (88). In the current model, synovial cells were cryopreserved within days of isolation to capture a population of both macrophages and fibroblasts, which would be in conjunction with the latter study. In combination, these studies demonstrate that both paracrine and juxtacrine signaling occurred between cells in the current model of synovitis.

In the literature, there have been some inconsistencies as to the necessity for contact to generate or amplify a signal. Some research has shown that direct contact is not required for suppression of T-cell proliferation by bone marrow stromal cells (89), indicating the possibility that soluble factors were solely responsible for the response. However, T cell suppression does not equal immune modulation. Crosstalk between signaling pathways has a tremendous effect on inflammatory signaling cascades. There appears to be more evidence that contact is important in cell-to-cell communication, but paracrine signaling plays a significant role as well (47). In the transwell and CM formats of our study, there was little to no cytokine production, indicating the importance for

contact. However, there is evidence of the importance of paracrine activity based on secretion of PGE_2 regardless of contact (Figure 4)

We found that the addition of chondrocytes increased secretion of IL-10. In the contact condition however, there was no difference in IL-10 secretion by MSC or DF co-cultures while CM and transwell co-cultures were significantly higher. The addition of chondrocytes reversed that effect. Contrary to our expectation that MSCs would secrete IL-10 to modulate inflammation, our findings demonstrate that SCs in contact with DFs and chondrocytes secrete more IL-10 than SCs in contact with MSCs and chondrocytes. Previous research has shown that MSCs pre-treated with IFN-γ suppress secretion of IL-10 by activated B cells in a contact-dependent manner through PGE_2 (90). Similar contact-dependent suppression could explain the lower concentration of IL-10, especially because PGE_2 secretion was high which was in accordance with the previous authors' findings that higher PGE_2 concentrations were required for suppression. Although cells in the current model were treated with IL1-β, a similar effect could be induced by other cytokines. Additionally, IL-10 has been shown not to exert chondroprotective effects on chondrocytes stimulated with IL1-β (91). Both studies provide support for the low production of IL-10 in our model. As mentioned, it has been proposed that DFs and MSCs may not be different based on their identical phenotypes (92), similar surface immunophenotype, proliferation and immunomodulation by both cell types (78). Although this creates some difficulty in drawing conclusions from differences between SC/MSC and SC/DF co-cultures, their immunomodulatory properties are likely tailored to their location and age, and we demonstrated that their

secretory behavior is in fact different. Our model demonstrates increased secretory activity in the presence of chondrocytes and possible inhibition of IL-10 through juxtacrine signaling.

We found that GRO secretion was affected by contact because GRO was increased in the SC/MSC contact condition. It was also significantly higher in the CM condition, showing that paracrine signaling plays a role in cellular communication in this model. The TAK/NFκB pathway, which is important for immunomodulation, has been shown to be activated by GRO (93). Although there was no difference in secretion by SC/MSC and SC/DF co-cultures, secretion was measurable in all conditions of contact, indicating paracrine based immunomodulation by GRO secretion.

We found that stimulation with IL1-β resulted in increased secretion of FGF and IL-8 which was not affected by contact. Low levels of FGF and IL-8 were detected in the culture supernatant, indicating production/secretion during the incubation period, but there were no differences in secretion between co-cultures of SCs with MSCs or DFs. Endogenous MSC recruitment has been shown to be enhanced by IL-8 (94), which has also been shown to enhance osteogenesis and chondrogenic differentiation (95). MSC secretion of FGF has been shown to promote proliferation of OA chondrocytes in co-culture (96). In our model, cells and explants were treated with IL1-β, which initiates the inflammatory response in OA. Although we did not measure proliferation of chondrocytes, secretion of FGF is supported by these findings. Secretion of IL-8 and FGF by co-cultures in this model supports the idea that MSCs have immunomodulatory capability and it is likely that low levels of secretion are due to limited incubation time.

We showed that a short period of inflammation does not result in substantial loss of proteoglycans by cartilage explants. In inflammatory arthritis, synovial cells secrete pro-inflammatory cytokines such as IL-6, PGE_2 and IL-8 in response to inflammatory stimulation which initiates the cascade of cartilage degradation. These pathways participate in normal joint homeostasis but become hyperactive in inflammation, which ultimately leads to irreversible damage over time (97). In osteoarthritis, extended inflammation leads to degradation of the extracellular matrix leading to changes in cartilage integrity (15). Thus, the results of this study are not surprising as cartilage damage that occurs during the progression of OA does not occur in the initial stages of synovitis. Although a longer incubation period may result in more dramatic changes to cartilage integrity, the lack of proper *in-vivo* environment would likely influence results based on cartilage integrity due to necrosis of the explant tissue. Cells are likely to migrate out of the explant and attach to the culture dish, further influencing morphology-based results.

While it is clear that the cellular secretome is affected by contact with local cells, some limitations exist. The benefits of *in-vitro* models, however, allow examination of individual hypotheses that build upon each other through successive experiments. Luminex data was split between two plates which potentially affected the comparisons of cytokine data between horses. While each horse's cells were contained on the same plate, it is difficult to compare data of horses from the two separate plates, as assay sensitivity may have affected interpolation of standard curves. While our efforts were to best mimic the natural joint environment, this *in-vitro* model of synovitis lacks some of

the essential components of the equine articular joint, such as synovial fluid. Future experiments should investigate the addition of synovial fluid to further mimic the joint environment. Paracrine signaling in this model may have been affected by the co-culture model and use of transwell membranes may have prevented complete exchange of signals, but there is increasing consensus that contact between synovial cells, and MSCs is required for MSC immunomodulatory function in joint disease and repair (58) (98).

Our results support previous findings that EVs play a role in MSC immunomodulation (99) (56), further warranting future studies with MSC derived EVs. Taken together, our findings demonstrate that communication between chondrocytes, synovial cells and MSCs involves both juxtacrine and paracrine signaling. This model may be used to further study MSC function during early inflammation.

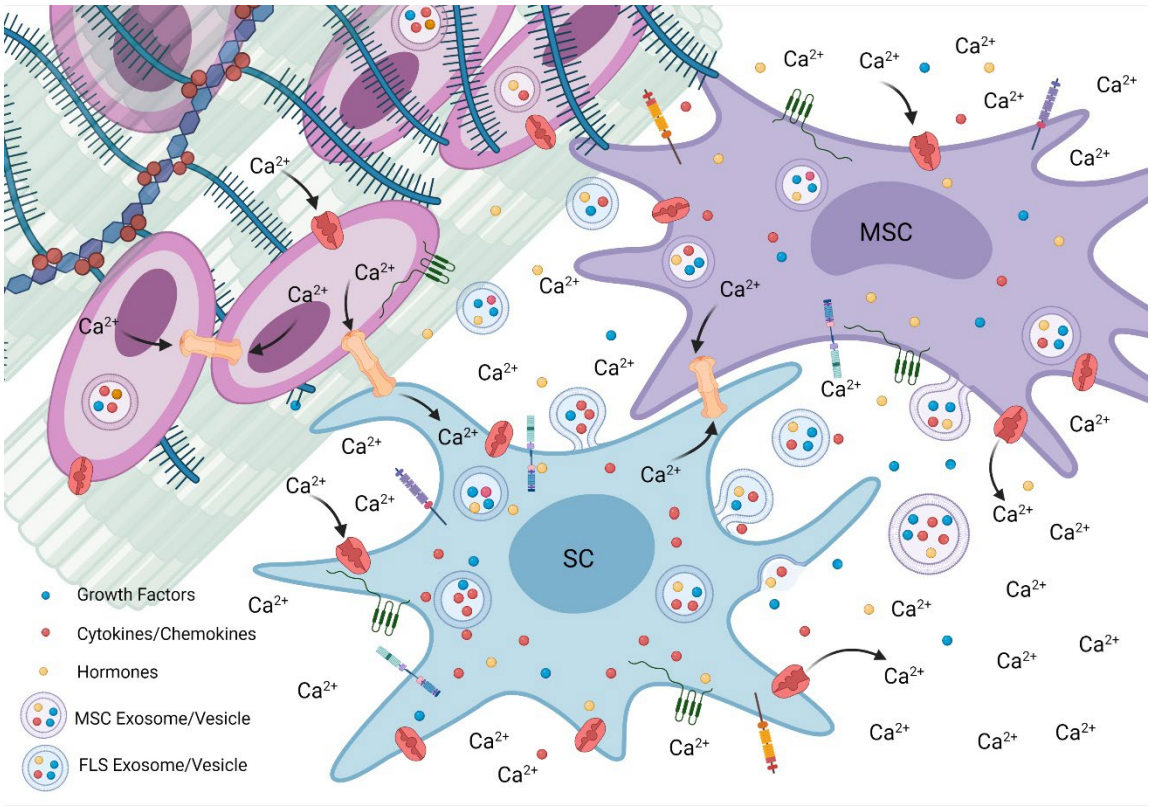

Figure 13. Juxtacrine and paracrine signaling between chondrocytes, SCs and MSCs. In direct contact, synovial cells (SCs) and mesenchymal stem cells (MSCs) exchange intracellular calcium through Notch signaling, gap junctions (yellow) and transport proteins (red) while growth factors, hormones and cytokines are exchanged through endocytosis and exocytosis of extracellular vesicles (EVs). Each cell type is shown with cell surface markers (CD 90, CD 44, VCAM), Notch signaling proteins, integrins in open and closed configurations and connexin 43 (green) for the formation of gap junctions between cells. Created with BioRender.com

Our group has previously shown that horses injected with haplotype matched MSCs increased endogenous progenitors in the joint compared to mismatched haplotypes, demonstrating that immunomodulation is working through paracrine mechanisms rather than cell replacement (50). From this study, we conclude that contact

is important for comprehensive communication between SCs, chondrocytes and MSCs in a controlled simulation of early inflammation. This leaves much potential for expansion on this work to further unravel the mechanism by which MSCs modulate inflammation. Further research is required to examine how MSCs function in a pro-inflammatory environment over time, eventually participating in tissue repair and regeneration.

CHAPTER III

TESTING THE USE OF SYNOVIAL FLUID IN A MODEL OF SYNOVITIS

Introduction

It is well established that osteoarthritis (OA) is common in both humans and horses and *in-vitro* studies are utilized to better understand disease progression and develop new therapies with the goal of tissue repair and regeneration. Cellular and cell-free therapies utilize MSCs and their secretions for this purpose, as they are associated with improved tissue repair and immunomodulation.

Before the progression to OA, synovitis occurs due to overloading the joint or changes within the microenvironment of the joint due to age or trauma. Synovitis in the articular joint triggers synovial cells to secrete enzymes that degrade and cause irreversible damage to the articular cartilage.

A widely accepted model to accurately mimic the equine synovial joint *in-vitro* is not available, so we tested several different formats in Chapter II to compare the juxtacrine and paracrine secretions of equine SCs with cartilage explants and MSCs or DFs. Our preliminary model demonstrated that MSC contact with synovial cells and chondrocytes increased immunomodulatory signaling, which is thought to be the mechanism by which MSCs contribute to tissue repair and regeneration. Although there is an increasing trend towards utilizing the MSC secretome and EVs as therapeutics, Notch signaling pathways and gap junctions are inaccessible to the synovial cells and chondrocytes due to lack of contact with MSCs. Intercellular communication through

Notch signaling (38) and gap junctions (100) (40) (41) occurs in homeostasis and inflammatory arthritis, which is consistent with or findings. The goal in our synovitis model was to mimic the inflamed equine joint as accurately as possible *in-vitro*. We also discovered that the presence of chondrocytes amplified secretory activity significantly. In our previous model, however, an important anatomical component, synovial fluid, was missing.

To further investigate the mechanisms of immunomodulation, we added synovial fluid instead of IL1-β from healthy and inflamed equine joints to the cartilage co-culture condition. Physiological concentrations of IL1-β in inflamed joints are under 0.5 ng/ml (101). Throughout the literature however, high concentrations are used for *in-vitro* studies (102) (80) (103) (104) (72). We hypothesized that synovial fluid from inflamed equine joints containing a combination of cytokines at different concentrations would more accurately mimic natural inflammation.

The objective of this study was to test our preliminary model of the equine joint with the addition of synovial fluid instead of IL1-β to better understand how MSCs function in synovitis. We found that healthy synovial fluid increased cytokine production compared to hyaluronic acid.

Methods

Experimental model

The experimental model (Figure 14) consisted of three conditions of direct co-culture with MSCs or DFs seeded on top SCs with the addition of a cartilage explant

and: (1) Hyaluronic acid (HA) (2) Healthy pooled donor synovial fluid (SFh) (3) Healthy donor pooled inflamed synovial fluid (SFi). Cells were lysed and stored for RNA isolation and gene expression analysis.

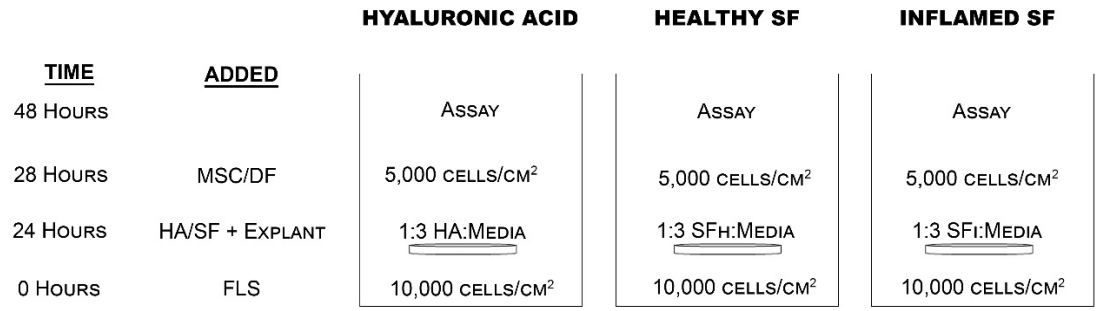

Figure 14. Experimental Model: Synovial fluid co-culture. Cells were harvested from the metacarpophalangeal joints and clean incision areas. Bone marrow was harvested from the sternum. Synovial cells (SCs), dermal fibroblasts (DFs) and mesenchymal stem cells (MSCs) were cryopreserved and later seeded onto 6 well plates. After overnight recovery, the cells were exposed to healthy donor pooled synovial fluid (SFh) or inflamed donor pooled synovial fluid (SFi) before addition of MSCs or DFs or no cells (not shown). Following treatment and overnight culture, media and cell lysates were collected and stored for future assays.

Cartilage Explants and Synovial Fluid

Cartilage explants and synovial fluid were collected from 5 horses that were euthanized for reasons unrelated to this study and previously described in Chapter 2. Synovial fluid was aseptically aspirated from the carpal joints and stifle joints (femorotibial, femoropatellar- middle, lateral, medial). Each donor horse provided explants for two co-culture experiments.

Assays

ELISA on cell culture supernatants, RT-qPCR on cartilage explants, DMMB assay on cell culture supernatants and cartilage explants and, and histology on cartilage explants (Modified Mankin Scoring, distance proteoglycan stain (Safranin O) loss were performed as in Chapter 2.

Statistical Analysis

All statistical analyses and graphs were created using GraphPad Prism software.

Data from MSC and DF co-cultures in all assays were compared using paired Wilcoxon Signed Rank: Cytokine (PGE_2, IL-6 and IL-10) concentrations between SC monoculture and MSC or DF co-cultures and between MSC and DF co-cultures ,ΔCt values between SC monoculture and MSC or DF co-cultures and between MSC and DF co-cultures, distances of Safranin O stain loss between SC monoculture and MSC or DF co-culture cartilage explants and between MSC and DF co-culture explants, modified Mankin scores between SC monoculture and MSC or DF co-cultures and between MSC and DF co-cultures, and percent loss of GAGs between SC monoculture and MSC or DF co-cultures and between MSC and DF co-cultures.

Results

We observed increased PGE_2 production by SC monocultures and SC/DF co-cultures compared in the presence of SFh compared to HA (Figure 15) PGE_2 concentrations (negative values are due to subtraction of baseline).

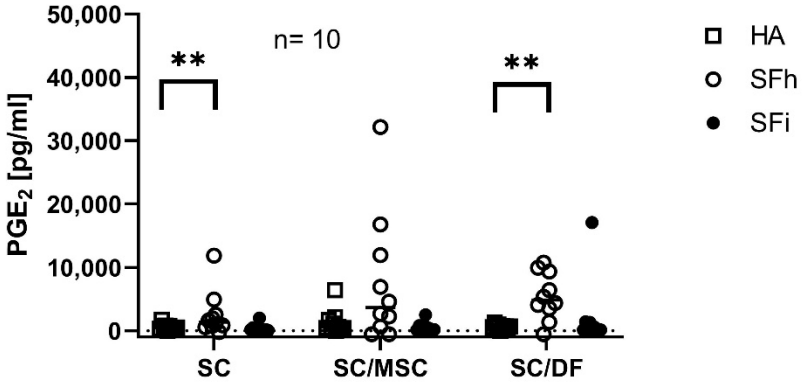

Figure 15. Prostaglandin E_2 (PGE_2) Production by synovial cells (SCs) and chondrocytes. Squares represent hyaluronic acid (HA), open circles represent healthy synovial fluid (SFh) and closed circles represent inflamed synovial fluid (SFi). Cytokine production was measured by enzyme linked immunosorbent assay (ELISA) using the cell culture supernatants. Increased PGE_2 production was observed (Wilcoxon signed rank) by SC monocultures ($p= 0.009$) and SC/DF co-cultures ($p= 0.005$) in the presence of healthy donor pooled synovial fluid (SFh) compared to hyaluronic acid (HA).

No significant differences were observed in IL-6 production between SC monocultures and either SC/MSC co-cultures or SC/DF co-cultures (Figure 16).

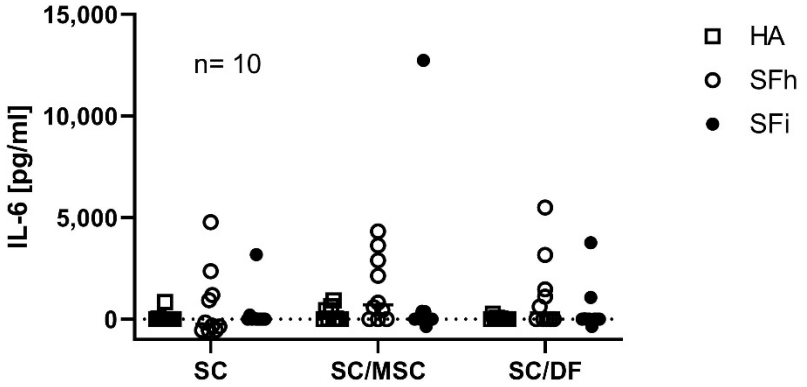

Figure 16. Interleukin-6 (IL-6) Production by synovial cells (SCs) and chondrocytes. Squares represent hyaluronic acid (HA), open circles represent healthy synovial fluid

(SFh) and closed circles represent inflamed synovial fluid (SFi). Cytokine production was measured by enzyme linked immunosorbent assay (ELISA) using the cell culture supernatants. There were no significant differences (Wilcoxon signed rank) between IL-6 concentrations between synovial cell (SC) monoculture and mesenchymal stem cell (MSC) or dermal fibroblast (DF) co-cultures or between SC/MSC and SC/DF co-cultures.

No significant differences were observed in IL-10 production between SC monocultures and either SC/MSC co-cultures or SC/DF co-cultures (Figure 17).

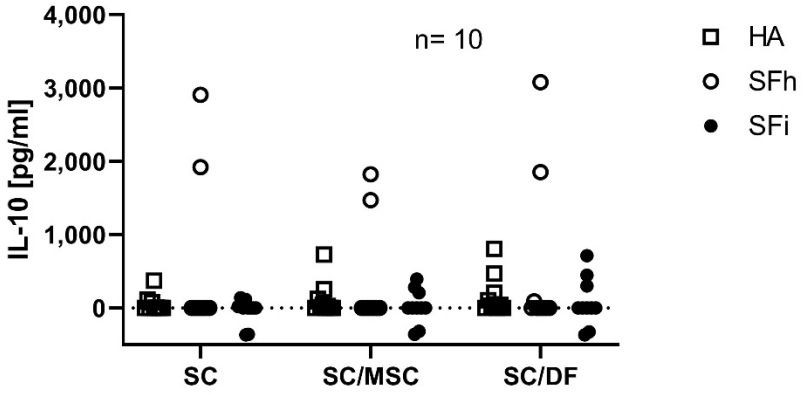

Figure 17. Interleukin-10 (IL-10) Production by synovial cells (SCs) and chondrocytes. Squares represent hyaluronic acid (HA), open circles represent healthy synovial fluid (SFh) and closed circles represent inflamed synovial fluid (SFi). Cytokine production was measured by enzyme linked immunosorbent assay (ELISA) using the cell culture supernatants. There were no significant differences (Wilcoxon signed rank) between IL-10 concentrations between synovial cell (SC) monoculture and mesenchymal stem cell (MSC) or dermal fibroblast (DF) co-cultures or between SC/MSC and SC/DF co-cultures.

Expression of *COX2* ($p= 0.002$) and *IL-6* ($p= 0.004$) were significantly increased in SCs exposed to SFh compared to HA (Figure 18). No differences in IL1-β expression were observed between HA and SFh or SFi.

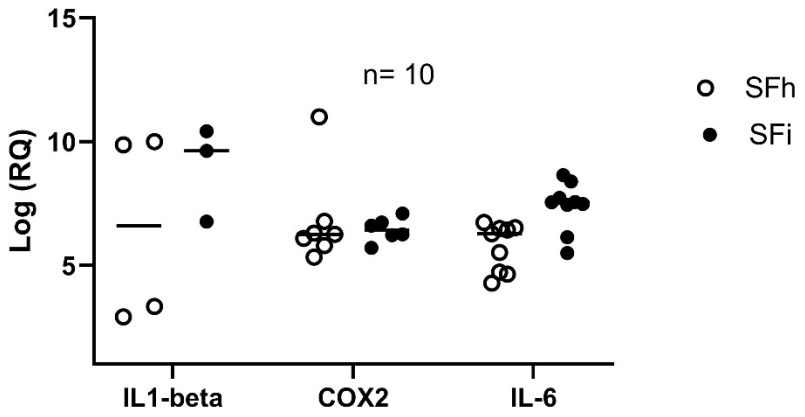

Figure 18. Steady state RNA levels of *IL1-β*, *COX2* and *IL-6*. Open circles represent healthy pooled donor synovial fluid (SFh) and closed circles represent pooled inflamed synovial fluid (SFi). Relative quantification of (ΔΔ Ct, log transformed) of interleukin-6 (*IL-6*), cyclooxygenase-2 (*COX-2*) and interleukin 1-beta (*IL1-β*) in synovial cell (SC) monocultures exposed SFh or SFi compared to hyaluronic acid (HA) control using glyceraldehyde 3-phosphate dehydrogenase (*GAPDH*) as a reference gene. *COX2* (p= 0.002) and *IL-6* (p= 0.004, Wilcoxon signed rank) were significantly upregulated in SFh compared to hyaluronic acid (HA).

There were no significant differences percent GAG loss (Figure 19), modified Mankin scores (Figure 22), distance between cartilage surface and the margin of stain loss (Figure 21) between SC/cartilage cultures exposed to HA, SFh or SFi.

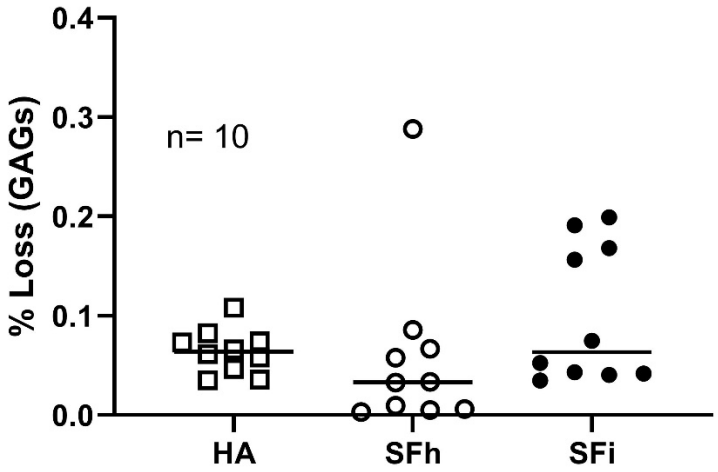

Figure 19. Percent loss of glycosaminoglycans (GAGs) by cartilage explants. Squares represent hyaluronic acid (HA), open circles represent healthy synovial fluid (SFh) and closed circles represent inflamed synovial fluid (SFi). Dimethylmethylene blue (DMMB) assay was performed with cell culture supernatants and cartilage explants to evaluate proteoglycan loss by explants in culture after exposure healthy donor pooled synovial fluid (SFh) or inflamed donor pooled synovial fluid (SFi). No significant difference was observed between synovial cell (SC) monoculture and mesenchymal stem cell (MSC) or dermal fibroblast (DF) co-cultures.

Figure 20. Cartilage explant histology images. Representative example of cartilage explants from mesenchymal stem cell synovial cell (SC) monocultures after tissue processing, sectioning, and staining with Safranin O and Fast green to visualize proteoglycan loss at the surface of the articular cartilage, chondrocyte morphology, and articular cartilage structure in SC monocultures exposed to hyaluronic acid (HA, A) donor pooled healthy synovial fluid (SFh, B) or donor pooled inflamed synovial fluid (SFi, C) at 200x magnification

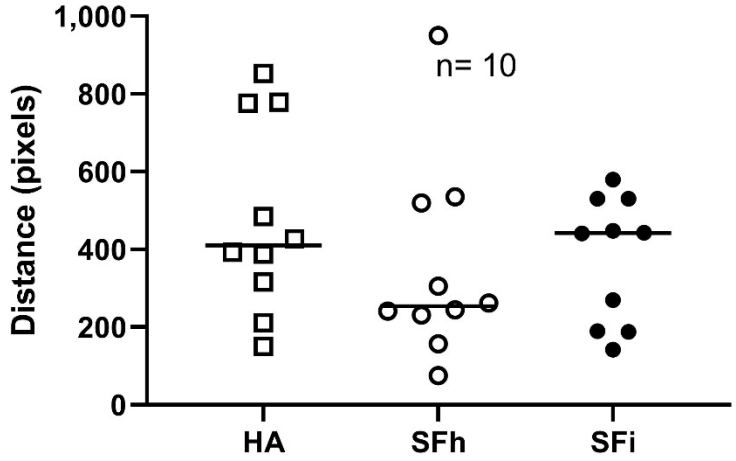

Figure 21. Cartilage Histology: Distance of proteoglycan stain (Safranin O) loss. Squares represent hyaluronic acid (HA), open circles represent healthy synovial fluid (SFh) and closed circles represent inflamed synovial fluid (SFi). The distance from the articular cartilage surface to the margin of stain loss was visually determined by drawing a line at the interface of stain loss. The distance was measured in pixels from the center of the image at the surface of the cartilage to the line. There were no differences in distances between synovial cell (SC) monoculture and mesenchymal stem cell (MSC) or dermal fibroblast (DF) co-cultures.

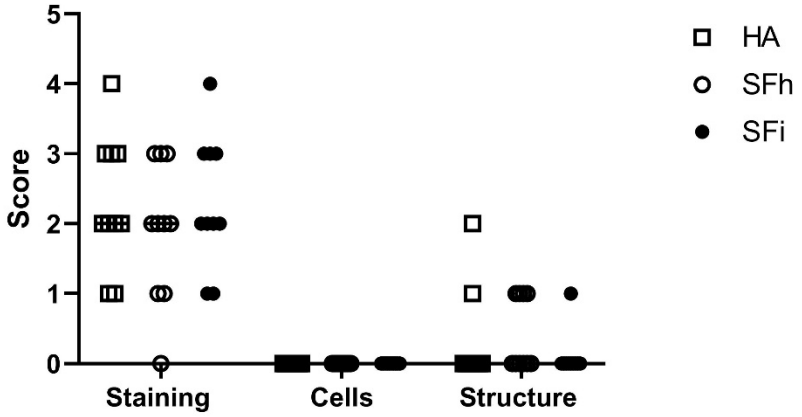

Figure 22. Cartilage Histology: Modified Mankin scores. Squares represent hyaluronic acid (HA), open circles represent healthy synovial fluid (SFh) and closed circles represent inflamed synovial fluid (SFi). There were no differences in loss of staining by visual observation into the superficial, middle or deep zones, chondrocyte clustering, cloning or hypocellularity and structure at the articular surface between synovial cell

(SC) monoculture and mesenchymal stem cell (MSC) or dermal fibroblast (DF) co-cultures exposed to healthy donor pooled synovial fluid (SFh) or inflamed donor pooled synovial fluid (SFi).

Discussion

In this study, we aimed to build on and compliment the previous co-culture *in-vitro* model with a more physiological inflamed joint microenvironment by using inflamed synovial fluid to induce inflammation. We tested the response of MSC or DF/cartilage explant/SC co-cultures and SC/explant monocultures with the addition of healthy synovial fluid, inflamed synovial fluid, and HA. PGE_2 was significantly increased in the SC monocultures and MSC/DF co-cultures in the presence of healthy SF relative to HA. There were no significant changes in *IL1-β*, *IL-6* or *COX2* RNA expression levels between healthy and inflamed synovial fluid. There was significantly higher PGE_2 production by SC monocultures and SC/DF co-cultures in the presence of SFh compared to HA, indicating some response to the healthy joint microenvironment. Our findings are consistent with the known role of PGE_2 in joint homeostasis, but it is unclear why the MSC co-culture response was not as pronounced. Perhaps it was due to MSC modulation of PGE_2 in the presence of SFh.

There were no significant differences in cartilage integrity between healthy and inflamed synovial fluid. This data suggests that the concentration of cytokine was too low or the incubation time too short to elicit a response. Furthermore, the data could also have been influenced by degradation of the inflamed SF by proteases during storage or transport. Additionally, preliminary experiments performed for the optimization of the model in chapter 2 (data not shown) demonstrated very little cytokine production in

response to 1.25 ng/ml IL1-beta, which is closer to the physiologic concentration of an inflamed equine joint. We suspected that the combination of cytokines present during inflammation may be necessary to better mimic inflammation, but overall, there was little response to adding synovial fluid to the cultures.

We also observed an interesting phenomenon while culturing the cells with the healthy donor synovial fluid. The cells in culture appeared to undergo increased cell death and morphological changes when SFh was added (Figure 23). This phenomenon was likely a major contributor to the lack of response to the synovial fluid among the aforementioned issues. This phenomenon was not observed in the previous co-culture models in chapter 2. These results suggested that there was an entity within the synovial fluid that was causing cytotoxicity to the MSCs. We suspected that this entity in the synovial fluid was an antibody within the SF that was causing cytotoxicity. The use of an autologous replacement to FBS could be of benefit since it would not contain bovine proteins and only equine proteins. Also, depletion of IgG from the synovial fluid could remedy cytotoxicity if it is being driven by an antibody. Future studies are needed to investigate the cause of cytotoxicity from the addition of SF to the cultures and alternatives to FBS.

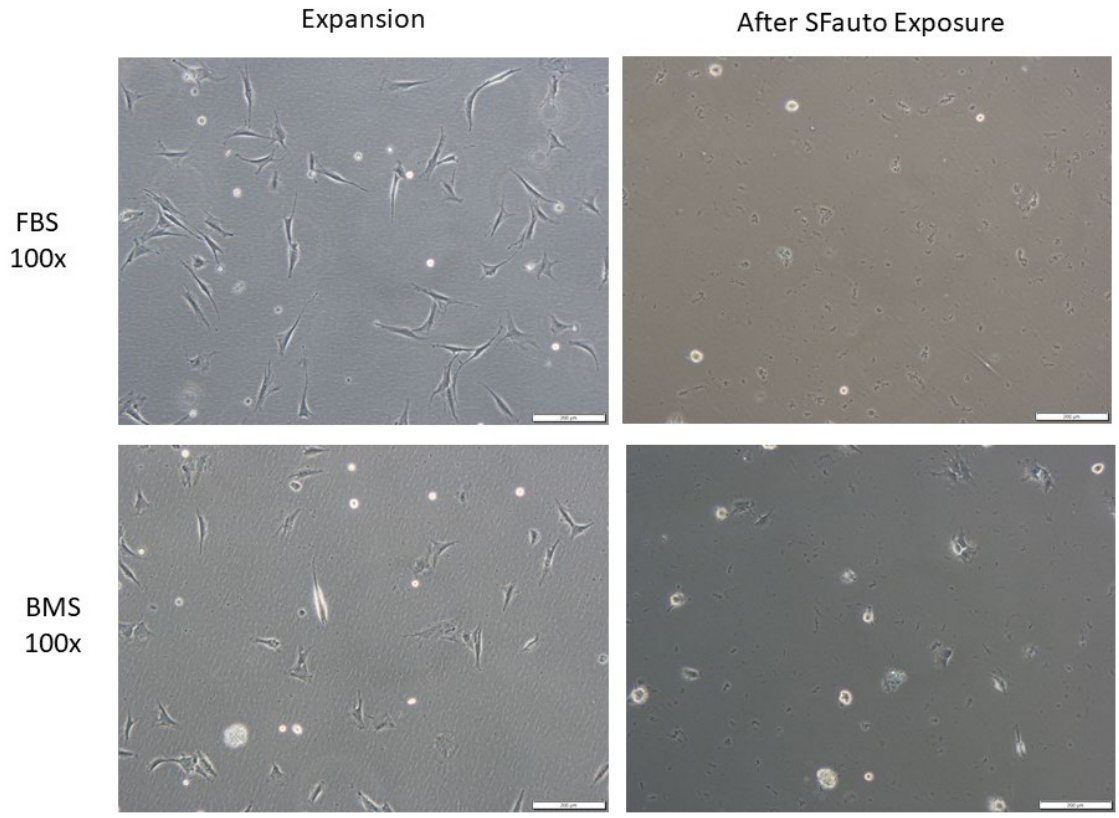

Figure 23. Images of BMS and FBS supplemented SCs before and after exposure to autologous synovial fluid at passage 2. Cells were plated, allowed to recover overnight, then exposed to autologous synovial fluid. After 24 hours, poor morphology and cell death were observed.

CHAPTER IV

DETECTION OF BOVINE SERUM ALBUMIN IN EQUINE MSCS GROWN IN FETAL BOVINE SERUM

Introduction

Cellular therapies are currently being used to treat a myriad of diseases despite the lack of understanding of the mechanisms of tissue repair and challenges associated with cellular expansion and application. While allogeneic therapy has been associated with positive outcomes (64), these therapies require the use of xenogeneic culture supplements for the expansion of cells. Fetal bovine serum (FBS) is the standard supplement for cell culture, as it contains proteins and growth factors that support the expansion of cells. However, xenogeneic proteins are taken up by the cells, leading to recognition by the host immune system and possible hypersensitivity. Additionally, xenogeneic proteins are recognized as antigens, presented on MHCI molecules, targeting the MSCs for lysis.

Hypersensitivity reactions after vaccination have been documented in horses and BSA specific immunoglobulin E (IgE) has been identified in horses after vaccination (105). Some horses produce excessive IgE after each vaccination, creating a higher risk for severe allergic reactions as the horse ages (106). Although the percentage of horses with this response is relatively small, it contributes to the need for a suitable replacement for FBS in therapeutic MSC culture.

Recent data from our lab demonstrated that MSCs supplemented with FBS during expansion do not survive in the joint cavity (33). Moreover, the addition of SF to the MSC/DF and SC co-cultures resulted in decreased cell viability and morphology changes. These observations suggest that there a factor in the synovial fluid that leads to toxicity of injected MSCs.

Previous data from our group demonstrated that MSCs supplemented with FBS throughout the culture period can uptake and store bovine proteins from the FBS resulting in inflammation after intra-articular injection and antibody-mediated cytotoxicity (34) (33) . Furthermore, our lab successfully developed an autologous replacement for FBS (BMS) with equal growth potential without causing inflammation and MSC rejection in the joint after intra-articular injection (33).

The cytotoxicity observations from the SF/co-culture and the FBS supplementation data suggest that the mediator of cytotoxicity within the SF is an antibody with specificity toward bovine proteins. Therefore, we hypothesize that MSCs grown in FBS endocytose bovine proteins, such as BSA, during expansion in culture and these bovine proteins are recognized by antibodies within equine serum or SF resulting in inflammation and cytotoxicity.

We were subsequently able to detect and purify an anti-BSA antibody from equine serum and show that MSCs grown in FBS were able to exocytose BSA into chemically defined media containing no albumin. We were also able to demonstrate that the anti-BSA antibody was eliciting cytotoxicity through complement-assisted antibody-directed complement cytotoxicity. Therefore, these data indicate that equine cells take up

bovine proteins during laboratory expansion in culture, and exposure to antibodies present in equine serum may lead to cellular cytotoxicity, negatively affecting the efficacy of MSC treatment and the use of equine cells in laboratory experiments. We propose the use of BMS for the culture expansion of equine cells for therapeutic use or research.

Data from chapter 3 also indicated the possibility of cytotoxicity after synovial cells were exposed to healthy synovial fluid. Our objective was to purify a BSA specific antibody from equine serum and demonstrate the presence of BSA in FBS grown cells. Additionally, our aim was to confirm the cellular cytotoxicity of equine MSCs in the presence of serum containing an anti-bovine antibody. We hypothesized that MSCs grown in FBS endocytose bovine proteins during expansion, and they may be detected in the culture supernatant after cells are starved of FBS and supplemented with a chemically defined, albumin free media for 24 hours. Figure 25 depicts exocytosis of bovine proteins over time after supplementation with FBS, followed by FBS starvation and replacement with chemically defined (CD) media. We successfully identified BSA as the target antigen for a bovine-specific equine IgG and detected exocytosed BSA using western blot with a purified BSA specific equine IgG. We recommend exploration of BMS as a replacement for FBS during the final stages of expansion, allowing exocytosis and clearance of bovine proteins from the cells.

Methods

Measurement of Anti-Bovine Titers in Commercial Equine Serum

Plates were incubated overnight with 100 µl/well of FBS, followed by four washes with phosphate buffered saline/Tris buffer (PBST). A serial dilution of HyEq was applied in triplicate (1:100- 1:814,000), with incubation at room temperature for 30 minutes. After four washes secondary antibody[xxxix] (goat-anti horse, SAB3700159), was applied (1:20,000 dilution, 100 µl) with incubation for 30 minutes at room temperature, four washes and addition of TMB substrate[xl], 15-minute incubation protected from light, followed by addition of stop solution[xli] and reading the plate at 450 nm.

Complement-Assisted Antibody Dependent Cellular Cytotoxicity

MSCs (passage 4) previously expanded in media supplemented with 10 % BMS or 10% FBS were thawed as described in chapter 2 and re-suspended in 233 µl Minimum Essential Medium [xlii], 100 µl HyClone Equine Serum (HyEq) [xliii], and 1µl DNase (3U/µl) [xliv] and incubated at 37°C for 30 minutes, with gentle mixing at 15 minutes. Then, 167 µl of rabbit complement [xlv] was added, followed by gentle vortex and the suspension was incubated at 37°C for 60 minutes with gentle mixing every 15-30 minutes. Samples were placed on ice prior to flow cytometry to assess viability in 10,000 single cells. An Amnis CellSteam flow cytometer was used with a 488 nm laser and viability was assessed with 7-AAD. Data were normalized to positive and negative controls to obtain accurate viability scores.

Fluorescent Labeling of Fetal Bovine Serum and imaging of FITC labeled MSCs

Undiluted FBS was diafiltered through a tangential flow filtration system for labeling of bovine proteins with fluorescein isothiocyanate[xlvi]. Fluorescently labeled FBS (fFBS) was added to MSC basal medium [DMEM 1g/l glucose supplemented with 10,000 U/ml Penicillin, 10 mg streptomycin sulfate, 25 µg/ml amphotericin B, HEPES buffer, 10 µg/ml human recombinant bFGF at a concentration of 10% and cells were incubated for 72 hours before imaging with an Olympus CKX41 light microscope. Images were captured with an Olympus DP73 camera mounted to the microscope and cellSense software was used to capture images. Image J was used to overlay light and fluorescent images.

Antibody Preparation Overview

The antibody was purified from HyEq using anion exchange chromatography by the Protein Chemistry Laboratory at Texas A&M. Following IgG purification, an affinity column was prepared by binding BSA to beads and eluting BSA specific IgG. Eluted fractions were combined and concentrated before measurement of protein concentration. Specificity was confirmed by SDS-PAGE after anion exchange chromatography and after affinity chromatography and specificity to BSA was confirmed by ELISA. Purified antibody was then brought to a concentration of 1 mg/ml (Figure 24).

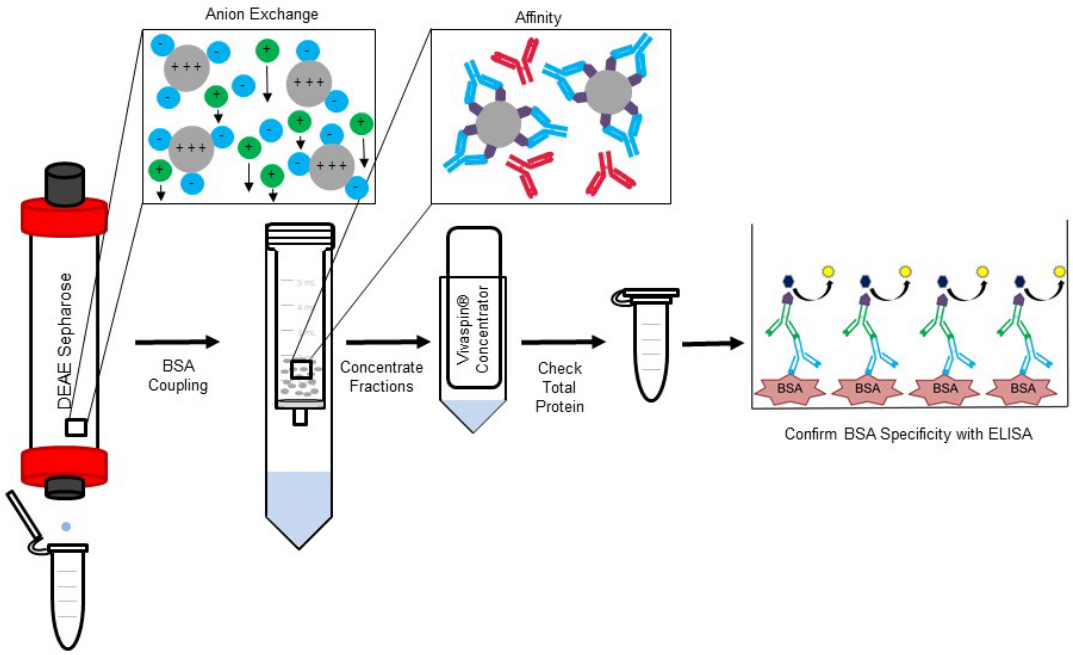

Figure 24. Overview of purification of equine anti-BSA IgG. Preparation of BSA specific IgG. DEAE Sepharose column was used to purify IgG from 50 ml of commercial equine serum, followed by SDS PAGE to confirm IgG specificity, affinity purification to obtain BSA specific IgG, concentration of fractions, total protein quantification and confirmation of specificity by ELISA.

Purification of IgG from commercially available equine serum

Equine serum as provided to the Texas A&M Protein Chemistry Laboratory (50 ml) for purification of equine IgG using a DEAE Sepharose column [xlvii]. Eluate was stored at -20°C.

IgG specificity

SDS Page

Samples were subjected to denaturing conditions prior to SDS-PAGE. Beta-mercaptoethanol[xlviii] (2.5%) and loading dye[xlix] were added before heating samples at

95°C for 10 minutes, followed by SDS-PAGE at 30 volts for 45 minutes, and 100 volts for 45 minutes. Gels were stained with Coomassie Blue[l] on an orbital shaker at room temperature overnight and de-stained prior to imaging.

Affinity purification of equine IgG for BSA specificity

Affinity purification columns were constructed by creating a matrix of AminoLink™ in centrifuge column[li] (5 ml) and coupling BSA (20 mg), blocking remaining active sites and a series of washes to remove uncoupled BSA from the column prior to affinity purification. Columns were equilibrated and IgG eluate applied followed by centrifugation, washing and elution of BSA specific IgG. Fractions were combined for concentration and buffer exchange[lii] (ab102778) and brought to a concentration of 1 mg/ml and conjugation to horseradish peroxidase (HRP) with a commercially available kit (abcam 102778)[liii]. A control column (PBS only, uncoupled) was also constructed comparison to confirm that the column does not bind proteins unspecifically.

Specificity of the Affinity Column to BSA

ELISA

Plates were incubated overnight with 100 µl/well of 2.5% BSA, followed by four washes with phosphate buffered saline/Tris buffer (PBST). Samples from washes 1-5 were and eluted fractions were applied in triplicate without dilution followed by incubation at room temperature for 30 minutes. After four washes the secondary antibody (goat-anti horse, SAB3700159) was applied (1:20,000) and incubated for 30

minutes at room temperature, followed by four washes and addition of TMB substrate, 15-minute incubation protected from light, addition of stop solution and reading the plate at 450 nm. Washes and fractions from control columns were also assayed to confirm that non-specific binding did not occur.

Specificity of the Purified Antibody to BSA

SDS-PAGE and Western blot

After affinity purification, BSA specificity was confirmed using SDS-PAGE as described above. Prior to concentration and buffer exchange, fractions were tested for specificity using western blot. Samples were subjected to denaturing conditions and SDS-PAGE as described previously. Mini Protean TGX gels[liv] (12% polyacrylamide) were transferred using a Trans-Blot Transfer System[lv] onto nitrocellulose membranes[lvi] and total protein was visualized with Ponceau S[lvii] stain and imaged using a ChemiDoc™ MP Imaging System[lviii]. After de-staining in Tris-phosphate buffered saline (TBST) for 10 minutes, blots were blocked for 1 hour with 5% rabbit serum[lix] and incubated with secondary antibody (goat anti-horse IgG+ HRP, 1: 1,000, SAB3700159) for one hour at room temperature on an orbital shaker with gentle rocking. Blots were rinsed in TBST for a total of three 1-hour washes before addition of the substrate[lx] and imaging. Membranes were exposed for 20 seconds with Image Lab software and exported for further analysis.

Detection of Bovine Proteins in FBS supplemented MSCs

After supplementation of FBS supplemented MSCs with fFBS for 72 hours, media was exchanged for media supplemented with 10% BMS, as it sustains growth similarly to FBS. Flow cytometry was performed using an Amnis® ImageStream®[lxi] flow cytometer with a 488nm laser to assess median fluorescence intensity (MFI) of FITC labeled cells over 4 days. Cells were collected at 24, 48, 72 and 96 hours. Exocytosis of bovine proteins was measured as loss of fluorescence from cells over time.

FBS supplemented MSCs were thawed, allowed to recover for 48 hours on 10% FBS supplemented media, rinsed twice with DPBS and switched to CD media. Supernatants were collected at 24 hours and stored at -20°C. SDS PAGE was performed as previously described on undiluted culture supernatant. Mini Protean TGX gels[lxii] (12% polyacrylamide) were transferred using a Trans-Blot Transfer System onto nitrocellulose membranes and total protein was visualized with Ponceau S stain and imaged as previously described. After de-staining in TBST for 10 minutes, blots were blocked for 1 hour with 5% rabbit serum and incubated with purified antibody (equine anti-BSA goat anti-horse IgG + HRP, 1: 20,000) overnight at 4°C on an orbital shaker with gentle rocking. Blots were rinsed in TBST for a total of three 1-hour washes before addition of the substrate and imaging. Membranes were exposed for 20 seconds with Image Lab software and exported for further analysis.

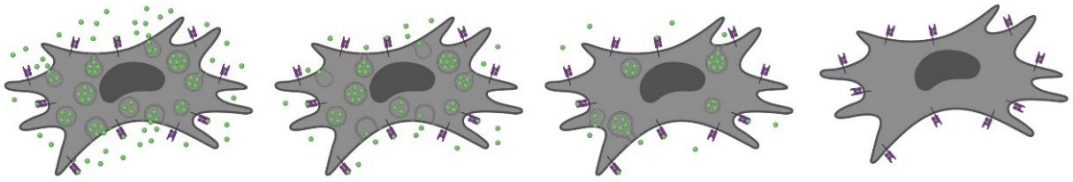

Figure 25. Representation of exocytosis and antigen presentation of bovine proteins by FBS supplemented MSCs. Fetal bovine supplemented MSCs endocytose fluorescently labeled bovine proteins during expansion. After starvation and replacement with chemically defined (CD) media, the cells begin to exocytose bovine proteins into the extracellular environment (left to right). *In-vivo*, cells present foreign proteins on MHCI, allowing recognition by the host immune system and over time, bovine proteins would diffuse into the body. *In vitro*, media exchange removes bovine proteins over time.

Statistical Analysis

Wilcoxon-signed rank was used to compare flow cytometry data (% dead cells) between BMS and FBS supplemented MSCs.

Results

Commercial Equine Serum Contains FBS antibodies

Anti-FBS antibodies were detected in HyEq at dilutions ranging from 1:100 to 1: 25,600 (Figure 25, 1:400 – 1: 204,800 shown).

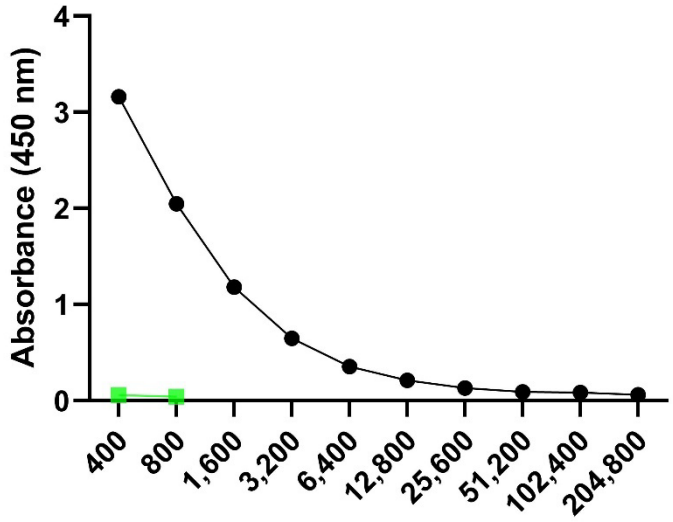

Figure 26. Anti- fetal bovine serum (FBS) titers in commercial equine serum (HyEq). Dilution factors are shown on the x axis. Serum was serially diluted from 1: 100 – 1: 814,000 and tested for anti-bovine antibodies by ELISA with FBS coated plates and an anti-equine IgG conjugated to horseradish peroxidase (HRP). The green squares represent fetal equine serum (FES) at a dilution of 1:400 and 1:800.

Antibody Dependent Cytotoxicity Affects Cells Grown in FBS Supplemented Media

Cells grown in FBS had a higher percent death after exposure to commercial equine serum containing the anti-bovine antibody ($p= 0.007$).

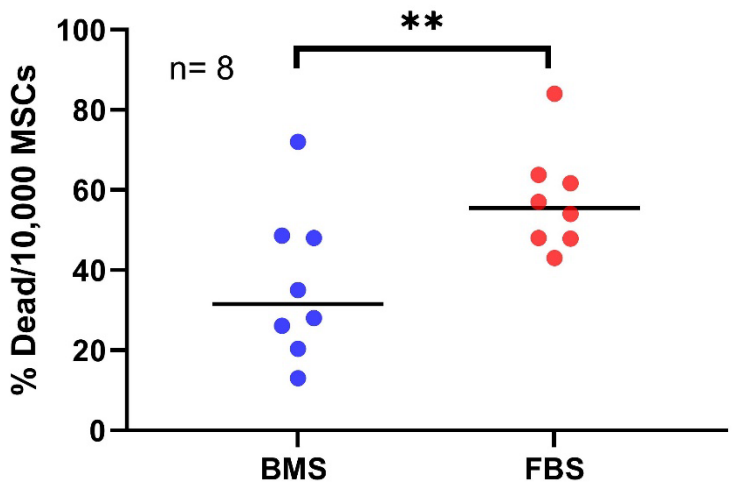

Figure 27. Cell death in fetal bovine serum (FBS) supplemented mesenchymal stem cells (MSCs). Complement-assisted Antibody-dependent Cellular Cytotoxicity (CAC) led to increased cell death in cells that were grown in 10% FBS supplemented media after exposure to commercial equine serum and complement as measured by flow cytometry (Wilcoxon signed rank, p= 0.007).

IgG Purification was Successful

After purification by anion exchange chromatography, IgG was detected by SDS-PAGE in diluted (1:8) and undiluted and Coomassie blue staining with heavy and light chain bands visible at 50 and 25 KDa respectively (Figure 28, left).

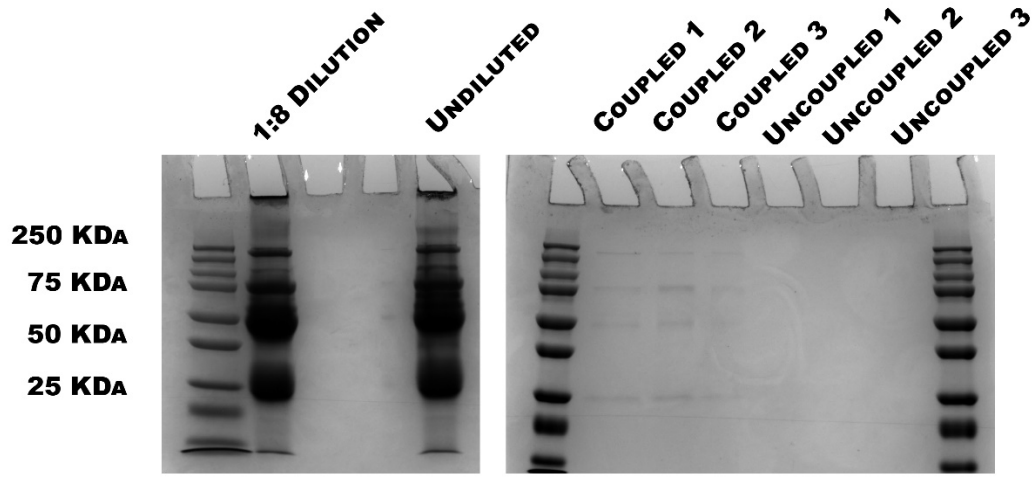

Figure 28. Identification of purified IgG by SDS-PAGE. SDS- PAGE and Coomassie blue staining of purified IgG after anion exchange chromatography (left) and BSA affinity purification (right).

Purified equine anti-BSA IgG is specific to bovine serum albumin

BSA specific IgG was eluted from the BSA coupled affinity column after 5 washes followed by detection by SDS-PAGE and Coomassie blue staining (Figure 28, right) followed by ELISA to confirm specificity compared to a control affinity column (buffer only) (Figure 29). Subsequently, specificity of each fraction eluted the BSA coupled column was also confirmed by western blot. Heavy (50 KDa) and light (25 KDa) chain bands were visible in each fraction and the positive control lane containing FBS (Figure 30).

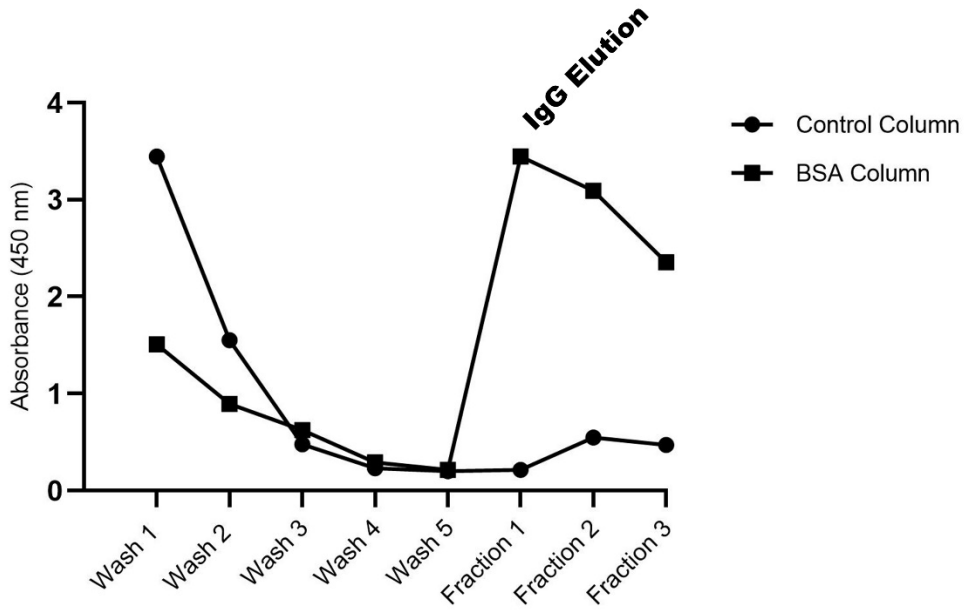

Figure 29. ELISA: Purified equine anti-BSA IgG is specific to bovine serum albumin (BSA). Detection of bovine serum albumin (BSA) by ELISA in columns coupled (BSA Column) and not coupled (Control Column) to BSA by affinity chromatography. The antibody is eluted at Fraction 1.

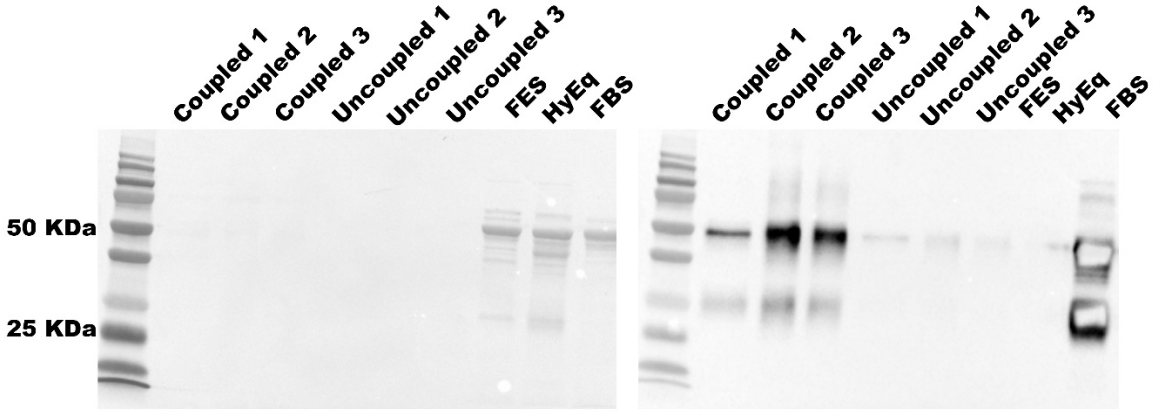

Figure 30. Western blot: Purified equine anti-bovine serum albumin (BSA) IgG is specific to BSA. Detection of affinity purified BSA specific IgG fractions (1-3) by western blot in columns coupled and not coupled to BSA. Left: Ponceau S total protein stain. Right: Probed blot.Negative controls: Fetal equine serum (FES), Commercial

equine serum (HyEq). Positive control: Fetal bovine serum (FBS). Heavy chain and light chain IgG bands shown in coupled fractions 1-3 at 50 and 25 KDa respectively.

BSA is detectable with purified antibody at low concentrations

The lowest concentration at which BSA can be detected in CD media is 0.0005% BSA (Figure 31).

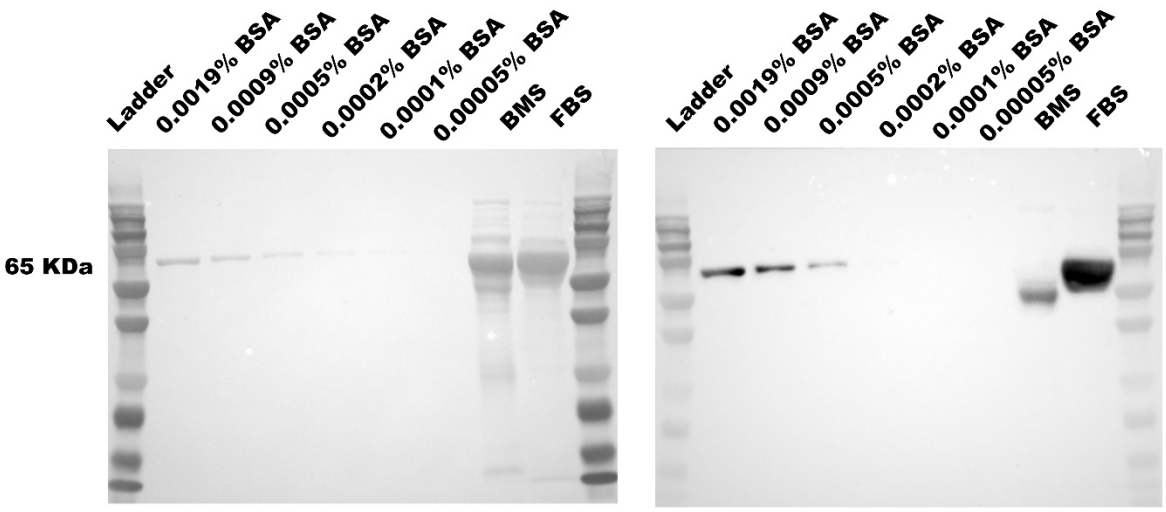

Figure 31. Serial dilution of bovine serum albumin (BSA) in chemically defined (CD) media. Determination of lowest concentration of bovine serum albumin (BSA) detectable by the purified BSA specific IgG using western blot. Negative control: Bone marrow supernatant (BMS). Positive control: Fetal bovine serum (FBS). The total protein stain is shown on the left, probed blot on the right.

Endocytosed BSA can be visualized intracellularly

BSA is visible by fluorescence microscopy after supplementation with fFBS (Figure 32).

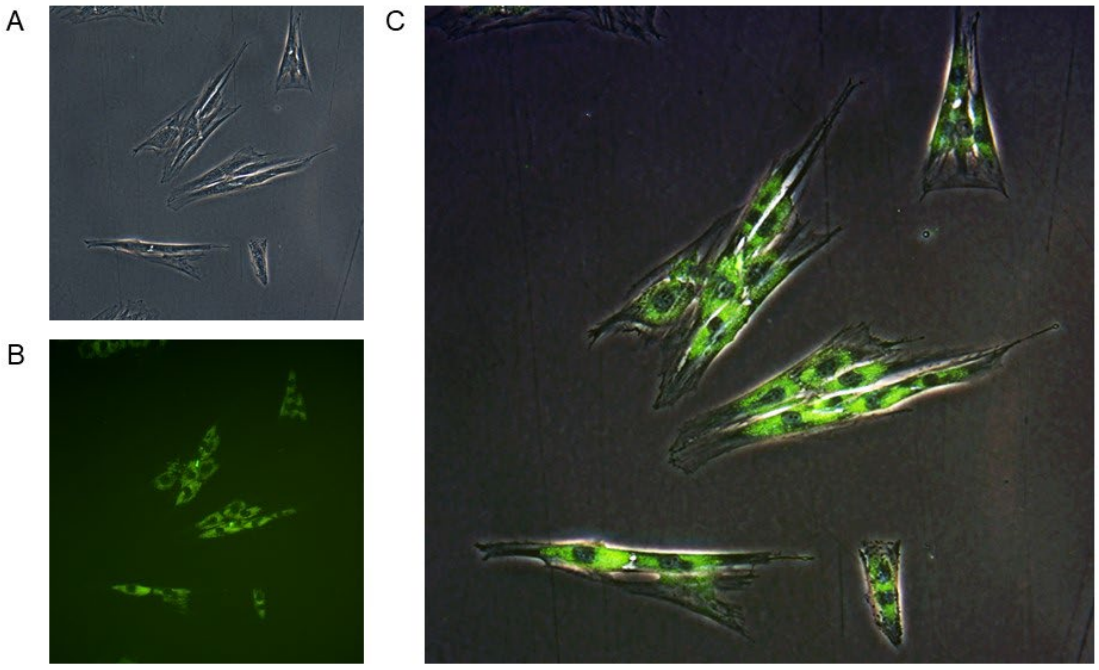

Figure 32. Fluorescent Images of endocytosed bovine proteins labeled with fluorescein (FITC). Mesenchymal stem cells (MSCs) were grown on fluorescently labeled fetal bovine serum (fFBS) for 96 hours for visualization of fFBS labeled bovine proteins within the cell. A) MSCs at 200x magnification without fluorescent filter B) MSCs at 200x magnification a 488 nm laser C) Image overlay to show location of fFBS within the cells.

BSA is exocytosed into the media by FBS supplemented cells

At the time of media exchange to 10% BMS MFI was measured at 736,496, decreasing to 18,594 after 96 hours on 10% BMS supplemented media indicating exocytosis of bovine proteins (Figure 33).

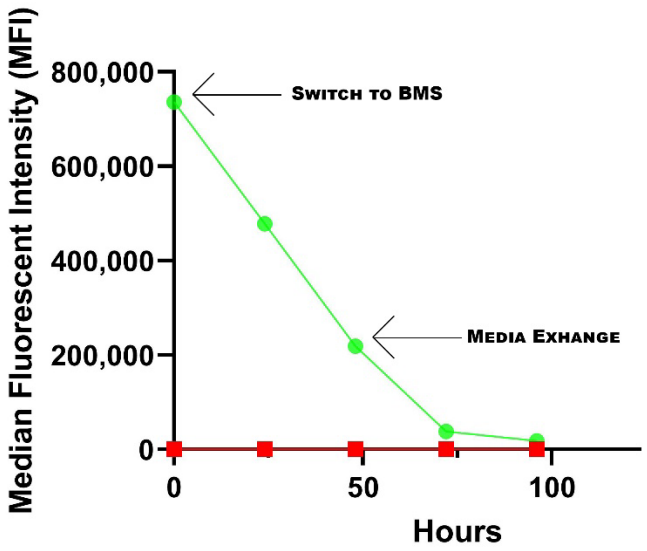

Figure 33. Fluorescein (FITC) labeled fetal bovine serum (FBS) to assess depletion of FBS from MSCs after switching to BMS supplementation. The green line represents FITC labeled fetal bovine serum (fFBS) and the red line represents unlabeled FBS used as a control. MSCs were seeded in 10% fFBS media for 96 hours. After switching to bone marrow supernatant (BMS), cells were collected at 24, 48, 72 and 96 hours for flow cytometry. fFBS was depleted to nearly undetectable levels by 96 hours.

BSA is exocytosed from cells grown in FBS and switched to chemically defined media after 24 hours (Figure 22, 34).

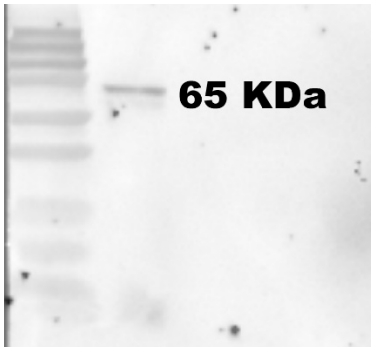

Figure 34. Western blot: Bovine serum albumin is present in FBS grown MSCs. Detection of bovine serum albumin (BSA) exocytosed from cells grown in fetal bovine serum (FBS). Mesenchymal stem cells (MSCs) grown in FBS were allowed to recover in FBS supplemented medium for 48 hours before switching to chemically defined (CD) medium. A 66 KDa band is visible after 24 hours on CD media.

Discussion

Despite growing evidence that FBS supplementation during culture of MSCs is harmful due to potential hypersensitivity reactions, alloreactivity and cell/antibody-mediated cytotoxicity of MSCs, the use of FBS in therapeutic cell lines and *in-vitro* studies is prevalent. Because the discovery of cytotoxicity of FBS supplemented MSCs is novel, the objectives of this chapter were to identify intracellular FBS, detect FBS expelled from MSCs into the media, and show that intracellular FBS results in increased cell death.

There are numerous reasons for the exploration of suitable replacements for FBS. One important argument includes the possibility of hypersensitivity to vaccines containing xenogeneic proteins from production. Anti-bovine IgE has been identified and documented in horses, sometimes leading to vaccine hypersensitivity and adverse reactions such as anaphylactic shock (105). Similarly, intra-articular injection of

allogeneic MSCs not depleted of FBS has resulted in significantly increased total nucleated cell count (TNCC) and pain compared to autologous, FBS depleted MSCs (34). These, among other challenges associated with the use of FBS in cell culture have sparked continued interest in FBS alternatives. Fortunately, depletion of FBS and replacement with BMS prior to cryopreservation would eliminate these concerns.

We developed a Complement-assisted Antibody-mediated Cytotoxicity (CAC) assay to determine if FBS supplemented cells were targeted for apoptosis in the presence of complement and anti-bovine antibody. Commercial equine serum contained an abundant amount of anti-FBS IgG, making it a suitable antibody component of the assay. We chose serum instead of purified antibody to represent a physiologic concentration of IgG, as this is what cells would be exposed to *in-vivo*. Complement is known to bind to the Fc region of antibodies and participate in cytotoxicity of target cells. Although it does have some cytotoxic effects alone, it can assist natural killer (NK) cells in antibody-dependent cellular cytotoxicity (ADCC) (107). Recent research is focused on enhancing ADCC as a mechanism used by the immune system to rid the body of cancer cells (108). In this assay, we observed significantly increased cell death when cells contained intracellular FBS from culture compared to cells grown in BMS. Some cell death was observed in both groups, likely due to the thawing process in which cells are removed from DMSO and brought back to their normal osmolarity. Because cells were exposed to complement and antibody, but not NK or T cells, the mechanism of cytotoxicity remains unknown. We suspect that the addition of PBMCs, containing, both NK and T cells would result in higher percent death. Future studies should address this with the

development of a cell based (CD8+ T cells) and antibody dependent cellular cytotoxicity (NK cells) assay to examine cellular synapses and apoptosis of target cells. Additionally, BSA has been shown to cause stress in the endoplasmic reticulum (ER) of renal tubule cells, leading to apoptosis (109). From the fluorescent images, FBS proteins appear perinuclear, suggesting that they are sequestered in the ER. Apoptosis resulting from BSA causing ER stress may also be examined in future studies.

We hypothesized that cells take up bovine proteins during culture and that they would be present intracellularly, then exocytosed by the cell into the surrounding media. To visualize FBS proteins intracellularly, FBS was labeled with FITC using tangential flow filtration, followed by culture for 96 hours, allowing the cells to take up fFBS proteins. Fluorescence and light microscopy were used to create a composite image of intracellular fFBS (Figure 32). Detection of exocytosed bovine proteins in the media required the purification of an antibody for western blot specific to the bovine proteins that would not cross-react with equine proteins.

As albumin is the most abundant protein in serum, we tested BSA binding of equine serum, followed by a monoclonal commercial anti-BSA, followed by IgG + HRP to BSA using ELISA (data not shown) to confirm that BSA is the target antigen. We then purified BSA specific IgG from commercial equine serum, which contain FBS specific IgG (Figure 26). We conjugated HRP directly to the primary antibody to avoid any potential cross-reactivity from a secondary antibody, as equine and bovine albumin share 74% amino acid similarity. In preliminary western blots commercial anti-BSA

primary antibodies paired with corresponding secondary antibodies yielded some cross-reactivity to equine proteins.

To confirm that IgG was still present after affinity purification, we visualized heavy (50 KDa) and light (25 KDa) on the gel (Figure 28). Using western blot, we also showed that the purified antibody is specific to BSA, as bands were visible after incubation with a monoclonal commercial anti-BSA antibody (Figure 30). To further confirm specificity to BSA and rule out the possibility of non-specific binding to the beads in the affinity column, we showed that the BSA coupled column and not the uncoupled column produced an eluate that bound to equine IgG (Figure 29).

Before using the antibody to detect bovine proteins exocytosed from MSCs, we tested the sensitivity of the antibody with a serial dilution of BSA (Figure 31) and found that the antibody is detectable at 0.0005% BSA. This information was used to optimize antibody concentrations for western blot.

Fluorescence microscopy indicated that there were abundant bovine proteins present in the cytoplasm of MSCs supplemented with 10% fFBS for 96 hours, proving that cells took up fFBS during culture. We also demonstrated exocytosis by depletion of fFBS and extracellular presence of BSA after removal from media containing albumin. Based on the fluorescence microscopy, we noted that there was possible evidence of BSA on the outside surface of the cell. Recent literature has examined BSA as a target molecule for drug delivery because of its function as a transport molecule (110), and ability to bind hydrophilic and hydrophobic molecules (111). It is also able to bind calreticulin (111), which is expressed on MSCs (112).

To begin the investigation into cytotoxicity resulting from intracellular BSA, we developed the CAC assay, as it is a simple starting point with few components. To elucidate the mechanism of cytotoxicity, the assay should be developed with additional component such PBMCs. Additionally, further research is needed to determine whether BSA is bound to a protein or molecule at the cell surface. This may be tested by labeling the purified anti-BSA with FITC, followed by incubation with FBS or CD supplemented MSCs and flow cytometry to visualize FITC labeled antibody on the cell surface. If BSA is present on the outer cell surface, antibodies can bind, leading to opsonization of the MSC and phagocytosis by immune cells, assisted by the complement pathway. Additionally, some leakage of BSA into the cytoplasm may occur during endocytosis, as some molecules have been found to escape the endosome during internalization (113). Intracellular proteins could be processed by the proteasome and presented as antigens on MHCI for recognition by the immune system, which would lead to CD8+ T cell-mediated cytotoxicity. Cell mediated cytotoxicity assays should be investigated to determine the mechanism of cell death after exposure to anti-BSA antibodies.

To show exocytosis of FBS during culture, we removed FBS from the culture media, replacing it with a CD media containing no albumin. Preliminary tests with cells switched to BMS supplemented media from FBS supplemented media indicated that equine albumin interfered with binding of bovine albumin to the antibody, preventing detection of exocytosed bovine proteins. Albumin is known to be abundant and prone to adhere to surfaces and other proteins due to its binding properties, and the use of CD media resolved unwanted binding of equine albumin that was observed with BMS

supplemented cells. Expelled BSA was detected at 24 hours, indicating that cells rapidly metabolized the FBS during culture.

We examined the time required for depleting FBS from cells because it has important therapeutic consequences. As discussed previously, intracellular FBS in therapeutic cells leads to joint swelling and pain in horses (33). While the use of BMS throughout the culture period would eliminate any xenogeneic contamination, it is difficult to obtain sufficient volumes of bone marrow supernatant for the entire culture period. Therefore, we investigated the time required for MSCs to fully expel bovine proteins. This would reduce the time required in BMS supplemented media, thus reducing the volume necessary to produce therapeutic cells free from xenogeneic proteins. We found that after 96 hours, FBS proteins are nearly undetectable in the cell (Figure 33). Clinically, this is useful because cells can be grown on FBS for several weeks to obtain a sufficient clinical dose, then switched to BMS supplemented media for the final passage, or a minimum of 96 hours prior to cryopreservation.

Our goal was to identify xenogeneic contamination in equine MSCs supplemented with FBS and show complement-assisted antibody-mediated cellular cytotoxicity. To accomplish this, we developed a flow cytometry-based assay and showed increased cellular death in FBS supplemented cells compared to BMS. Using fFBS, we showed intracellular FBS proteins and discovered that FBS is depleted from cells in culture after 4 days of starvation and replacement with another supplement suitable for survival and proliferation. A purified antibody was used to detect bovine proteins expelled from MSCs into the surrounding media, further confirming metabolism

of FBS. We emphasize that BMS is a suitable replacement for FBS and should be considered in therapeutic cell lines. Additionally, BMS should be considered for *in-vitro* studies in which cells may be exposed to xenogeneic proteins from culture in FBS.

There is a possibility that adaptive immunity plays a role in cell death. A CD8+ T cell with a receptor that matches a bovine peptide loaded on MHCI may also lead to cytotoxicity. We suggest the development of an assay that can detect cell based (CD8+ T cell) cytotoxicity and/or phagocytosis of MSCs after anti-BSA exposure to determine the mechanism of cell death.

CHAPTER V

CONCLUSIONS

Cellular Contact is Important for MSC Immunomodulation

There is continued promise of clinical use of MSCs and translation of animal models to humans and market approval. Our goal was to investigate the mechanism by which MSCs modulate inflammation. We developed a model of synovitis to evaluate how cellular contact influences cellular secretions in early inflammation. This work has shed light on cellular signaling between MSCs, synovial cells and chondrocytes in an equine model of synovitis.

We provided evidence that cellular contact works in tandem with paracrine signaling to maximize MSC immunomodulation. We also demonstrated that while use of synovial fluid in a model of synovitis may be useful, the presence of anti-bovine antibodies in synovial fluid presents a challenge due to cell and or/antibody mediated cytotoxicity. Additionally, we have shown that the addition of IL1-β is required to mimic an inflamed synovial environment.

Collectively, the findings of this research led to the design of a new synovitis model using the same format, with the addition of synovial fluid and IL1-β. The proposed conditions include SC monoculture, SC/MSC co-culture, SC/MSC co-culture with EVs, SC/EV co-culture and SC/DF co-culture using the cartilage co-culture format for all conditions to further evaluate SC/MSC secretory activity in a synovitis model (Figure 35). A control group in which cells are not treated with IL1-β should be included

for data normalization and comparison of GAG loss by cartilage explants in control versus inflamed conditions. Because research has shown that DFs may actually be MSCs (92) (78), they should not be used as controls, and untreated controls should be used for comparisons. However, SC/DF EVs may be isolated and used in additional conditions for comparison of immunomodulatory functions.

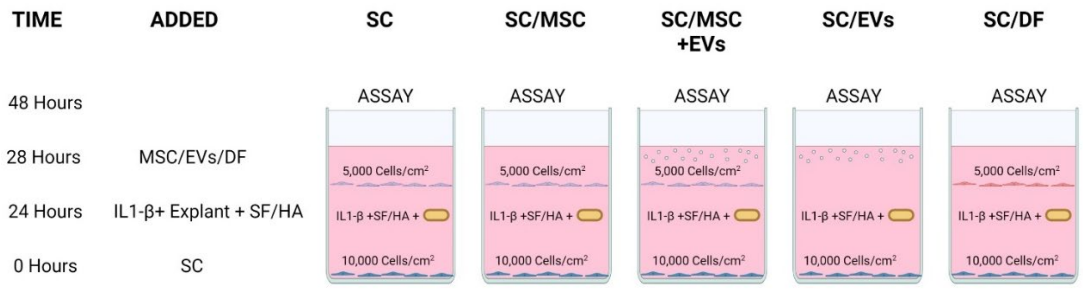

Figure 35. Model of proposed experiment. After overnight recovery, the SCs will be exposed to 10 ng/ml IL1-β plus autologous synovial fluid (SFa), inflamed donor pooled synovial fluid (SFi) or hyaluronic acid (HA) before addition of MSCs with or without EVs, EVs alone or DFs. Following treatment and overnight culture, media and cell lysates will be collected and stored for future assays. Created with BioRender.com

Intracellular Bovine Proteins Lead to Cytotoxicity of MSCs

We purified an equine anti-BSA IgG that binds specifically to BSA exocytosed into albumin-free media by MSCs grown in FBS and showed intracellular FBS presence by fluorescence microscopy. We also showed that FBS is depleted from cells 96 hours replacing the culture supplement. While not all cell lines metabolize nutrients at an equal rate, this information can greatly reduce the amount of time that cells need to be cultured

on BMS supplemented media prior to cryopreservation. This reduces the need for large volumes of BMS, which are difficult to obtain. We propose the use of BMS supplemented or albumin free media to further investigate the presence of bovine contaminants in cell cultures that may be used for both *in-vitro* studies and clinical therapeutics.

The presence of anti-bovine antibodies and observation of cytotoxicity after exposure to these antibodies led to two questions. How are horses stimulated to produce anti-bovine antibodies? Are these antibodies related to cytotoxicity of FBS supplemented MSCs? Several mechanisms of immune recognition that should be examined. Due to the binding properties of albumin, it is probable that BSA is present on the outer surface of the cell. This would allow complement to bind to the antibody and initiate cell lysis or assist NK cells in cytotoxicity (Figure 36; 1, 4). There is a possibility that internalized molecules can escape the endo-lysosomal pathway (113), allowing processing by the proteasome and presentation on MHCI (Figure 36, 2). These peptides are not likely to lead to antibody recognition, but may be recognized by a CD8+ T cell, leading to cytotoxicity (Figure 36, 3). Lastly, if MSCs are primed with IFN-γ, they are stimulated to upregulate expression of MHCII (114) (115), which would allow processing through the endo-lysosomal pathway leading to recognition by CD4+ T cells (Figure 36, 5). This may be a mechanism of antibody production, which might contribute to differences in antibody titers between horses. However, antibody production after vaccination is based on individual immune responses, which would also lead to differences in antibody titers. A previous study in horses showed the presence of

anti-BSA antibodies in horses before and after MSC treatment, but no increase in production of anti-bovine antibodies two weeks after injection of FBS supplemented MSCs (116). While this finding seems to indicate that anti-BSA antibodies are produced in response to vaccination rather than B cell activation by CD4+ T cells, it is not possible to determine based on their experimental design.

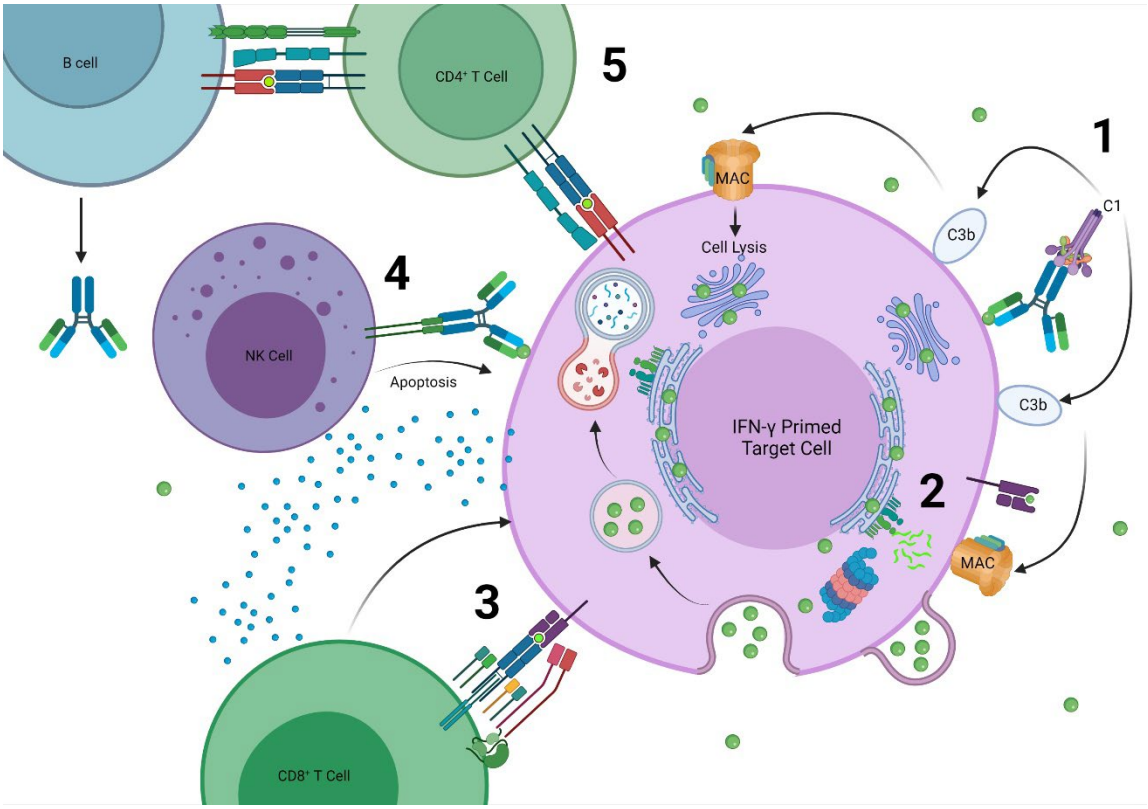

Figure 36. Possible mechanisms of cytotoxicity of FBS supplemented MSCs and antibody production by MSCs exposed to FBS through vaccination. Bovine proteins are endocytosed during expansion, processed and presented for recognition by the host immune system. We propose several possible mechanisms for recognition and target for apoptosis or antibody production. 1. Exocytosed bovine serum albumin (BSA) may become stuck to the cell surface and recognized by complement, triggering lysis. 2. If BSA leaks into the cytoplasm during endocytosis or through cross presentation, it may

be processed by the proteasome and presented on MHCI, but would not be recognized by antibodies therefore not targeted for cytotoxicity. 3. BSA leaked into the cytoplasm may be presented on MHCI and recognized by CD8+ cytotoxic T cells, leading to apoptosis. 4. Exocytosed BSA stuck to the cell membrane may be recognized by circulating anti-BSA antibodies and targeted for apoptosis by natural killer (NK cells) 5. If MSCs are primed with IFN-γ, MHCII may be upregulated and processing by endo-lysosomal pathway may lead to presentation and recognition by CD4+ T cells followed by antibody production, explaining differences in titers between individuals. Created with BioRender.com

Imaging flow cytometry has been used to visualize synapse formation between target and effector cells and quantify apoptosis during antibody dependent cell-mediated cytotoxicity (117). Future experiments may investigate apoptosis of FBS supplemented MSCs by cell or antibody mediated cytotoxicity by designing an imaging flow cytometry-based assay in which immune synapses can be observed between target cells (MSCs) and immune cells (NK cells or T cells). Previous research has shown that synapses between target and effector cells can be visualized with imaging flow cytometry and apoptosis can be quantified with the corresponding software (117). Cell mediated cytotoxicity can be imaged and measured between target cells and CD8+ cytotoxic T-cells that possess a T-cell receptor specific to bovine antigens. Visualizing synapses between MSCs and CD4+ and CD8+ T cells that are tagged with different fluorescent labels would elucidate mechanisms of cytotoxicity and antibody production. These assays may be useful as diagnostic tools and prediction of cell survival after exposure to specific antibodies.

In summary, this body of work has demonstrated the importance of cellular contact and paracrine signaling for MSC immunomodulation and identified cytotoxicity

resulting from several possible mechanisms: antibody binding to xenogeneic proteins stuck to the outside of the cell followed by lysis by the complement cascade, bovine peptides presented on MHCI and recognized by CD8+ cytotoxic T cells due to leakage into the cytoplasm during endocytosis or cross presentation, or bovine peptides presented on MHCII after upregulation by IFN-γ. Thus, this research has provided new insight on MSC function in synovitis and discovered important consequences of traditional cell culture methods. This opens the door for mechanistic studies on MSC communication within the synovial joint through gap junctions and Notch signaling as well as studies on cellular cytotoxicity.

REFERENCES

(1) Lambert NC. How twin studies help to understand inflammatory joint disease. *Joint, bone, spine: revue du rhumatisme* (2016) **83**:637-643. doi: 10.1016/j.jbspin.2016.02.008.

(2) Macfarlane E, Seibel MJ, Zhou H. Arthritis and the role of endogenous glucocorticoids. *Bone research* (2020) **8**:33. doi: 10.1038/s41413-020-00112-2.

(3) Anonymous Am Fam Physician 2018 Wasserman RA common questions about diagnosis and management.

(4) Peláez P, Damiá E, Torres-Torrillas M, Chicharro D, Cuervo B, Miguel L, et al. Cell and Cell Free Therapies in Osteoarthritis. *Biomedicines* (2021) **9**:1726. doi: 10.3390/biomedicines9111726.

(5) David O, Hunter J, Bierma-Zeinstra S. Lancet 2019 Hunter Osteoarthritis. *Seminar www.thelancet.com*.

(6) Xie F, Kovic B, Jin X, He X, Wang M, Silvestre C. Economic and humanistic burden of osteoarthritis: a systematic review of large sample studies. *PharmacoEconomics* (2016) **34**:1087-1100. doi: 10.1007/s40273-016-0424-x.

(7) Mcilwraith CW, Frisbie DD, Kawcak CE. The horse as a model of naturally occurring osteoarthritis. *Bone Joint Res* (2012) **1**:297. doi: 10.1302/2046-3758.111.

(8) Boyde A. The Bone Cartilage Interface and Osteoarthritis. *Calcif Tissue Int* (2021) **109**:303-328. doi: 10.1007/s00223-021-00866-9.

(9) McIlwraith CW, Fortier LA, Frisbie DD, Nixon AJ. PMC4297134; Equine Models of Articular Cartilage Repair. *Cartilage* (2011) **2**:317-326. doi: 10.1177/1947603511406531.

(10) McCoy AM. Animal Models of Osteoarthritis. *Veterinary pathology* (2015) **52**:803-818. doi: 10.1177/0300985815588611.

(11) Mandl LA. Osteoarthritis year in review 2018: clinical. *Osteoarthritis and cartilage* (2019) **27**:359-364. doi: 10.1016/j.joca.2018.11.001.

(12) Griffin TM, Scanzello CR. Clin Exp Rheumatol 2019 Innate inflammation and synovial macrophages in OA pathophysiology. *Clin Exp Rheumatol* (2019) **37**:57.

(13) Culemann, S. Grüneboom, A. Nicolás-Ávila, JÁ Weidner, D. Lämmle, K. F. Rothe, T. Quintana, J. A. Kirchner, P. Krljanac, B. Eberhardt, M. Ferrazzi, F. Kretzschmar, E.

Schicht, M. Fischer, K. Gelse, K. Faas, M. Pfeifle, R. Ackermann, J. A. Pachowsky, M. Renner, N. Simon, D. Haseloff, R. F. Ekici, A. B. Bäuerle, T. Blasig, I. E. Vera, J. Voehringer, D. Kleyer, A. Paulsen, F. Schett, G. Hidalgo, A. Krönke, G. Locally renewing resident synovial macrophages provide a protective barrier for the joint. *Nature* (2019) **572**:670-675.

(14) Alquraini A, Jamal M, Zhang L, Schmidt T, Jay GD, Elsaid KA. PMC5423025; The autocrine role of proteoglycan-4 (PRG4) in modulating osteoarthritic synoviocyte proliferation and expression of matrix degrading enzymes. *Arthritis Res Ther* (2017) **19**:89. doi: 10.1186/s13075-017-1301-5.

(15) Akkiraju H, Nohe A. PMC4916494; Role of chondrocytes in cartilage formation, progression of osteoarthritis and cartilage regeneration. *J Dev Biol* (2015) **3**:177-192. doi: 10.3390/jdb3040177.

(16) Li Z, Huang Z, Bai L. Cell Interplay in Osteoarthritis. *Frontiers in cell and developmental biology* (2021) **9**:720477. doi: 10.3389/fcell.2021.720477.

(17) Chou C, Jain V, Gibson J, Attarian DE, Haraden CA, Yohn CB, et al. Synovial cell cross-talk with cartilage plays a major role in the pathogenesis of osteoarthritis. *Sci Rep* (123456789) **10**. doi: 10.1038/s41598-020-67730-y.

(18) Hu Y, Chen X, Wang S, Jing Y, Su J. Subchondral bone microenvironment in osteoarthritis and pain. *Bone Res* (2021) **9**. doi: 10.1038/s41413-021-00147-z.

(19) Mathiessen A, Conaghan PG. Synovitis in osteoarthritis: current understanding with therapeutic implications. *Arthritis Res Ther* (2017) **19**. doi: 10.1186/s13075-017-1229-9.

(20) Donell S. Subchondral bone remodelling in osteoarthritis. *EFORT Open Reviews* (2019) **4**:221-229. doi: 10.1302/2058-5241.4.180102.

(21) Zhang H, Cai D, Bai X. Macrophages regulate the progression of osteoarthritis. *Osteoarthritis and cartilage* (2020) **28**:555-561. doi: 10.1016/j.joca.2020.01.007.

(22) Scanzello CR, Goldring SR. PMC3372675; The role of synovitis in osteoarthritis pathogenesis. *Bone* (2012) **51**:249-257. doi: 10.1016/j.bone.2012.02.012.

(23) Silawal, S, Triebel, J,Bertsch, T. Osteoarthritis and the complement cascade *Clin Med Insights: Arthritis Musculoskeletal Disord*. Osteoarthritis and the complement cascade. (2018) **11**. doi: 10.1177/1179544117751430

(24) Ipseiz N, Pickering RJ, Rosas M, Tyrrell VJ, Davies LC, Orr SJ, et al. Tissue-resident macrophages actively suppress IL-1beta release via a reactive prostanoid/IL-10 pathway. *EMBO J* (2020) **39**. doi: 10.15252/embj.2019103454.

(25) Behrendt P, Preusse-Prange A, Klüter T, Haake M, Rolauffs B, Grodzinsky AJ, et al. IL-10 reduces apoptosis and extracellular matrix degradation after injurious compression of mature articular cartilage. *Osteoarthritis and Cartilage* (2016) **24**:1981-1988. doi: https://doi.org/10.1016/j.joca.2016.06.016.

(26) Cameron AD, Even KM, Linardi RL, Berglund AK, Schnabel LV, Engiles JB, et al. Adeno-associated virus-mediated overexpression of interleukin-10 affects the immunomodulatory properties of equine bone marrow-derived mesenchymal stem cells. *Human Gene Therapy* (2021) **32**:907. doi: 10.1089/hum.2020.319.

(27) Murray PJ. Macrophage Polarization. *Annual review of physiology* (2017) **79**:541-566. doi: 10.1146/annurev-physiol-022516-034339.

(28) Zhu X, Lee C, Xu H, Wang Y, Yung PSH, Jiang Y, et al. Phenotypic alteration of macrophages during osteoarthritis: a systematic review. *Arthritis Res Ther* (2021) **23**. doi: 10.1186/s13075-021-02457-3.

(29) Palm W, Thompson CB. Nutrient acquisition strategies of mammalian cells. *Nature (London)* (2017) **546**:234-242. doi: 10.1038/nature22379.

(30) Doherty GJ, McMahon HT. Mechanisms of Endocytosis. *Annual Review of Biochemistry* (2009) **78**:857-902. doi: 10.1146/annurev.biochem.78.081307.110540.

(31) Mathieu M, Martin-Jaular L, Lavieu G, Théry C. Specificities of secretion and uptake of exosomes and other extracellular vesicles for cell-to-cell communication. *Nat Cell Biol* (2019) **21**:9. doi: 10.1038/s41556-018-0250-9.

(32) Canton J. Macropinocytosis: New Insights into Its underappreciated role in innate immune cell surveillance. *Frontiers in immunology* (2018) **9**:2286. doi: 10.3389/fimmu.2018.02286.

(33) Rowland AL, Burns ME, Levine GJ, Watts AE. Preparation Technique Affects recipient immune targeting of autologous mesenchymal stem cells. *Frontiers in veterinary science* (2021) **8**. doi: 10.3389/fvets.2021.724041.

(34) Joswig A, Mitchell A, Cummings KJ, Levine GJ, Gregory CA, Smith 3, Roger, et al. Repeated intra-articular injection of allogeneic mesenchymal stem cells causes an adverse response compared to autologous cells in the equine model. *Stem cell research & therapy* (2017) **8**:42. doi: 10.1186/s13287-017-0503-8.

(35) Karnieli O, Friedner OM, Allickson JG, Zhang N, Jung S, Fiorentini D, et al. A consensus introduction to serum replacements and serum-free media for cellular therapies. *Cytotherapy (Oxford, England)* (2017) **19**:155-169. doi: 10.1016/j.jcyt.2016.11.011.

(36) Gilbert SF. "Juxtacrine Signaling,". In: Anonymous *Developmental Biology. 6th edition*: Sunderland (MA): Sinauer Associates (2000).

(37) Alabi RO, Lora J, Celen AB, Maretzky T, Blobel CP. Analysis of the conditions that affect the selective processing of endogenous Notch1 by ADAM10 and ADAM17. *IJMS* (2021) **22**. doi: 10.3390/ijms22041846.

(38) Šućur A, Filipović M, Flegar D, Kelava T, Šisl D, Lukač N, et al. Notch receptors and ligands in inflammatory arthritis – a systematic review. *Immunology letters* (2020) **223**:106-114. doi: 10.1016/j.imlet.2020.04.010.

(39) Takam Kamga P, Bazzoni R, Dal Collo G, Cassaro A, Tanasi I, Russignan A, et al. The Role of Notch and Wnt Signaling in MSC Communication in Normal and Leukemic Bone Marrow Niche. *Front Cell Dev Biol* (2021) **8**. doi: 10.3389/fcell.2020.599276.

(40) Mayan MD, Gago-Fuentes R, Carpintero-Fernandez P, Fernandez-Puente P, Filgueira-Fernandez P, Goyanes N, et al. Articular chondrocyte network mediated by gap junctions: role in metabolic cartilage homeostasis. doi: 10.1136/annrheumdis-2013-204244.

(41) Carpintero-Fernandez P, Gago-Fuentes R, Wang HZ, Fonseca E, Caeiro JR, Valiunas V, et al. Intercellular communication via gap junction channels between chondrocytes and bone cells. *Biochimica et biophysica acta. Biomembranes* (2018) **1860**:2499-2505. doi: 10.1016/j.bbamem.2018.09.009.

(42) Pearson MJ, Herndler-Brandstetter D, Tariq MA, Nicholson TA, Philp AM, Smith HL, et al. IL-6 secretion in osteoarthritis patients is mediated by chondrocyte-synovial fibroblast cross-talk and is enhanced by obesity. *Scientific reports* (2017) **7**:3451-11. doi: 10.1038/s41598-017-03759-w.

(43) Tonon R, Andrea P. Interleukin-1β Increases the functional expression of connexin 43 in articular chondrocytes: Evidence for a Ca2+-dependent mechanism. *Journal of bone and mineral research* (2000) **15**:1669-1677. doi: 10.1359/jbmr.2000.15.9.1669.

(44) Bootman MD, Berridge MJ, Roderick HL. Calcium signalling: dynamics, homeostasis and remodelling. *Nature reviews. Molecular cell biology* (2003) **4**:517-529. doi: 10.1038/nrm1155.

(45) Liang K, Wei L, Chen L. Exocytosis, endocytosis, and their coupling in excitable cells. *Frontiers in molecular neuroscience* (2017) **10**:109. doi: 10.3389/fnmol.2017.00109.

(46) Caffi V, Espinosa G, Gajardo G, Morales N, Durán MC, Uberti B, et al. Pre-conditioning of equine bone marrow-derived mesenchymal stromal cells increases their

immunomodulatory capacity. *Frontiers in veterinary science* (2020) **7**:318. doi: 10.3389/fvets.2020.00318.

(47) Zou J, Bai B, Yao Y. Progress of co-culture systems in cartilage regeneration. *Expert Opin Biol Ther* (2018) **18**:1151-1158. doi: 10.1080/14712598.2018.1533116.

(48) Pas HI, Winters M, Haisma HJ, Koenis MJ, Tol JL, Moen MH. Stem cell injections in knee osteoarthritis: a systematic review of the literature. *Br J Sports Med* (2017). doi: 10.1136/bjsports-2016-096793.

(49) Prządka P, Buczak K, Frejlich E, Gąsior L, Suliga K, Kiełbowicz Z. The Role of Mesenchymal Stem Cells (MSCs) in Veterinary Medicine and Their Use in Musculoskeletal Disorders. *Biomolecules (Basel, Switzerland)* (2021) **11**:1141. doi: 10.3390/biom11081141.

(50) Rowland AL, Miller D, Berglund A, Schnabel LV, Levine GJ, Antczak DF, et al. Cross-matching of allogeneic mesenchymal stromal cells eliminates recipient immune targeting. *Stem cells translational medicine* (2021) **10**:694-710. doi: 10.1002/sctm.20-0435.

(51) Berglund AK, Fortier LA, Antczak DF, Schnabel LV. Immunoprivileged no more: measuring the immunogenicity of allogeneic adult mesenchymal stem cells. *Stem cell research & therapy* (2017) **8**:288. doi: 10.1186/s13287-017-0742-8.

(52) Berglund AK, Schnabel LV. PMC5425313; Allogeneic major histocompatibility complex-mismatched equine bone marrow-derived mesenchymal stem cells are targeted for death by cytotoxic anti-major histocompatibility complex antibodies. *Equine Vet J* (2017) **49**:539-544. doi: 10.1111/evj.12647.

(53) Dostert G, Mesure B, Menu P, Velot É. PMC5293793; How do mesenchymal stem cells influence or are influenced by microenvironment through extracellular vesicles communication?. *Front Cell Dev Biol* (2017) **5**:6. doi: 10.3389/fcell.2017.00006.

(54) Li Z, Li M, Xu P, Ma J, Zhang R. Compositional variation and functional mechanism of exosomes in the articular microenvironment in knee osteoarthritis. *Cell Transplantation* (2020) **29**:963689720968495. doi: 10.1177/0963689720968495.

(55) L PK, Kandoi S, Misra R, S V, K R, Verma RS. The mesenchymal stem cell secretome: A new paradigm towards cell-free therapeutic mode in regenerative medicine. *Cytokine & growth factor reviews* (2019) **46**:1-9. doi: 10.1016/j.cytogfr.2019.04.002.

(56) Arévalo-Turrubiarte M, Baratta M, Ponti G, Chiaradia E, Martignani E. Extracellular vesicles from equine mesenchymal stem cells decrease inflammation

markers in chondrocytes in vitro. *Equine veterinary journal* (2021) **00**:1. doi: 10.1111/evj.13537.

(57) Zhang Q, Fu LL, Liang Y, Guo Z, Wang L, Ma C, et al. Exosomes originating from MSCs stimulated with TGF-β and IFN-γ promote Treg differentiation. *J Cell Physiol* (2018) **233**:6832. doi: 10.1002/jcp.26436.

(58) Mancuso P, Raman S, Glynn A, Barry F, Murphy JM. Mesenchymal Stem Cell Therapy for Osteoarthritis: The critical role of the cell secretome. *Front Bioeng Biotechnol* (2019) **7**. doi: 10.3389/fbioe.2019.00009.

(59) Dahlin RL, Ni M, Meretoja VV, Kasper FK, Mikos AG. PMC3844679; TGF-β3-induced chondrogenesis in co-cultures of chondrocytes and mesenchymal stem cells on biodegradable scaffolds. *Biomaterials* (2014) **35**:123-132. doi: 10.1016/j.biomaterials.2013.09.086.

(60) Meretoja VV, Dahlin RL, Kasper FK, Mikos AG. Enhanced chondrogenesis in co-cultures with articular chondrocytes and mesenchymal stem cells. *Biomaterials* (2012) **33**:6362-6369.

(61) Wu L, Prins HJ, Helder MN, van Blitterswijk CA, Karperien M. Trophic effects of mesenchymal stem cells in chondrocyte co-cultures are independent of culture conditions and cell sources. *Tissue Eng Part A* (2012) **18**:1542-1551. doi: 10.1089/ten.TEA.2011.0715.

(62) McIlwraith CW, Frisbie DD, Rodkey WG, Kisiday JD, Werpy NM, Kawcak CE, et al. Evaluation of intra-articular mesenchymal stem cells to augment healing of microfractured chondral defects. *Arthroscopy* (2011) **27**:1552-1561. doi: 10.1016/j.arthro.2011.06.002.

(63) Broeckx SY, Martens AM, Bertone AL, Van Brantegem L, Duchateau L, Van Hecke L, et al. The use of equine chondrogenic-induced mesenchymal stem cells as a treatment for osteoarthritis: a randomised, double-blinded, placebo-controlled proof-of-concept study. *Equine Vet J* (2019). doi: 10.1111/evj.13089.

(64) Hotham WE, Henson FMD. The use of large animals to facilitate the process of MSC going from laboratory to patient—'bench to bedside'. *Cell Biol Toxicol* (2020) **36**:103. doi: 10.1007/s10565-020-09521-9.

(65) Rowland AL, Miller D, Berglund A, Schnabel LV, Levine GJ, Antczak DF, et al. Cross-matching of allogeneic mesenchymal stromal cells eliminates recipient immune targeting. *Stem cells translational medicine* (2021) **10**:694-710. doi: 10.1002/sctm.20-0435.

(66) Ni Z, Zhou S, Li S, Kuang L, Chen H, Luo X, et al. Exosomes: roles and therapeutic potential in osteoarthritis. *Bone research* (2020) **8**:25. doi: 10.1038/s41413-020-0100-9.

(67) Joo HS, Suh JH, Lee HJ, Bang ES, Lee JM. Current Knowledge and Future Perspectives on mesenchymal stem cell-derived exosomes as a new therapeutic agent. *International journal of molecular sciences* (2020) **21**:727. doi: 10.3390/ijms21030727.

(68) Bogatcheva NV, Coleman ME. Conditioned medium of mesenchymal stromal cells: a new class of therapeutics. *Biochemistry Mosc* (2019) **84**:1375-1389. doi: 10.1134/s0006297919110129.

(69) Kim YG, Choi J, Kim K. Mesenchymal Stem Cell-Derived Exosomes for Effective Cartilage tissue repair and treatment of osteoarthritis. *Biotechnology journal* (2020) **15**:e2000082-n/a. doi: 10.1002/biot.202000082.

(70) Peters AE, Watts AE. PMC4789557; Biopsy needle advancement during bone marrow aspiration increases mesenchymal stem cell concentration. *Front Vet Sci* (2016) **3**:23. doi: 10.3389/fvets.2016.00023.

(71) Mitchell A, Rivas KA, Smith R, 3, Watts AE. PMC4661990; Cryopreservation of equine mesenchymal stem cells in 95% autologous serum and 5% DMSO does not alter post-thaw growth or morphology in vitro compared to fetal bovine serum or allogeneic serum at 20 or 95% and DMSO at 10 or 5. *Stem Cell Res Ther* (2015) **6**:231. doi: 10.1186/s13287-015-0230-y.

(72) Byron CR, Trahan RA. PMC5611359; Comparison of the effects of interleukin-1 on equine articular cartilage explants and cocultures of osteochondral and synovial explants. *Front Vet Sci* (2017) **4**:152. doi: 10.3389/fvets.2017.00152.

(73) Thomas CM, Fuller CJ, Whittles CE, Sharif M. Chondrocyte death by apoptosis is associated with cartilage matrix degradation. *Osteoarthr Cartil* (2007) **15**:27-34. doi: 10.1016/j.joca.2006.06.012.

(74) Thomas CM, Fuller CJ, Whittles CE, Sharif M. Chondrocyte death by apoptosis is associated with the initiation and severity of articular cartilage degradation. *Int J Rheum Dis* (2011) **14**:191-198. doi: 10.1111/j.1756-185X.2010.01578.x.

(75) van der Sluijs, J. A., Geesink RG, van der Linden, A. J., Bulstra SK, Kuyer R, Drukker J. The reliability of the Mankin score for osteoarthritis. *J Orthop Res* (1992) **10**:58-61. doi: 10.1002/jor.1100100107.

(76) Mankin HJ, Dorfman H, Lippiello L, Zarins A. Biochemical and metabolic abnormalities in articular cartilage from osteo-arthritic human hips. II. Correlation of

morphology with biochemical and metabolic data. *J Bone Joint Surg Am* (1971) **53**:523-537.

(77) Noss EH, Brenner MB. The role and therapeutic implications of fibroblast-like synoviocytes in inflammation and cartilage erosion in rheumatoid arthritis. *Immunol Rev* (2008) **223**:252-270. doi: 10.1111/j.1600-065X.2008.00648.x.

(78) Soundararajan M, Kannan S. Fibroblasts and mesenchymal stem cells: Two sides of the same coin?. *Journal of cellular physiology* (2018) **233**:9099-9109. doi: 10.1002/jcp.26860.

(79) Haniffa MA, Wang XN, Holtick U, Rae M, Isaacs JD, Dickinson AM, et al. Adult human fibroblasts are potent immunoregulatory cells and functionally equivalent to mesenchymal stem cells. *J Immunol* (2007) **179**:1595-1604.

(80) Benito MJ, Veale DJ, FitzGerald O, van den Berg, W. B., Bresnihan B. Pmc1755629; Synovial tissue inflammation in early and late osteoarthritis. *Ann Rheum Dis* (2005) **64**:1263-1267. doi: 10.1136/ard.2004.025270.

(81) Ross TN, Kisiday JD, Hess T, McIlwraith CW. Evaluation of the inflammatory response in experimentally induced synovitis in the horse: a comparison of recombinant equine interleukin 1 beta and lipopolysaccharide. *Osteoarthr Cartil* (2012) **20**:1583-1590. doi: 10.1016/j.joca.2012.08.008.

(82) Kaplanski G, Marin V, Montero-Julian F, Mantovani A, Farnarier C. IL-6: a regulator of the transition from neutrophil to monocyte recruitment during inflammation. *Trends Immunol* (2003) **24**:25-29. doi: 10.1016/s1471-4906(02)00013-3.

(83) Guerne PA, Desgeorges A, Jaspar JM, Relic B, Peter R, Hoffmeyer P, et al. Effects of IL-6 and its soluble receptor on proteoglycan synthesis and NO release by human articular chondrocytes: comparison with IL-1. Modulation by dexamethasone. *Matrix Biol* (1999) **18**:253-260. doi: 10.1016/s0945-053x(99)00021-9.

(84) Kapoor M, Martel-Pelletier J, Lajeunesse D, Pelletier JP, Fahmi H. Role of proinflammatory cytokines in the pathophysiology of osteoarthritis. *Nat Rev Rheumatol* (2011) **7**:33-42. doi: 10.1038/nrrheum.2010.196.

(85) Srirangan S, Choy EH. PMC3383508; The role of interleukin 6 in the pathophysiology of rheumatoid arthritis. *Ther Adv Musculoskelet Dis* (2010) **2**:247-256. doi: 10.1177/1759720x10378372.

(86) Lee CM, Kisiday JD, McIlwraith CW, Grodzinsky AJ, Frisbie DD. PMC3620939; Synoviocytes protect cartilage from the effects of injury in vitro. *BMC Musculoskelet Disord* (2013) **14**:54. doi: 10.1186/1471-2474-14-54.

(87) Atukorala I, Kwoh CK, Guermazi A, Roemer FW, Boudreau RM, Hannon MJ, et al. Synovitis in knee osteoarthritis: a precursor of disease?. *Ann Rheum Dis* (2014). doi: 10.1136/annrheumdis-2014-205894.

(88) Wongchana W, Palaga T. Direct regulation of interleukin-6 expression by Notch signaling in macrophages. *Cellular & molecular immunology* (2012) **9**:155-162. doi: 10.1038/cmi.2011.36.

(89) Beekhuizen M, Bastiaansen-Jenniskens Y, Koevoet W, Saris DB, Dhert WJ, Creemers LB, et al. Osteoarthritic synovial tissue inhibition of proteoglycan production in human osteoarthritic knee cartilage: establishment and characterization of a long-term cartilage-synovium coculture. *Arthritis Rheum* (2011) **63**:1918-1927. doi: 10.1002/art.30364.

(90) Hermankova B, Zajicova A, Javorkova E, Chudickova M, Trosan P, Hajkova M, et al. Suppression of IL-10 production by activated B cells via a cell contact-dependent cyclooxygenase-2 pathway upregulated in IFN-γ-treated mesenchymal stem cells. *Immunobiology (1979)* (2015) **221**:129-136. doi: 10.1016/j.imbio.2015.09.017.

(91) Radons J, Falk W, Schubert TE. Interleukin-10 does not affect IL-1-induced interleukin-6 and metalloproteinase production in human chondrosarcoma cells, SW1353. *Int J Mol Med* (2006) **17**:377-383.

(92) Denu RA, Nemcek S, Bloom DD, Goodrich AD, Kim J, Mosher DF, et al. fibroblasts and mesenchymal stromal/stem cells are phenotypically indistinguishable. *Acta haematologica* (2016) **136**:85-97. doi: 10.1159/000445096.

(93) Yung MM, Tang HW, Cai PC, Leung TH, Ngu S, Chan KKW, et al. GRO-α and IL-8 enhance ovarian cancer metastatic potential via the CXCR2-mediated TAK1/NFκB signaling cascade. *Theranostics* (2018) **8**. doi: 10.7150/thno.22536.

(94) Park MS, Kim YH, Jung Y, Kim SH, Park JC, Yoon DS, et al. In Situ Recruitment of human bone marrow-derived mesenchymal stem cells using chemokines for articular cartilage regeneration. *Cell transplantation* (2015) **24**:1067-1083. doi: 10.3727/096368914X681018.

(95) Yang A, Lu Y, Xing J, Li Z, Yin X, Dou C, et al. IL-8 Enhances therapeutic effects of BMSCs on bone regeneration via CXCR2-mediated PI3k/Akt signaling pathway. *Cellular physiology and biochemistry* (2018) **48**:361-370. doi: 10.1159/000491742.

(96) Wu L, Leijten J, van Blitterswijk CA, Karperien M. fibroblast growth factor-1 Is a Mesenchymal stromal cell-secreted factor stimulating proliferation of osteoarthritic chondrocytes in co-culture. *Stem cells and development* (2013) **22**:2356-2367. doi: 10.1089/scd.2013.0118.

(97) Chang SK, Gu Z, Brenner MB. Fibroblast-like synoviocytes in inflammatory arthritis pathology: the emerging role of cadherin-11. *Immunol Rev* (2010) **233**:256-266. doi: 10.1111/j.0105-2896.2009.00854.x.

(98) Barry F, Murphy M. Mesenchymal stem cells in joint disease and repair. *Nature reviews. Rheumatology* (2013) **9**:584-594. doi: 10.1038/nrrheum.2013.109.

(99) Del Fattore A, Luciano R, Pascucci L, Goffredo BM, Giorda E, Scapaticci M, et al. Immunoregulatory effects of mesenchymal stem cell-derived extracellular vesicles on T lymphocytes. *Cell Transplant* (2015). doi: 10.3727/096368915x687543.

(100) Donahue HJ, Qu RW, Genetos DC. Joint diseases: from connexins to gap junctions. *Nature reviews. Rheumatology* (2017) **14**:42-51. doi: 10.1038/nrrheum.2017.204.

(101) McNulty AL, Rothfusz NE, Leddy HA, Guilak F. PMC4037157; Synovial fluid concentrations and relative potency of interleukin-1 alpha and beta in cartilage and meniscus degradation. *J Orthop Res* (2013) **31**:1039-1045. doi: 10.1002/jor.22334.

(102) Gregg AJ, Fortier LA, Mohammed HO, Mayr KG, Miller BJ, Haupt JL. Assessment of the catabolic effects of interleukin-1beta on proteoglycan metabolism in equine cartilage cocultured with synoviocytes. *Am J Vet Res* (2006) **67**:957-962. doi: 10.2460/ajvr.67.6.957.

(103) Vezina Audette R, Lavoie-Lamoureux A, Lavoie JP, Laverty S. Inflammatory stimuli differentially modulate the transcription of paracrine signaling molecules of equine bone marrow multipotent mesenchymal stromal cells. *Osteoarthr Cartil* (2013) **21**:1116-1124. doi: 10.1016/j.joca.2013.05.004.

(104) Reesink HL, Sutton RM, Shurer CR, Peterson RP, Tan JS, Su J, et al. Galectin-1 and galectin-3 expression in equine mesenchymal stromal cells (MSCs), synovial fibroblasts and chondrocytes, and the effect of inflammation on MSC motility. *Stem Cell Res Ther* (2017) **8**:243. doi: 10.1186/s13287-017-0691-2.

(105) Gershwin LJ, Netherwood KA, Norris MS, Behrens NE, Shao MX. Equine IgE responses to non-viral vaccine components. *Vaccine* (2012) **30**:7615-7620. doi: 10.1016/j.vaccine.2012.10.029.

(106) Behrens NE, Gershwin LJ. Immune modulation of T regulatory cells and IgE responses in horses vaccinated with West Nile virus vaccine combined with a CpG ODN. *Vaccine* (2015) **33**:5764-5771. doi: 10.1016/j.vaccine.2015.09.049.

(107) Duensing TD, Watson SR. Assessment of antibody-dependent cellular cytotoxicity by flow cytometry. *Cold Spring Harb Protoc* (2018) **2018**. doi: 10.1101/pdb.prot093815.

(108) Zahavi D, AlDeghaither D, O'Connell A, Weiner LM. Enhancing antibody-dependent cell-mediated cytotoxicity: a strategy for improving antibody-based immunotherapy. *Antibody therapeutics* (2018) **1**:7-12. doi: 10.1093/abt/tby002.

(109) Lee YJ, Suh HN, Han HJ. Effect of BSA-induced ER stress on SGLT protein expression levels and α-MG uptake in renal proximal tubule cells. *American Journal of Physiology - Renal Physiology* (2009) **296**:1405-1416. doi: 10.1152/ajprenal.90652.2008.

(110) Merlot AM, Kalinowski DS, Richardson DR. Unraveling the mysteries of serum albumin: more than just a serum protein. *Frontiers in physiology* (2014) **5**. doi: 10.3389/fphys.2014.00299.

(111) Spada A, Emami J, Tuszynski JA, Lavasanifar A. The uniqueness of albumin as a carrier in nanodrug delivery. *Mol Pharmaceutics* (2021) **18**:1862. doi: 10.1021/acs.molpharmaceut.1c00046.

(112) Qiu Y, Marquez-Curtis LA, Janowska-Wieczorek A. Mesenchymal stem cells express the surface receptor calreticulin (cC1qR) and complement C1q chemoattracts Them. *Blood* (2010) **116**:3855. doi: 10.1182/blood.V116.21.3855.3855.

(113) Brock DJ, Kondow-McConaghy HM, Hager EC, Pellois J. Endosomal escape and cytosolic penetration of macromolecules mediated by synthetic delivery agents. *Bioconjugate chemistry* (2019) **30**:293-304. doi: 10.1021/acs.bioconjchem.8b00799.

(114) Schnabel LV, Pezzanite LM, Antczak DF, Felippe MJ, Fortier LA. Pmc4055004; Equine bone marrow-derived mesenchymal stromal cells are heterogeneous in MHC class II expression and capable of inciting an immune response in vitro. *Stem Cell Res Ther* (2014) **5**:13. doi: 10.1186/scrt402.

(115) Cassano JM, Schnabel LV, Goodale MB, Fortier LA. Inflammatory licensed equine MSCs are chondroprotective and exhibit enhanced immunomodulation in an inflammatory environment. *Stem cell research & therapy* (2018) **9**:82. doi: 10.1186/s13287-018-0840-2.

(116) Owens SD, Kol A, Walker NJ, Borjesson DL. PMC5018342; Allogeneic mesenchymal stem cell treatment induces specific alloantibodies in horses. *Stem Cells Int* (2016) **2016**:5830103. doi: 10.1155/2016/5830103.

(117) Helguera G, Rodríguez JA, Luria-Pérez R, Henery S, Catterton P, Bregni C, et al. Visualization and quantification of cytotoxicity mediated by antibodies using imaging flow cytometry. *Journal of immunological methods* (2011) **368**:54-63. doi: 10.1016/j.jim.2011.03.003.

[i] Lonza, Walkersville, MD, USA

[ii] Mediatech, Inc., Manassas, VA, USA

[iii] Mediatech, Inc., Manassas, VA, USA

[iv] Mediatech, Inc., Manassas, VA, USA

[v] HyClone, Thermo Scientific, Logan, UT, USA

[vi] MilliporeSigma, Burlington, MA, USA

[vii] EMD Chemicals, Inc., Calbiotech, San Diego, CA, USA

[viii] EMD Chemicals, Inc., Calbiotech, San Diego, CA, USA

[ix] 175 cm2 Polystyrene Tissue Culture Flask with Vented Caps Corning, Corning, NY, USA

[x] Trypsin EDTA, Corning, Corning, NY, USA

[xi] Dimethyl Sulfoxide, MilliporeSigma, Burlington, MA, USA

[xii] Corning, Corning, NY, USA

[xiii] Integra® Miltex Disposable Biopsy Punch, Integra York PA, Inc., USA

[xiv] Corning, Corning, NY, USA

[xv] MilliporeSigma, Burlington, MA

[xvi] R&D Systems, Minneapolis, MN, USA

[xvii] ThermoFisher Bond-Breaker™ TCEP Solution, Rockford, IL, USA

[xviii] Corning, Corning, NY, USA

[xix] R&D Systems, Minneapolis, MN, USA

[xx] R&D Systems, Minneapolis, MN, USA

[xxi] R&D Systems, Minneapolis, MN, USA

[xxii] MilliporeSigma, Burlington, MA, USA

[xxiii] Bio-Plex 200 System, BioRad, Hercules, CA, USA

[xxiv] PureLink RNA Mini Kit, Thermofisher, Waltham, MA, USA

[xxv] Tape Station 2200, Agilent Technologies, Santa Clara, CA, USA

[xxvi] OligoArchitect™, Sigma-Aldrich, St. Louis, MO, USA

[xxvii] MilliporeSigma, Burlington, MA, USA

[xxviii] MilliporeSigma, Burlington, MA, USA

[xxix] Cytation 7, BioTek Instruments Winooski, Vermont, USA

[xxx] MilliporeSigma, Burlington, MA, USA

[xxxi] MilliporeSigma, Burlington, MA, USA

[xxxii] MilliporeSigma, Burlington, MA, USA

[xxxiii] cellSense Imaging Software, Olympus Corporation, Shinjuku City, Tokyo, Japan

[xxxiv] ImageJ Software, National Institutes of Health, Public Domain

[xxxv] Thermofisher, Waltham, MA, USA

[xxxvi] Thermofisher, Waltham, MA, USA

[xxxvii] Amnis ® CellStream ® Flow Cytometer, Luminex, Austin, TX, USA

[xxxviii] GraphPad Prism Software, Inc., USA

[xxxix] MilliporeSigma, Burlington, MA, USA

[xl] GenWay Biotech Inc., San Diego, CA, USA

[xli] GenWay Biotech Inc., San Diego, CA, USA

[xlii] Corning, Corning, NY, USA

[xliii] HyClone, Thermo Scientific, Logan, UT, USA

[xliv] Invitrogen, Waltham, MA, USA

[xlv] One Lambda, Inc., Los Angeles, CA, USA

[xlvi] Thermofisher, Waltham, MA, USA

[xlvii] GE Healthcare, Chicago, IL, USA

[xlviii] MilliporeSigma, Burlington, MA, USA

[xlix] Bio-Rad, Hercules, CA, USA

[l] Bio-Rad, Hercules, CA, USA

[li] Pierce™, Thermo Scientific, Waltham, MA, USA

[lii] Abcam, Cambridge, UK

[liii] Abcam, Cambridge, UK

[liv] Bio-Rad, Hercules, CA, USA

[lv] Bio-Rad, Hercules, CA, USA

[lvi] Bio-Rad, Hercules, CA, USA

[lvii] Bio-Rad, Hercules, CA, USA

[lviii] Bio-Rad, Hercules, CA, USA

[lix] Thermo Scientific, Waltham, MA, USA

[lx] Bio-Rad, Hercules, CA, USA

[lxi] Amnis ® ImageStream ® Flow Cytometer, Luminex, Austin, TX, USA

[lxii] Bio-Rad, Hercules, CA, USA